Impacts of climate change and agricultural managements on major global cereal crops

Xuhui Wang

THESE DE DOCTORAT

DE

SORBONNE UNIVERSITÉ

(UNIVERSITÉ PIERRE ET MARIE CURIE)

ÉCOLE DOCTORALE N°129

Sciences de l'environnement d'Ile-de-France

Spécialité de doctorat : Météorologie, océanographie, physique de l'environnement

Par

M. Xuhui WANG

Impacts of climate change and agricultural managements on major global cereal crops

Titre: Impacts du changement climatique et des pratiques agricoles sur la culture des principales céréales du monde

Mots clés: changement climatique, irrigation, phénologie, rendement, Chine

Résumé:

Les terres cultivées représentent un cinquième de la surface émergée de la Terre. Elles fournissent des nutriments à l'homme, modifient le cycle biogéochimique et l'équilibre énergétique de la terre. L'évolution des terres cultivées dans le contexte du changement climatique et avec une intensification des actions anthropiques constitue un enjeu important pour la sécurité alimentaire et les exigences environnementales du développement durable. Le manuscrit de thèse s'inscrit dans cette thématique en exploitant les données de différentes sources et la modélisation numérique. Les données utilisées sont : les statistiques de rendements, les observations agro-météorologiques à long terme, les résultats des sites d'expérimentation avec du réchauffement, les jeux de données globales issus des processus de fusion ou d'assimilation, les données climatiques historiques et de projection future. La modélisation fait appel aux modèles statistiques et aux modèles de processus. Le manuscrit est composé d'une série de travaux de détection et d'attribution. Ils explorent la phénologie, le rendement et leurs réponses aux changements climatiques et aux pratiques de gestion. Ils sont soit sur l'échelle régionale soit sur l'échelle globale, en fonction de la disponibilité des données et de leur pertinence.

Le chapitre 2 décrit la construction et l'utilisation d'un modèle statistique avec des données provinciales de rendement au Nord-est de Chine et des données climatiques historiques. Les résultats montrent un effet asymétrique de la température diurne sur le rendement du maïs. Le rendement du maïs augmente de 10.0±7.7% en réponse à une augmentation moyenne de 1°C pendant la saison de croissance quand il s'agit de la température minimale de nuit (Tmin), mais le rendement diminue de 13,4±7,1% quand il s'agit de la température maximale de jour (Tmax). Il y a une grande disparité spatiale pour la réponse à Tmax, ce qui peut s'expliquer partiellement par le fort gradient spatial de la température pendant la saison de croissance ($R = -0,67$, $P < 0,01$). La réponse du rendement aux précipitations dépend aussi des conditions d'humidité. Malgré la détection d'impacts significatifs du changement climatique sur le rendement, une part importante de ses variations n'est pas expliquée par les variables climatiques, ce qui souligne le besoin urgent de pouvoir attribuer proprement les variations de rendement au changement climatique et aux pratiques de gestion.

Le chapitre 3 présente le développement d'un algorithme d'optimisation basé sur la théorie de Bayes pour optimiser les paramètres importants contrôlant la phénologie dans le modèle ORCHIDEE-crop. L'utilisation du modèle optimisé permet de distinguer les effets de la gestion de ceux du changement climatique sur la période de croissance du riz (LGP). Les résultats du modèle optimisé ORCHIDEE-crop suggèrent que le changement climatique

affecte la LGP différemment en fonction des types du riz. Le facteur climatique a fait raccourcir la LGP du riz précoce (-2,0±5,0 jour / décennie), allonger la LGP du riz tardif (1,1±5,4 jour / décennie). Il a peu d'effet sur la LGP du riz unique (-0,4±5,4 jour / décennie). Les résultats du modèle ORCHIDEE-crop montrent aussi que les changements intervenus dans la date de transplantation ont provoqué un changement généralisé de la LGP, mais seulement pour les sites de riz précoce. Ceci compense à la hauteur de 65% le raccourcissement de la LGP provoquée par le changement climatique. Le facteur dominant du changement LGP varie suivant les trois types de riz. La gestion est le principal facteur pour les riz précoce et unique. Ce chapitre démontre aussi qu'un modèle optimisé peut avoir une excellente capacité à représenter des variations régionales complexes de LGP. Les études futures devraient mieux cerner les défauts d'observation et documenter les différentes pratiques de gestion afin de réduire les incertitudes qui existent encore dans l'attribution de causes pour le changement de LGP. Elles devraient aussi faciliter l'intégration de la modélisation et de l'observation.

Le chapitre 4 présente des résultats issus d'une exploration conjointe avec les données de sites, d'un côté, et la modélisation globale, de l'autre côté. L'observation est un ensemble de données avec du réchauffement contrôlé, coordonné sur 48 sites du monde pour les quatre cultures les plus répandues (blé, maïs, riz et soja). La modélisation est assise sur un ensemble de modèles de cultures sur des mailles régulières couvrant le globe. Le but est d'estimer les réponses du rendement de ces céréales au changement de température (ST), l'estimation étant contrainte par les données d'expérimentation. Le nouveau cadre avec contraintes intègre des données de sites d'observation avec un réchauffement contrôlé et la modélisation globale des cultures. Les résultats montrent, avec une probabilité > 95%, que des températures plus chaudes réduisent les rendements du maïs (-7,1 ± 2,8% K-1), du riz (-5,6 ± 2,0% K-1) et du soja (-10,6 ± 5,8% K-1). Pour les blés, ST étant moins négatif, il y a seulement 89% de probabilité pour que son rendement soit négatif (-2,9 ± 2,3% K-1). Les contraintes apportées par les observations de terrain avec du réchauffement contrôlé permettent de réduire les incertitudes associées au réchauffement global. La réduction est de 12 à 54% pour les quatre cultures. Une principale implication de ces résultats s'applique aux évaluations des conséquences climatiques dans le cadre de l'Accord de Paris qui préconise des efforts nécessaires pour que le réchauffement global soit limité à 2 K au-dessus du niveau de l'époque préindustrielle. Dans ce cas, les rendements des principales cultures connaissent une réduction de 3% à 13%, sans tenir compte des effets de CO2. Même si le réchauffement est limité à 1,5 K, aucun des principaux pays de ces cultures ne bénéficierait des températures plus chaudes sans une adaptation efficace. Le maïs, le riz et le soja seraient plus vulnérables à l'augmentation des températures que le blé.

Le chapitre 5 présente une estimation cohérente (une sorte de ré-analyse) sur la contribution de l'irrigation au rendement mondial du blé et du maïs, tout en poursuivant le même cadre bayésien intégrant les mesures de terrain et la modélisation des cultures. La ré-analyse ainsi obtenue a plus de précision que toutes autres estimations simples lorsque le résultat est confronté aux statistiques nationales des Etats-Unis. A l'échelle mondiale,

l'irrigation contribue respectivement à 34%±25% et 22%±23% au rendement irrigué pour le blé et le maïs. Les grandes variations spatiales de la contribution de l'irrigation au rendement sont davantage attribuables à l'approvisionnement climatique en eau qu'à la demande. En accord avec les ressources de ruissellement disponibles, la priorité de construire des installations d'irrigation se déplace vers l'Europe de l'Est et l'Inde pour le blé et vers le Brésil pour le maïs. Si l'on transforme les terres cultivées pluviales en terres irriguées, 30 à 47% des terres pluviales actuelles ne disposent pas de ressources locales suffisantes à la demande d'irrigation, y compris certaines régions importantes (par exemple le Nord de la Chine et le Centre-Ouest des États-Unis) qui devraient développer des projets d'extraction d'eau souterraine ou des projets de transfert d'eau inter-bassin. En considérant qu'il y a d'importantes surestimations de la contribution de l'irrigation au rendement des cultures dans la plupart des modèles antérieurs, on doit ici préconiser que les analyses, fondées sur ces résultats surestimés, concernant l'économie agricole et de l'hydrologie devrait être réexaminée.

Enfin, pour clôturer le manuscrit, une discussion est présentée autour de l'implication des résultats des chapitres précédents sur le développement continu du modèle ORCHIDEE-crop et son application potentielle pour la modélisation couplée terre-atmosphère.

Title: Impacts of climate change and agricultural managements on major global cereal crops

Key words: climate change, irrigation, phenology, yield, China

Abstract:

Croplands accounts for one-fifth of global land surface, providing calories for human beings and altering the global biogeochemical cycle and land surface energy balance. The response of croplands to climate change and intensifying human managements is of critical importance to food security and sustainability of the environment. The present manuscript of thesis utilizes various types of data sources (yield statistics, long-term agrometeorological observations, field warming experiments, data-driven global datasets, gridded historical climate dataset and projected climate change) and also modelling approaches (statistical model vs. process model). It presents a series of detection and attribution studies exploring how crop phenology and crop yield respond to climate change and some management practices at regional and global scales, according to data availability.

In Chapter 2, a statistical model is constructed with prefecture-level yield statistics and historical climate observations over Northeast China. There are asymmetrical impacts of daytime and nighttime temperatures on maize yield. Maize yield increased by 10.0±7.7% in response to a 1 ^{o}C increase of daily minimum temperature (*Tmin*) averaged in the growing season, but decreased by 13.4±7.1% in response to a 1 ^{o}C warming of daily maximum temperature (*Tmax*). There is a large spatial variation in the yield response to *Tmax*, which can be partly explained by the spatial gradient of growing season mean temperature ($R=-0.67$, $P<0.01$). The response of yield to precipitation is also dependent on moisture conditions. In spite of detection of significant impacts of climate change on yield variations, a large portion of the variations is not explained by climatic variables, highlighting the urgent research need to clearly attribute crop yield variations to change in climate and management practices.

Chapter 3 presents the development of a Bayes-based optimization algorithm that is used to optimize key parameters controlling phenological development in ORCHIDEE-crop model for discriminating effects of managements from those of climate change on rice growth duration (LGP). The results from the optimized ORCHIDEE-crop model suggest that climate change has an effect on LGP trends, but with dependency on rice types. Climate trends have shortened LGP of early rice (-2.0±5.0 day/decade), lengthened LGP of late rice (1.1±5.4 day/decade) and have little impacts on LGP of single rice (-0.4±5.4 day/decade). ORCHIDEE-crop simulations further show that change in transplanting date caused widespread LGP change only for early rice sites, offsetting 65% of climate-change-induced LGP shortening. The primary drivers of LGP change are thus different among the three types of rice. Management is predominant driver of LGP change for early and single rice. This chapter demonstrated the capability of the optimized crop model to represent complex

regional variations of LGP. Future studies should better document observational errors and management practices in order to reduce large uncertainties that exist in attribution of LGP change and to facilitate further data-model integration.

In Chapter 4, a harmonized data set of field warming experiments at 48 sites across the globe for the four most-widely-grown crops (wheat, maize, rice and soybean) is combined with an ensemble of gridded global crop models to produce emergent constrained estimates of the responses of crop yield to changes in temperature (S_T). The new constraining framework integrates evidences from field warming experiments and global crop modeling shows with >95% probability that warmer temperatures would reduce yields for maize (-7.1±2.8% K^{-1}), rice (-5.6±2.0% K^{-1}) and soybean (-10.6±5.8% K^{-1}). For wheat, S_T was less negative and only 89% likely to be negative (-2.9±2.3% K^{-1}). The field-observation based constraints from the results of the warming experiments reduced uncertainties associated with modeled S_T by 12-54% for the four crops. The key implication for impact assessments after the Paris Agreement is that with global warming limited within 2 K above pre-industrial levels will still reduce yields of major crops by 3% to 13%, without considering effects of atmospheric CO_2 concentrations. Even if warming was limited to 1.5 K, none of the major producing countries of these crops would likely benefit from the warmer temperatures without effective adaptation. Maize, rice and soybean would be more vulnerable to increasing temperatures than wheat.

In addition to model-data integration for assessing climate change impacts, Chapter 5 reanalyzed irrigation contribution to global wheat and maize yield with the Bayesian framework integrating estimates from both field measurements and crop modelling. The reanalysis has more precision than any single estimate when confronted with US statistics. At global scale, irrigation contributes to 34%±25% and 22%±23% of irrigated yield for wheat and maize respectively. The large spatial variations in irrigation contribution to crop yield are driven more by climatic water supply than by climatic water demand. When matching with available runoff resources, the priority of building irrigation facilities shift to eastern Europe and India for wheat and to Brazil for maize. If shifting global rainfed croplands into irrigated ones, 30% - 47% of current rainfed croplands do not have sufficient local runoff resources to meet irrigation demand, including some hotspots (e.g. northern China and mid-western US), which will have to rely on groundwater or trans-basin water transfer program. The large overestimates in crop-model-simulated irrigation contribution to crop yield suggest that previous model-based analyses of agricultural economy and hydrology will have to be revisited.

Finally, a discussion is given around the implication of findings in previous chapters on the ongoing development of ORCHIDEE-crop and its potential application for the land-atmospheric coupled modelling.

Acknowledgements

When reviewing my thesis, I am truly grateful to many, who have significantly helped my studies and making my researches different. First, I am grateful to my advisors, Dr. Shilong Piao and Dr. Laurent Li. I have worked with Dr. Piao since my undergraduate years. The training and working experience I got from him has transferred me from an ecology student interest in science and information technology to a researcher trying to explore the cutting edge of global change studies. It is a truly great honor for me to learn from the best and to work closely with him. The guidance and training I had from him shapes my views of sciences and researches. I am deeply indebted to him. Since the first day I came to Paris, Dr. Li has been my ultimate solution for all problems I encountered. He gave me the freedom to explore and discover the question of my interest, sponsored me to participate academic conference, encouraged me and shared with me new ideas and thoughts from worldwide colleagues. The training I had for the LMDZOR model will become a powerful tool for my continuing researches. He also made my life, an English/Chinese speaker in France, possible and easier. I am also deeply indebted. Without him, I would not be able to make it.

I am also grateful to Dr. Philippe Ciais, who has provide inspiring suggestions for almost every manuscript I made, supporting me financially for researches and conference participations, and providing the opportunity to continue my researches with ORCHIDEE. Working with Dr. Ciais is also an eye-opening experience, for his broad and deep understanding on every topic I am interested in. The guidance from him has made my work detoured less and my publishing experience more enjoyable. Thanks very much for the continuous help.

The work presented in this thesis has also got help from younger students, including but not limited to Liqing Peng and Chuang Zhao, working with them is also quite a pleasure. Analyses using crop model ensembles will not be possible without the support from the colleagues in global gridded crop model intercomparison project (GGCMI), in particular Dr. Christoph Muller and Dr. Joshua Elliot. I thank them for the opportunities.

Senior colleagues in LMD, SOFIE and LSCE have made my years of PhD studies enjoyable. The list of names I should thank is very long, Shushi Peng, Tao Wang, Nicolas Viovy, Jinfeng Chang, Yue Li, Xiuchen Wu, Josefine Ghattas and Nicolas Vuichard. It is a pleasure working with them. My Chinese friends here in France has made my life more colorful. Discussions we had also help me move my researches. Thanks a lot to them, Yilong Wang, Wei Li, Chao Yue, Bo Zheng, Xin Lin, Dan Zhu, Yi Yin, Shan Li, Zun Yin…

Finally, I dedicated the thesis also to my wife, Huihui Dong, who has made my life different. Marrying her is the other big difference I made during my pursuing of the science. Thanks also to the supports from my families, and sorry for my absence in their lives because

I am either in Beijing or in Paris.

I made this journey with all your supports. Thank you very much for helping me make it!

Table of contents

Chapter 1 Introduction

Food security under changing climate is a critical global issue, with rising population projected to reach 9.6 billion ~2050s (UN, 2012). To feed such huge population, global food production has to increase by more than 70% (FAO, 2012). This estimates will have to be even larger (~110%), if considering potential change in diets (Tilman et al., 2011). The anthropogenic climate change (IPCC, 2013) has been an important factor limiting sustainable food supply and causing fluctuations of supply-demand balance global crop production (Godfray et al., 2010; Beddington et al., 2012; Lesk et al., 2016). Therefore, studying climate change impacts on crop ecosystems is vital for sustainability of the society.

The human managements on croplands not only produces food, but also left its footprint on biophysics and biogeochemical cycle of the earth system. According to Ramankutty et al. (2008), croplands comprise 20% of global land surface, which accounts ~25% of greenhouse gas emission to the atmosphere (Foley et al., 2005; World Resource Institute, 2013; Tian et al., 2016). The global carbon cycle has also been modified by croplands. For example, studies have shown that, the “Green Revolution” over the past five decades has significantly change seasonal variations of atmospheric CO_2 (Gray et al., 2014; Zeng et al., 2014). In addition, human management has profoundly affected the energy and water balance of the land surface. The annual water withdraw for irrigation accounts for ~70% of global water withdraw from the river runoff. Therefore, it is essential to explore the relationship between climate and croplands as the component of the earth system models.

As the Introduction of the thesis, we first overview knowledge on how climate change has influenced crop phenology, yield, energy balance and water cycle. Then we synthesize status of crop model developments. In the end, we present the objective and structure of the thesis.

1.1 The impact of climate change on croplands

Phenology and yield

The growth duration of a crop determine the time length of light interception and photosynthesis, therefore the crop yield and its water and energy balance. As sensitivity of crop to climate variations are not equally sensitive across the growing season (Porter & Semenov, 2005), which can be particularly sensitive to climate variations at certain reproductive phase (e.g. Hatfield et al., 2011; Espe et al., 2017), the timing of key phenological events are also of great importance. Thus, understanding how phenology respond to climate change is a prerequisite to understand how climate change affects crop ecosystems.

It has long been recognized that climate change has significant impacts on crop growth duration. Each 1°C of warmer temperature shorten growth duration by ~7 days by average (Muchow et al., 1990; IPCC, 2007). However, this average sensitivity cannot really represent the theories and observations. A widely-adopted theory of cardinal temperatures suggest that, crop growth accelerates with warmer temperature when it is below the optimum temperature for crop development (e.g. Hatfield et al., 2011), which shorten the growth duration. However, when temperature is above its optimum, the acceleration with higher temperature may disappear. This critical temperature threshold (the optimum temperature) may differ largely across crops and varieties ranging from 20°C to 35°C (Sanchez et al., 2014). It should be noted that how crop-climate relationship may change above the optimum temperature is largely uncertain and differ across crops (Craufurd & Wheeler, 2009). For example, some studies found rapid senescence of wheat after exposure to 32-34ºC during flowering period (Asseng et al., 2011; Lobell et al., 2013). However, for rice, the limited number of researches indicate that growth duration is not responsive to temperature when it goes beyond the optimum (Yoshida, 1983). These observational evidences, however, have not been well accounted in many widely used crop models (Sanchez et al., 2014). For example, the CERES model used for assessing food security under climate change in China (e.g. Xiong et al., 2009; Xiong et al., 2010) only considers the acceleration effects of warming but not the high temperature stress (e.g. Lobell et al., 2013)。

For natural ecosystems, many studies have consistently shown that global warming over the past few decades has advanced the spring onset date (e.g. Menzel et al., 2006; Wang et al., 2015), lengthening the growing season (e.g. Garonna et al., 2014), though it may reverse over a few regions due to climate fluctuations (e.g. Piao et al., 2011). However, unlike the consistency found for natural ecosystem, the trend in crop growth duration was quite diversified in different researched. For example, Siebert et al. (2012) found growth duration of oat over Germany is shortening by 0.1-0.4 day/10a over past five decades; Tao et al. (2006) found growth duration for rice over China have also shortened over past two decades. However, more recent researched over past two to three decades found growth duration for major cereal crops (rice, wheat and maize) over China has become longer (e.g. Liu et al., 2012; Liu et al., 2013; Tao et al., 2013; Xiao et al., 2013; Li et al., 2014). These results appear contradictory, but can be reconciled with adaptation measures by selecting long-duration varieties.

Crop yield can be affected by temperature change through different pathways. First, rising temperature directly drives change in photosynthetic rate (Figure 1.1). When temperature is below the optimum temperature, rising temperature will enhance photosynthetic rate, while it suppress photosynthetic rate when temperature goes beyond the optimum. Respiration processes also subject to temperature regulations. However, the optimum temperature for respiration is usually higher than that of photosynthesis and outside measurement range (Figure 1.1). It is therefore commonly believed that higher temperature will lead to higher respiration rate. The net effect of temperature on photosynthesis and respiration is the temperature effects on crop productivity. Night-time warming was believed to negatively affect crop yield as respiration increase while photosynthesis is still zero (Peng et al., 2004; Lobell et al., 2012a). However, due to potential compensation effects that enhance photosynthesis on the day (Wan et al., 2009), warmer nighttime temperature may also improve crop productivity. Second, certain phase of crop reproductive growth (e.g. silking and grain filling) is sensitivity to high/low temperature stress (e.g. Schar et al., 2004; Espe et al., 2017). For example, high temperature stress can lead to failure of flowering, grain formation and grain filling, leading to reduced crop yield (Schar et al., 2004; Porter & Semenov, 2005; Asseng et al., 2011; Teixeira et al.,

2013). Third, as mentioned in previous paragraph, temperature change will affect the length of growing duration, which affect the accumulation of photosynthesis and thus yield. Usually, higher temperature lead to shorter growing duration and lower yield (e.g. Iqbal et al., 2009; Giannakopoulos et al., 2009; Lobell et al., 2012b). Finally, increase in temperature lead to exponential increment of vapor pressure deficit, which may also stress the productivity of croplands (e.g. Lobell et al., 2013).

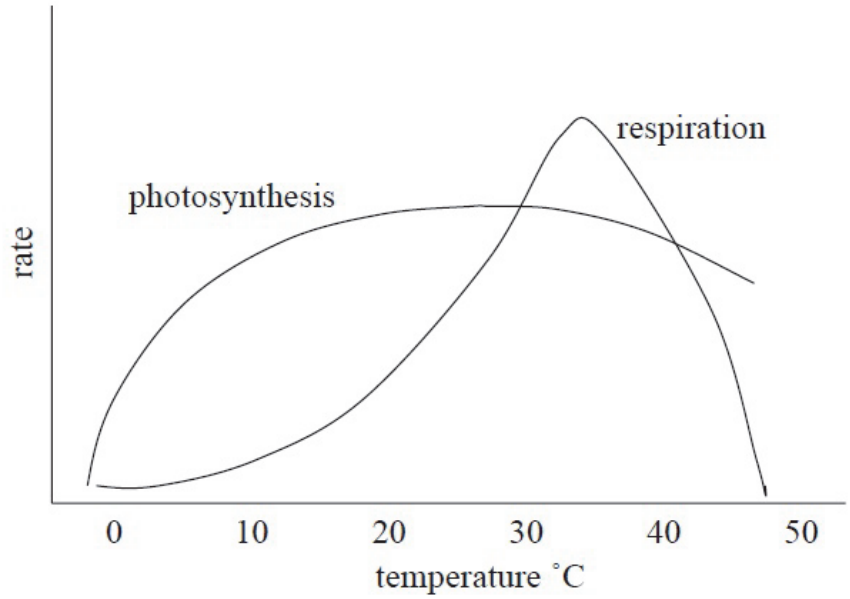

Figure 1.1 Schematic diagram for relationship between temperature and rates of photosynthesis and respiration (Porter & Semenov, 2005)

The impact of precipitation change on crop yield remains more controversial. Some studies show that 20% decrease in precipitation will still have limited impacts on maize yield over USA (Lobell et al., 2013), while other studies found precipitation change as more dominant factor than change in temperature and atmospheric CO_2 on crop yield (Ko et al., 2010). Probably due to expansion of irrigation, which may alleviate the water stress to crop production, the studies on impact of precipitation on crop yield is much less than that of temperature. However, climate change will lead to change in irrigation demands (Elliot et al., 2014) and spatio-temporal distribution of available water resources. Whether sufficient irrigation water can be provided is a urgent research question to answer. In addition, projected increase in exteme events, such as droughts and flood (IPCC, 2012), may also leads to fluctuations of global crop productions (Lesk et al., 2016).

Solar radiation reaching the land surface is the energy source of photosynthesis and thus crop productivity. Interannual variations of solar radiation has significant impacts on rice yield over China (Zhang et al., 2010). However, it is so commonly assumed that crop growth was more stressed by temperature and water availability (Hatfield et al., 2011), the impact of variations of solar radition on crop yield remains largely uncertain.

Despite growing knowledge on the mechanism how climate change could influence crop yield, our knowledge on the key parameters (e.g. cardinal temperature) and dominant climatic factors driving yield change remains unclear. Regional and inter-crop differences may further complex situation. Large uncertainties, therefore, still exist in quantifying climate change impacts on crop production (IPCC, 2013a). A synthesis of 66 studies on climate change impacts on crop yield (IPCC, 2013a) found that warming of 1-2 ^{o}C may lead to decline of wheat and maize yield. However, rice in tropical region and maize in temperate regions show different response to warming in different studies. As a result, even qualitative conclusions are difficult to make. Different global studies drew different conclusions on how rice yield respond to climate change. For example, Lobell et al. (2011) found climate change over past three decades may slightly enhance the yield, while recent multi-model intercomparison study (Rosenzweig et al., 2014) found climate change will reduce rice yield, without considering the CO_2 fertilization effect. Therefore, detailed regional studies are warranted in order to reduce the uncertainties. However, regional studies based on statistics, long-term agro-meteorological site observations and crop models drew contrast conclusions on how climate change affects rice yield over China (Lin et al., 2005; Yao et al., 2007; Tao et al., 2008; Xiong et al., 2007; Xiong et al., 2009; Zhang et al., 2010; Welch et al., 2010; Tao et al., 2012), highlighting large uncertainties in the estimates. Single model studies are prevalent among previous ones (e.g. Lin et al., 2005; Xiong et al., 2007; Yao et al., 2007; Xiong et al., 2009; Tao and Zhang, 2012) , but the uncertainties related to model structures and parameters remains largely unexplored. Recent studies seems indicating the multi-model ensemble may improve confidence in projecting how crop yield may respond to the changing climate (Asseng et al., 2015; Martre et al., 2015; Li et al., 2015).

Land surface energy and water exchange

Irrigation accounts for ~70% of global water widraw (Shiklomanov & Rodda, 2003), which is also a key variable for projecting crop production and food security (IPCC, 2013a). The irrigation water requirements of croplands are determined by balance of precipitation and evapotranspiration, both of which are affected by climate change. Anthropogenic climate change is projected to alter the spatial distribution of annual precipitation (IPCC, 2013b), which will change the water availability over contemporary cropping area. The seasonal distribution of precipitation may also altered (IPCC, 2013b), which may induced seasonal shortage of water supply during growing season.

Climate change affect evapotranspiration through three pathways. First, it affects crop productivity, which consume water affect the rate of evapotranspiration; Second, it regulates length of growing season, which affects the annual sum of evapotranspiration; Finally, warmer temperature will directly change saturated water vapor pressure and stomatal conductance, the net effect of which may accelerate the crop evapotranspiration (e.g. Ben-Asher et al., 2008). One factor often dismissed in studies on crop evapotranspiration is the impact of solar radiation (Hatfield et al., 2011), which directly alter the energy balance of the land surface (Wild et al,. 2005). The commonly used empirical equation (Penmman-monteith) in crop models does not include effects of solar radiation, which may underestimate variations of evapotranspiration. Rising atmospheric CO_2 will lead to decrease of stomatal conductance and thus reducing transpiration (Leaky et al., 2006). Across different FACE experiments, stomatal conductance by average reduce by 20% in response to enhanced CO_2 at 550 ppm (Ainsworth et al., 2005). The reduction of stomatal conductance may further enhanced to 30%-40% under doubling CO_2 concentration (Hatfield et al., 2011). However, at canopy level, the observed change of evapotranspiration under double CO_2 is only 8%-13% (Hatfield et al., 2011), which can result from negative feedbacks result from higher CO_2 induced higher leaf temperature and photosynthetic rate (Leaky et al., 2009; Burkart et al., 2011). Rising atmospheric CO_2 and temperature drive change evapotranspiration in different direction, which is a hotspot for impact studies and remains largely uncertain (Liu & Tao, 2013). Complex interactions among climate change factors in affecting evapotranspiration may have not been fully understood and incorporated in the models. For example, rising CO_2 may enhance vegetation growth, and thus surface

roughness, resulting in reduced wind speed (Vautard et al., 2010). The lower wind speed resulted from rising CO_2 may thus reduce evapotranspiration.

Overall, experimental and model studies show that warmer temperature lead to increasing cropland evapotranspiration (e.g. Guo et al., 2010; Hoff et al., 2010; Gerten et al., 2011). Field observational studies in general agree that rising atmospheric CO2 will lead to decrease of cropland evapotranspiration (e.g. Reddy et al., 1995; Leaky et al., 2006; Bernacchi et al., 2007). Assuming no change of crop varieties, the global modelling study show the overall effect of climate change following RCP8.5 will be reducing global crop irrigation demand by 8%-15% (Elliot et al., 2014), but the sign and magnitude change across crops and regions. Uncertainties are still large, as hydrological models and crop models differ, by average two times, in the estimate of crop irrigation demand (Elliot et al., 2014).

1.2 Crop models, from sites to the globe

Crop models are the essential tool integrating our knowledge of climate change impacts on croplands. The field-scale crop model started from 1960s with two genres: The waegningen group led by de Wit (1965) developed crop growth model based on light use efficiency module. Crop models such as WOFOST and ORYZA(Bouman & Van Laar, 2006) are evolution of this type of models. The other genre is the CERES type of model (Ritchie et al., 1985) based on earlier work by Duncan (1967), including CROPGRO. DSSAT is the platform integrating both CERES and CROPGRO. APSIM is an Australian model also belongs to this genre. Despite the differences among these models, there are some resemblance on them, such as the use of radiation use efficiency (RUE) module or water use efficiency (WUE) module, the thermal accumulation module to drive crop phenology, the use of variants of Penman-Monteith equation for calculation of evapotranspiration. These traditional crop model have strong suits in detailed simulation of organ developments, given a large number of parameters. However, the equations used are often highly empirical. For example, the water and nutrient stress to crop phenology development, the ratio of actual to potential evapotranspiration are often empirical parameter between 0 and 1. Such formulation of equations will easily lead to over-parameterization and uniformality issues in representing physiological process. The photosynthesis in these models are semi-empirical

WUE or RUE model (Soussana et al., 2010), instead of the physiology based Farquhar(Farquhar & Sharkey, 1982). Under contemporary climate, these crop models may be parameterized to reflect the characteristics of the croplands, but its robustness to be extrapolated into future and project impacts of climate change could be dubious (Nowak et al., 2004; Soussana et al., 2010). For example, Wang et al. (2012) show WUE and RUE model may predict contrast response of productivity to climate change over China. There are a long list of this type of crop models developed by researches from different countries (e.g. STICS (Brisson et al., 2008), SIMRIW(Horie, 1987; Zhang et al., 2014), Agro-C (Huang et al., 2009), RiceGrow (Tang et al., 2009), McWLA(Tao and Zhang, 2012)), which have been developed and tuned for a certain crop-region. As a result , in recent model intercomparison of crop models for wheat, maize and rice, no models can out-perform others in four test sites at different regions of the globe (Li et al., 2015; Martre et al., 2015).

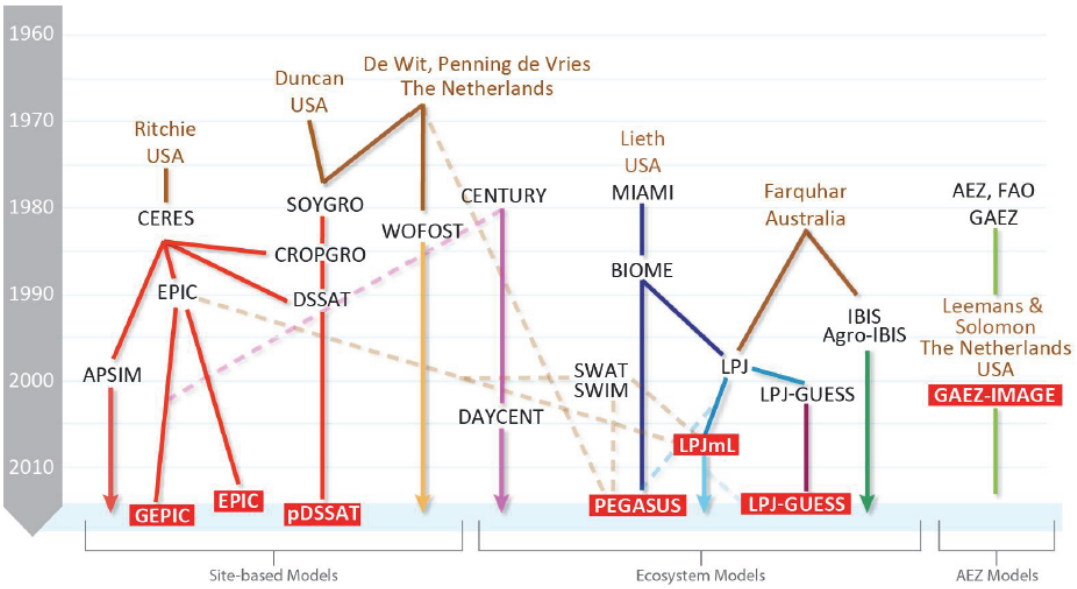

Figure 1.2 evolution of some crop models (Rosenzweig et al., 2014)

Researchers have realized the difficult in applying the site-scale model at regional and global scales (Challinor et al., 2009), at which climate change impacts and economy models have to operate. The other generation of crop models was thus developed to explore large scale crop-climate relationships, such as IMAGE (Leeman & Solomon, 1993). These model typically divide the globe into several agro-ecological zones. Empirical relationship between climate and yield was then built usually with agro-statistics. Some selective process may also be incorporated into these models for model improvements, such as

GLAM (Challinor et al., 2004). Compared with traditional crop models mentioned in previous paragraph, these models have far less input requirements and parameters and low requirement of computing resources, which facilitates large-scale applications. However, its empirical nature may hurdle further exploration on how management practices may affect the croplands' response to climate change (Challinor et al., 2004). When climate change beyond its contemporary range of variations (Mora et al., 2013), it is hard to prove whether the contemporary empirical relationship may still apply. Similar issues also apply for different types of statistical models (e.g. Lobell et al., 2011).

Compared with previously mentioned models, terrestrial ecosystem models have more physiology-based formulations. However, previous studies often neglect or simplified representation of crop ecosystems (e.g.Piao et al., 2009). The simplified module cannot represent the generally short growth duration of crops (Smith et al., 2010) and different allocation strategy of croplands than natural ecosystems (Bondeau et al., 2007). All earth system models in CMIP5 did not include a specific crop module. As croplands role in global biogeochemical cycle being gradually brought more attentions, there are some efforts introducing crop modules into the ecosystem models (Drewniak et al., 2013). For example, Kucharik (2003) bring crop phenology, irrigation and fertilization module into IBIS model, resulting in better representation of spatio-temporal variations of maize yield over US due to climate and management differences (Kucharik, 2003; Kucharik, 2008). Levis et al. (2012) bring Agro-IBIS into community land model, finding improved representation of dynamics in leaf area index (LAI), net ecosystem exchange and thus seasonal variations of atmospheric CO_2 concentration. Bondeau et al. (2007) introduce crop functional type to LPJ. The improved LPJmL model, though only introduce improvements of phenology at that time, simulated 24% less global vegetation carbon pool than original LPJ model and produce significant difference in spatio-temporal variations of net primary productivity. Similarly, ORCHIDEE has also tried to introduce STICS model for simulating crop phenology, finding the model become better representing interannual variations of LAI and net primary production. Overall, the introduction of crop module can improve ecosystem models in representing spatio-temporal variations of cropland ecosystems, making it an alternative choice to study regional and global croplands, how they may respond to climate change.

Despite the large differences in the complexity of introduced crop module, the agro-ecosystem models still have limitations in representing the crop growth dynamics, such as the morphology of crop organs, the grain quality, and the lack of nutrient cycling, particularly for micro-nutrients such as potassium. In addition, the process-based ecosystem models usually requires larger amount of computational resources following the same protocol of simulations. The consumption of computing resource by ORCHIDEE-crop is one magnitude larger than that required by pDSSAT and pAPSIM (Elliot & Wang, personal communication). It becomes a bottleneck for the application of agro-ecosystem models, though increasing computing power globally may gradually alleviate the pressure.

The Global Gridded Crop Model Inter-comparison (GGCMI) project brought different types of crop models together to perform simulations forced with consistent climate and management forcing (Elliot et al., 2015). This ongoing global effort will help us further understand the advantage and disadvantage of different crop models and reduce large uncertainties in estimating crop yield response to climate change at global and regional scale.

1.3 Objectives and structure of this thesis

The general goal of this PhD thesis is to describe the efforts using both statistical tools and processed based crop models to 1) detect climate change impacts on crop phenology and yield, identifying key climatic factors regulating crop yield variations and estimating the temperature sensitivity of crop yield, and 2) attribute the crop yield change to climate and management factors, at regional and global scale.

In Chapter 2, I built statistical models using yield statistics at prefecture scale during the past three decades over Northeast China, along with contemporary historical climate data, to explore the yield-climate relationship and its spatial variations. In addition, I explored how climate-yield relationship evolve along the climate gradient.

In Chapter 3, I developed a Bayes-based parameterization system to optimized parameters of ORCHIDEE-crop model to represent the spatio-temporal variations of rice

growing season duration during past three decades over China. The carlibrated ORCHIDEE-crop model is then driven by historical change in climate and management in order to attribute observed change in China's rice phenology.

In Chapter 4, An emergent constraint framework was built to integrate global gridded crop models and field warming experiments in order to reanalyze and refine global crop yield response to warmer temperature. The implications for crop yield change under climate change goal of Paris Agreement and data and knowledge gap for reducing uncertainties are explored.

In Chapter 5, Using global gridded crop models and data-driven model for global rainfed and irrigated crop yield, I applied Bayesian model average to reanalyze potential contribution of irrigation to global crop yield. Based on the reanalysis, the supply-demand balance of irrigation water demand and surface runoff supply was also analyzed.

In Chapter 6, I summarized the findings of previous chapters. Implications of the studies on ongoing development of ORCHIDEE-crop model and the IPSL earth system model are explored and discussed.

References

Ainsworth EA, Rogers A, Nelson R, et al. (2004) Testing the "source–sink" hypothesis of down-regulation of photosynthesis in elevated CO_2 in the field with single gene substitutions in Glycine max. Agricultural and Forest Meteorology, 122, 85-94.

Ainsworth EA & Long SP (2005) What have we learned from 15 years of free-air CO_2 enrichment (FACE)? A meta-analytic review of the responses of photosynthesis, canopy properties and plant production to rising CO_2. New Phytologist, 165, 351-372.

Asseng S, Foster IAN & Turner NC. (2011) The impact of temperature variability on wheat yields. Global Change Biology, 17, 997-1012.

Asseng S, Ewert F, Martre P et al. (2015) Rising temperatures reduce global wheat production. Nature Climate Change, 5, 143-147.

Ben-Asher J, Garcia AGY, Hoogenboom G. (2008) Effect of high temperature on photosynthesis and transpiration of sweet corn (Zea mays L. var. rugosa). Photosynthetica, 46 (4): 595-603.

Bernacchi CJ, Pimentel C & Long SP (2003) In vivo temperature response functions of parameters required to model RuBP-limited photosynthesis. Plant, Cell & Environment,

26, 1419-1430.
Bernacchi CJ, Kimball BA, Quarles DR, et al. (2007) Decreases in stomatal conductance of soybean under open-air elevation of CO_2 are closely coupled with decreases in ecosystem evapotranspiration. Plant Physiology, 143, 134-144.
Bondeau A, Smith PC, Zaehle S, et al. (2007) Modelling the role of agriculture for the 20th century global terrestrial carbon balance. Global Change Biology, 13, 679-706.
Boote KJ, Jones JW & Hoogenboom G (1998) Simulation of crop growth: CROPGRO model.
Bouman BAM, van Laar HH (2006) Description and evaluation of the rice growth model ORYZA2000 under nitrogen-limited conditions. Agricultural Systems, 87, 249–273 (doi: 10.1016/j.agsy.2004.09.011)
Brisson N & Delecolle R (1991) Developpement et modeles de simulation de culture. Agronomie, 12, 253-263
Brisson N, Gary C, Justes E, et al. (2003) An overview of the crop model stics. European Journal of Agronomy, 18, 309-332.
Brisson N, Beaudoin N & Mary B (2008) Conceptual basis, formalisations and parameterization of the STICS crop model, Editions Quae.
Burkart S, Manderscheid R, Wittich KP, et al. (2011) Elevated CO_2 effects on canopy and soil water flux parameters measured using a large chamber in crops grown with free-air CO_2 enrichment. Plant Biology, 13, 258-269.
Challinor AJ, Wheeler TR, Craufurd PQ, et al. (2004) Design and optimisation of a large-area process-based model for annual crops. Agricultural and Forest Meteorology, 124, 99-120.
Challinor AJ & Wheeler TR (2008) Use of a crop model ensemble to quantify CO_2 stimulation of water-stressed and well-watered crops. Agricultural and Forest Meteorology, 148, 1062-1077.
Craufurd PQ & Wheeler TR (2009) Climate change and the flowering time of annual crops. Journal of Experimental Botany, 60, 2529-2539.
De Wit CT (1965) Photo synthesis of leaf canopies. Agricultural Research Report, 663, 1-56.
Deryng D, Sacks WJ, Barford CC, et al. (2011) Simulating the effects of climate and agricultural management practices on global crop yield. Global Biogeochemical Cycles, 25(2).
Drewniak B, Song J, Prell J, et al. (2013) Modeling agriculture in the Community Land Model. Geoscientific. Model Development, 6, 495-515.
Duncan WG, Loomis RS, Williams WA, et al. (1967) A model for simulating photosynthesis in plant communities. Hilgardia, 38: 181-205.
Elliott J, Deryng D, Müller C, et al. (2014) Constraints and potentials of future irrigation water availability on agricultural production under climate change. Proceedings of the National Academy of Sciences, 111, 3239-3244.
Elliott J, Müller C, Deryng D, et al. (2015) The Global Gridded Crop Model

Intercomparison: data and modeling protocols for Phase 1 (v1.0). Geoscientific Model Development, 8, 261-277.

Espe MB, Hill JE, Hijmans RJ *et al.* (2017) Point stresses during reproductive stage rather than warming seasonal temperature determine yield in temperate rice. *Glob Chang Biol,* 23, 4386-4395.

FAO (2012) World Agriculture Towards 2030-2050, Agricultural Development Economics Division, Food and Agriculture Organization of the United Nations.

Farquhar GD & Sharkey TD (1982) Stomatal conductance and photosynthesis. Annual Review of Plant Physiology and Plant Molecular Biology, 33, 317-345.

Foley JA, DeFries R, Asner GP, et al. (2005) Global consequences of land use. Science, 309, 570-574.

Garonna I, de Jong R, de Wit AJ, et al. (2014) Strong contribution of autumn phenology to changes in satellite-derived growing season length estimates across Europe (1982-2011). Global Change Biology, 20, 3457-70.

Gerten D, Heinke J, Hoff H, et al. (2011) Global water availability and requirements for future food production. Journal of Hydrometeorology, 12, 885-899.

Giannakopoulos C, Le Sager P, Bindi M, et al. (2009) Climatic changes and associated impacts in the Mediterranean resulting from global warming. Global Planet Change, 68, 209–224.

Gray JM, Frolking S, Kort EA, et al. (2014) Direct human influence on atmospheric CO_2 seasonality from increased cropland productivity. Nature, 515, 398-401.

Godfray HCJ, Beddington JR, Crute IR et al. (2010) Food security: The challenge of feeding 9 billion people. Science, 327, 812-818.

Guo R, Lin Z, Mo X. et al. (2010) Responses of crop yield and water use efficiency to climate change in the North China Plain. Agricultural Water Management, 97, 1185-1194.

Hatfield JL (2011) Climate Impacts on Agriculture: Implications for Crop Production. *Agronomy Journal,* 103, 351-370.

Hoff H, Falkenmark M, Gerten D, et al. (2010) Greening the global water system. Journal of Hydrology, 384, 177-186.

Horie T, Nakagawa H, Centeno HGS, Kropff MJ (1995) The rice crop simulation model SIMRIW and its testing. In: Modeling the impact of climate change on rice production in Asia (eds Matthews RB, Kropff MJ, Bachelet D, et al.), pp. 51–56. Wallingford, Oxon, UK: CAB International in association with International Rice Research Institute.

Huang Y, Yu Y, Zhang W, et al. (2009) Agro-C: A biogeophysical model for simulating the carbon budget of agroecosystems. Agricultural and Forest Meteorology, 149, 106-129.

IPCC (2013a) Food security and food production systems. in Climate Change 2014: Impacts, Adaptation and Vulnerability (eds Field CB, Barros VR, Dokken DJ, et al.). Cambridge University Press, Cambridge, United Kingdom and New York, NY, USA, pp. 485-533.

IPCC (2013b) Climate Change 2013: The Physical Science Basis. Contribution of Working Group I to the Fifth Assessment Report of the Intergovernmental Panel on Climate Change (Cambridge University Press, Cambridge, 2013).

Iqbal J, Hu R, Lin S, et al. (2009) CO_2 emission in a subtropical red paddy soil (Ultisol) as affected by straw and N-fertilizer applications: A case study in Southern China. Agriculture, Ecosystems & Environment, 131, 292-302.

Ko J, Ahuja L, Kimball B, et al. (2010) Simulation of free air CO_2 enriched wheat growth and interactions with water, nitrogen, and temperature. Agricultural and Forest Meteorology, 150, 1331-1346.

Kucharik CJ (2003) Evaluation of a process-based Agro-Ecosystem model (Agro-IBIS) across the U.S. corn belt: Simulations of the interannual variability in maize yield. Earth Interactions, 7, 1-33.

Kucharik CJ (2008) Contribution of planting date trends to increased maize yields in the central United States all rights reserved. No part of this periodical may be reproduced or transmitted in any form or by any means, electronic or mechanical, including photocopying, recording, or any information storage and retrieval system, without permission in writing from the publisher. Agronomy Journal, 100, 328-336.

Leemans R & Solomon AM (1993) Modeling the potential change in yield and distribution of the earth's crops under a warmed climate. Climate Research, 3, 79-96.

Leakey AD, Uribelarrea M, Ainsworth EA, et al. (2006) Photosynthesis, productivity, and yield of maize are not affected by open-air elevation of CO_2 concentration in the absence of drought. Plant Physiology, 140, 779-790.

Lesk C, Rowhani P, Ramankutty N (2016) Influence of extreme weather disasters on global crop production. *Nature,* 529, 84-87.

Li T, Hasegawa T, Yin X, et al. (2015) Uncertainties in predicting rice yield by current crop models under a wide range of climatic conditions. Global Change Biology, 21, 1328-1341.

Li Z, Yang P, Tang H, et al. (2014) Response of maize phenology to climate warming in Northeast China between 1990 and 2012. Regional Environmental Change, 14, 39-48.

Lin E, Xiong W, Ju H, et al. (2005) Climate change impacts on crop yield and quality with CO_2 fertilization in China. Philosophical Transactions of the Royal Society B: Biological Sciences, 360, 2149-2154.

Liu L, Wang E, Zhu Y, et al. (2012) Contrasting effects of warming and autonomous breeding on single-rice productivity in China. Agriculture, Ecosystems & Environment, 149, 20-29.

Lobell DB, Schlenker W & Costa-Roberts J (2011) Climate trends and global crop production since 1980. Science, 333, 616-20.

Lobell DB, Bonfils CJ, Kueppers LM, et al. (2008) Irrigation cooling effect on temperature and heat index extremes. Geophysical Research Letters, 35, L09705.

Lobell DB & Gourdji SM (2012a) The influence of climate change on global crop productivity. Plant Physiology, 160, 1686-1697.

Lobell DB, Sibley A & Ivan Ortiz-Monasterio J (2012b) Extreme heat effects on wheat senescence in India. Nature Climate Change, 2, 186-189.

Lobell DB, Hammer GL, McLean G, et al. (2013) The critical role of extreme heat for maize production in the United States. Nature Climate Change, 3, 497-501.

Martre P, Wallach D, Asseng S, et al. (2015) Multimodel ensembles of wheat growth: Many models are better than one. Global Change Biology, 21, 911-925.

Menzel A, Sparks TH, Estrella N, et al. (2006) European phenological response to climate change matches the warming pattern. Global Change Biology, 12, 1969-1976.

Mora C, Frazier AG, Longman RJ, et al. (2013) The projected timing of climate departure from recent variability. Nature, 502, 183-187.

Muchow RC, Sinclair TR & Bennett JM (1990) Temperature and solar radiation effects on potential maize yield across locations. Agronomy Journal, 338-343.

Peng SB, Huang JL, Sheehy JE, et al. (2004) Rice yields decline with higher night temperature from global warming. Proceedings of the National Academy of Sciences of the United States of America, 101, 9971-9975.

Piao S, Cui M, Chen A, et al. (2011) Altitude and temperature dependence of change in the spring vegetation green-up date from 1982 to 2006 in the Qinghai-Xizang Plateau. Agricultural and Forest Meteorology, 151, 1599-1608.

Piao S, Ciais P, Friedlingstein P, et al. (2009) Spatiotemporal patterns of terrestrial carbon cycle during the 20th century. Global Biogeochemical Cycles, 23, GB4026.

Porter JR & Semenov MA (2005) Crop responses to climatic variation. Philosophical Transactions of the Royal Society B: Biological Sciences, 360, 2021-2035.

Priestley CHB & Taylor RJ (1972) On the assessment of surface heat flux and evaporation using large-scale parameters. Monthly Weather Review, 100, 81-82.

Ramankutty N, Evan AT, Monfreda C, et al. (2008) Farming the planet: 1. Geographic distribution of global agricultural lands in the year 2000. Global Biogeochemical Cycles, 22, GB1003.

Reddy VR, Reddy KR & Hodges HF (1995) Carbon dioxide enrichment and temperature effects on cotton canopy photosynthesis, transpiration, and water-use efficiency. Field Crops Research, 41, 13-23.

Ritchie JT & Otter S (1985) Description and performance of CERES Wheat: A user oriented wheat yield model. Willis W O. ARS wheat yield project. US: USDA-ARS, ARS238, 159-175.

Richter GM & Semenov MA (2005) Modelling impacts of climate change on wheat yields in England and Wales: assessing drought risks. Agricultural Systems, 84, 77-97.

Rosenzweig C, Jones JW, Hatfield JL, et al. (2013) The Agricultural Model Intercomparison and Improvement Project (AgMIP): Protocols and pilot studies. Agricultural and Forest Meteorology, 170, 166-182.

Rosenzweig C, Elliott J, Deryng D, et al. (2014) Assessing agricultural risks of climate change in the 21st century in a global gridded crop model intercomparison. Proceedings of the National Academy of Sciences of the United States of America, 111,

3268-3273.
Sánchez B, Rasmussen A & Porter JR (2014) Temperatures and the growth and development of maize and rice: a review. Global Change Biology, 20, 408-417.
Schar C *et al.* (2004) The role of increasing temperature variability in European summer heatwaves. In: *Nature.* pp Page, Nature Publishing Group.
Shiklomanov IA & Rodda JC (2003) World water resources at the beginning of the 21st century. International Hydrology Series (Cambridge Univ Press, Cambridge, UK).
Siebert S & Ewert F (2012) Spatio-temporal patterns of phenological development in Germany in relation to temperature and day length. Agricultural and Forest Meteorology, 152, 44-57.
Smith PC, De Noblet-Ducoudré N, Ciais P, et al. (2010) European-wide simulations of croplands using an improved terrestrial biosphere model: Phenology and productivity. Journal of Geophysical Research, 115, G01014.
Soussana JF, Graux AI & Tubiello FN (2010) Improving the use of modelling for projections of climate change impacts on crops and pastures. Journal of Experimental Botany, 61, 2217-2228.
Tao F, Yokozawa M, Xu Y, et al. (2006) Climate changes and trends in phenology and yields of field crops in China, 1981-2000. Agricultural and Forest Meteorology, 138, 82-92.
Tao F, Yokozawa M, Liu J, et al. (2008) Climate-crop yield relationships at provincial scales in China and the impacts of recent climate trends. Climate Research, 38, 83-94.
Tao F, Zhang Z, Zhang S, et al. (2012) Response of crop yields to climate trends since 1980 in China. Climate Research, 54, 233-247.
Tao F & Zhang Z (2012) Climate change, high-temperature stress, rice productivity, and water use in Eastern China: A new superensemble-based probabilistic projection. Journal of Applied Meteorology and Climatology, 52, 531-551.
Tao F, Zhang Z, Shi W, et al. (2013) Single rice growth period was prolonged by cultivars shifts, but yield was damaged by climate change during 1981-2009 in China, and late rice was just opposite. Global Chang Biology, 19, 3200-9.
Teixeira EI, Fischer G, Van Velthuizen H, Walter C, Ewert F (2013) Global hot-spots of heat stress on agricultural crops due to climate change. *Agricultural And Forest Meteorology,* 170, 206-215.
Tian H, Lu C, Ciais P *et al.* (2016) The terrestrial biosphere as a net source of greenhouse gases to the atmosphere. *Nature,* 531, 225-228.
Tilman D, Balzer C, Hill J, et al. (2011) Global food demand and the sustainable intensification of agriculture. Proceedings of the National Academy of Sciences, 108, 20260-20264.
Tubiello FN, Soussana JF & Howden SM (2007) Crop and pasture response to climate change. Proceedings of the National Academy of Sciences, 104, 19686-19690.
United Nations. 2012. World population prospects: The 2012 revision.
Vautard R, Cattiaux J, Yiou P, et al. (2010) Northern Hemisphere atmospheric stilling partly attributed to an increase in surface roughness. Nature Geoscience, 3, 756-761.

Wan S, Xia J, Liu W, et al. (2009) Photosynthetic overcompensation under nocturnal warming enhances grassland carbon sequestration. Ecology, 90, 2700-2710.

Wang H, Prentice IC & Ni J (2012) Primary production in forests and grasslands of China: contrasting environmental responses of light- and water-use efficiency models. Biogeosciences, 9, 4689-4705.

Wang XH, Piao SL, Xu XT, Ciais P, Macbean N, Myneni RB, Li L (2015) Has the advancing onset of spring vegetation green-up slowed down or changed abruptly over the last three decades? *Global Ecology And Biogeography,* 24, 621-631.

Welch JR, Vincent JR, Auffhammer M, et al. (2010) Rice yields in tropical/subtropical Asia exhibit large but opposing sensitivities to minimum and maximum temperatures. Proceedings of the National Academy of Sciences, 107, 14562-14567.

Xiao D, Tao F, Liu Y, et al. (2013) Observed changes in winter wheat phenology in the North China Plain for 1981-2009. International Journal of Biometeorology, 57, 275-285.

Wild M, Gilgen H, Roesch A, et al. (2005) From dimming to brightening: Decadal changes in solar radiation at earth's surface. Science, 308, 847-850.

Xiong W, Conway D, Lin E, et al. (2009) Potential impacts of climate change and climate variability on China's rice yield and production. Climate Research, 40, 23-35.

Xiong W, Lin E, Ju H, et al. (2007) Climate change and critical thresholds in China’s food security. Climatic Change, 81, 205-221.

Yao F, Xu Y, Lin E, et al. (2007) Assessing the impacts of climate change on rice yields in the main rice areas of China. Climatic Change, 80, 395-409.

Zeng N, Zhao F, Collatz GJ, et al. (2014) Agricultural green revolution as a driver of increasing atmospheric CO_2 seasonal amplitude. Nature, 515, 394-397.

Zhang T, Zhu J & Wassmann R (2010) Responses of rice yields to recent climate change in China: An empirical assessment based on long-term observations at different spatial scales (1981–2005). Agricultural and Forest Meteorology, 150, 1128-1137.

Chapter 2 Detecting climate change impacts on maize yield in Northeast China

Summary

Northeast China (NEC), the most productive maize growing area in China, has experienced pronounced climate change. However, the impacts of historical climate changes on maize production and their spatial variations remain uncertain. In this study, we used yield statistics at prefecture scale over the past three decades, along with contemporary climate data, to explore the yield-climate relationship and its spatial variations. At the regional scale, maximum and minimum temperature changes had opposite impacts on maize yield, which increased by 10.0±7.7% in response to a 1 ºC increase in growing season mean daily minimum temperature (*Tmin*), but decreased by 13.4±7.1% in response to a 1 ºC increase in growing season mean daily maximum temperature (*Tmax*). Variations in precipitation seemed to have small impacts on the maize yield variations (-0.9±5.2 %/100mm). However, these responses of maize yield to climate variations were subject to large spatial differences in terms of both the sign and the magnitude. ~30% of the prefectures showed a positive response of maize yield to rising *Tmax*, which was in contrast to the negative response at the regional scale. Our results further indicate that the spatial variations in the yield response to climate change can be partly explained by variations in local climate conditions. The growing season mean temperature was significantly correlated with the response of maize yield to *Tmax* ($R=-0.67$, $P<0.01$), which changes from positive to negative when the growing season mean temperature exceeds 17.9±0.2 ºC. Precipitation became the dominant climatic factor driving maize yield variations when growing season precipitation was lower than ~400 mm, but had a weaker influence than temperature over most of the study area. We conclude that, although NEC is a region spanning only one more millions of kilometer squares, the divergence of the yield response to climatic variations highlights the need to analyze the yield-climate relationship at fine spatial scales. This chapter has been published as Wang X *et al.* (2014) Divergence of climate impacts on maize yield in Northeast China. *Agriculture, Ecosystems & Environment,* **196**, 51-58.

1. Introduction

Understanding how climate change has been affecting crop production is a prerequisite to ensure global food security and to inform adaptation decisions (IPCC, 2007; Schmidhuber and Tubiello, 2007; Godfray, 2011). Both modeling and empirical studies have indicated that maize yield is negatively affected by climate change at the global scale (IPCC, 2007; Lobell et al., 2011). However, global analyses could have hidden regional winners and losers (Godfray et al., 2010). Detailed regional analyses are thus required to explore possible mechanisms for the spatial differences in impacts of climate change on maize yield.

Maize is one of the staple food crops in China, which is currently the world's second largest maize producer (Meng et al., 2006). Although maize is cultivated in every province in China, the three provinces in Northeast China (NEC) alone account for more than 30% of China's maize production and 27% of its maize growing area (National Bureau of Statistics in China (NBSC), 2011). Part of this region is also the most productive maize growing area in China, known as the golden maize belt. Over the past decades, NEC has experienced faster warming than the lower latitudes of China, along with pronounced precipitation changes (Piao et al., 2010; Editorial Board of National Climate Change Assessment Report (EBNCCAR), 2011). Understanding how this historical climate change could have influenced maize production in NEC is thus critical to China's food production and to decisions on climate change mitigation.

A variety of approaches, including statistical analyses and crop models, have been used to explore the influence of climate change on maize production in NEC (e.g. Xiong et al., 2007; Tao et al., 2008; Chen et al., 2011; Liu et al., 2012; Zhang and Huang, 2012). The estimates of the response of maize yield to climate change are, however, largely uncertain as they differ even in their signs. Some modeling studies (Xiong et al., 2007; Liu et al., 2012) indicate that warming, in particular an increase in maximum temperature, could reduce maize yield in NEC. For example, simulations by Liu *et al.* (2012) showed that a 1 ^{o}C warming in maximum temperature would reduce maize yield by 2 – 9% at different sites in NEC. On the contrary, another analysis indicated that 1 ^{o}C warming could improve maize yield by more than 20% in parts of NEC (Wang et al., 2007), which is in line with some

other studies indicating warming has benefited maize yield in NEC (EBNCCAR, 2011; Chen et al., 2011). Consequently, more empirical evidence is still needed to reduce the uncertainties in diagnosing and predicting the response of maize yield to climate change.

Empirical yield-climate relationships are often explored with yield statistics at province, county or farm scale (e.g. Tao et al., 2008; Chen et al., 2011; Liu et al., 2012; Zhang et al., 2012). It was found that the response of crop yield to climate change is scale-dependent (Tao et al., 2008; Zhang et al., 2010). As the relationship between maize yield and climate at prefecture scale has not yet been explored, it is of need to fill this gap. Moreover, a prefecture in NEC usually spans a relatively homogeneous geographic area from ~5 to ~54 thousand km^2, covering a few grids of the high-resolution gridded climate dataset (Mitchell & Jones, 2005). The match of scale in statistics and climate data makes it suitable to explore yield-climate relationship. In addition to the scale issue, previous studies show large spatial variations in the response of crop yield to climate change (e.g. Tao et al., 2008; Chen et al., 2011), but these differences often remain unexplained or qualitatively attributed to regional differences in crop management, soils, crop varieties and other factors (e.g. Tao et al., 2008; Lobell et al., 2008). Hence, in this study, we analyzed both the yield-climate relationship and its spatial variations over 36 prefectures in NEC during 1980-2009. The objectives of this study were (1) to understand how maize yield, at regional and prefecture scale, has responded to historical climate change over the past three decades, and (2) to explore whether spatial variations in these responses can be explained by differences in local climate conditions.

2. Datasets and Methods

2.1 Study Area

Northeast China (NEC) is located in northernmost China (38ºN-54ºN) (Figure 1). It has a cool summer (mean June-August temperature 20 ºC) and long winter (five months), which results in a short thermal growing season (May - September) that only allows single cropping. As Figure 2a shows, the mean growing season temperature in maize planting areas generally follows a latitudinal gradient from 10 ºC in the north to 22 ºC in the south, except for some high-altitude mountainous areas (Daxing'anling, Xiaoxing'anling and Changbai mountain range) which are cooler than other regions on the same latitude. The growing season precipitation exhibits a southeast-northwest gradient, decreasing from more

than 800 mm to less than 400 mm (Figure 2b).

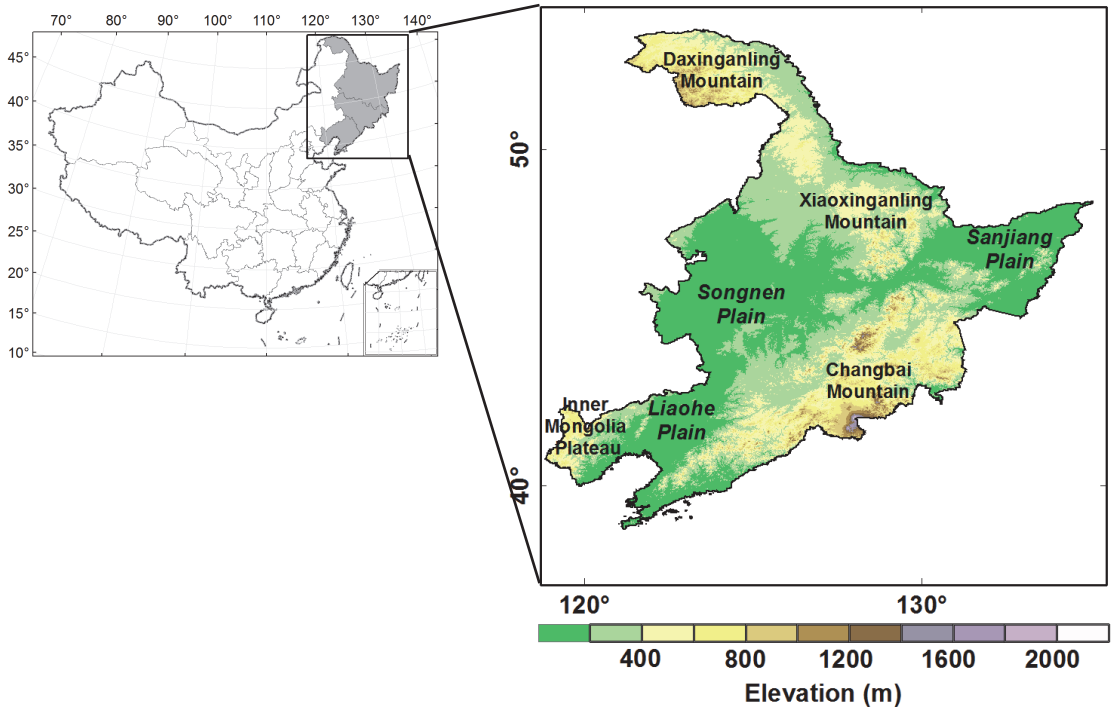

Figure 1. Geographic location of Northeast China (NEC) and spatial distribution of the elevation over NEC.

The prefecture is a mid-level administration that is part of a province and containing several counties. The NEC is comprised of 36 prefectures with their area range from 4.8×10^3 km^2 (Liaoyang) to 5.44×10^4 km^2 (Heihe).

Maize is widely cultivated in NEC (Figure 2c). The total maize growing area is about 6 million hectares. The average yield is about 5000 kg/ha, ranging from 3575 to 9051 kg/ha among different prefectures with warmer area tending to have larger yield (Figure S2). The most productive area concentrated in Songliao Plain (Figure 2d).More than 90% of the maize fields over this region is rainfed (NBSC, 2011), with average precipitation more than 300mm during the maize growing season (Figure S2).

2.2 Datasets

Yield statistics for each prefecture area and in each province were obtained from the Agricultural Yearbook (1980-2009) of Liaoning Province, Jilin Province, and Heilongjiang Province, the three provinces comprising NEC (Figure S1), accessed from

http://data.cnki.net. It should be noted that prefecture-level statistics for Heilongjiang during 1980-1985 and for Liaoning during 1980-1991 are not available from the database.

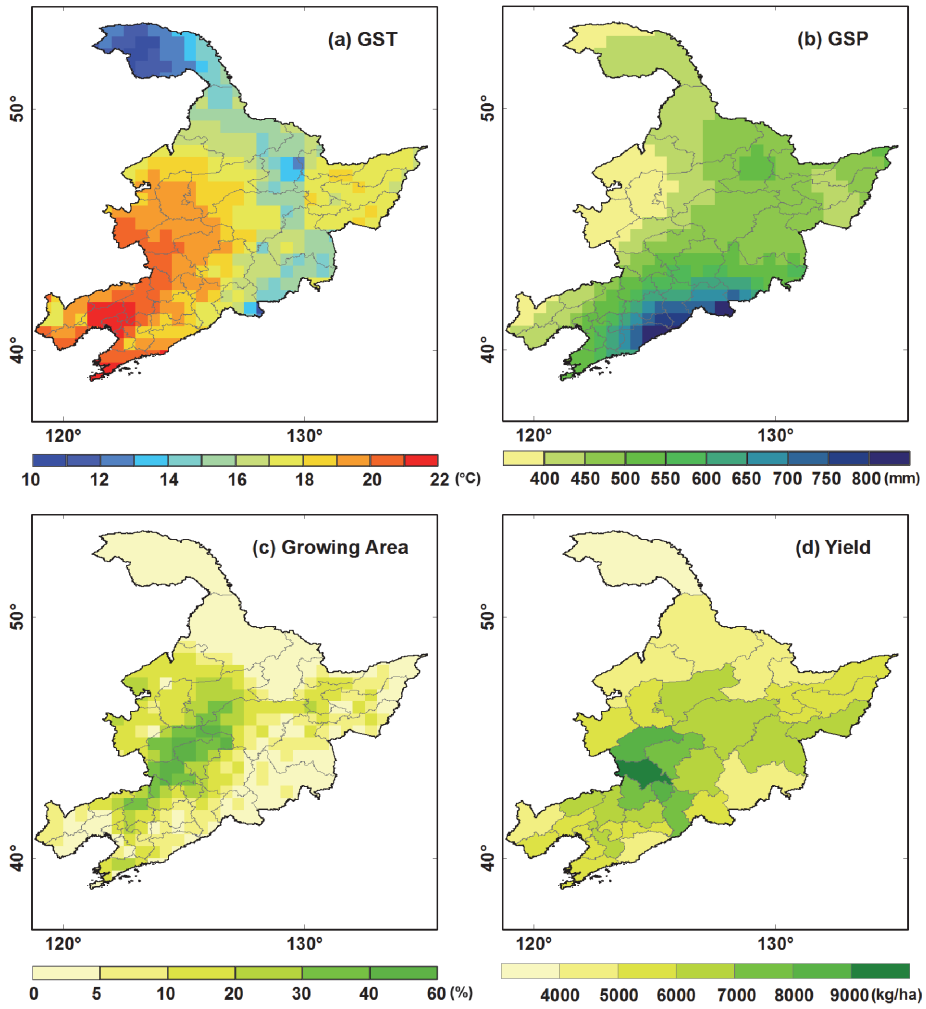

Figure 2. Spatial distribution of (a) mean growing season temperature, (b) growing season precipitation, (c) maize cultivation fraction, and (d) maize yield over NEC during 1980-2009.

Monthly temperature and precipitation data during 1980-2009 were obtained from the Climatic Research Unit (CRU, University of East Anglia), at a spatial resolution of 0.5 degrees (Mitchell and Jones, 2005). We defined the maize growing season as the period from May to September according to the typical cropping system in NEC (Meng et al., 2006). The maize growing area was obtained from the Maps of Cropland Distribution in China (Frolking et al., 2002), which has a spatial resolution of 0.5 degrees.

2.3 Analyses

For each prefecture area, growing season mean daily maximum temperature (*Tmax*), growing season mean daily minimum temperature (*Tmin*) and growing season precipitation (*Pre*) were calculated as the maize growing area weighted averages during May-September each year.

To explore the relationship between variations in yield and climate, our analyses were based on the first difference time series of the maize yield and climate variables, which is a commonly applied approach to minimize the influence of slowly varying factors such as changes in crop management and varieties (Nicholls, 1997; Lobell and Field, 2007; Tao et al., 2008). The first difference time series of maize yield, *Tmax, Tmin* and *Pre* are denoted hereafter as *Δyield, ΔTmax*, *ΔTmin* and *ΔPre,* respectively. Pearson correlation and partial correlation analyses were applied to measure the relationships between maize yield and climate variables. P = 0.10 was chosen *a priori* as the significance level for statistical tests, which was intended to reduce the risk of Type II error. Multiple linear regression (Eq. 1) was applied to calculate the response of maize yield to climate change:

$$\Delta yield = a\Delta Tmax + b\Delta Tmin + c\Delta Pre + I + \varepsilon \qquad \text{(Eq. 1)}$$

where *a, b* and *c* are the response of maize yield to change in *Tmax*, *Tmin* and *Pre*, respectively. *I* is the intercept of the regression, and ε is the residual.

The covariations between climate variables have long been recognized but remain a challenge in understanding the yield-climate relationship (Evans and De Datta, 1979; Sheehy et al., 2006). Our multiple regression approach was considered to be capable of minimizing the impacts of the covariations, in order to obtain reasonable estimates of the climate impacts on the yield (Welch et al., 2010).

The changing maize varieties could also contribute to the variations in *Δyield*, but we do not include the varieties in the equation because we do not have access to year-to-year variations on maize varieties applied in each prefecture area. However, this should have limited impacts on our analyses since a recent study indicated the climate sensitivity for some physiological parameters seems to be invariant between different varieties (Parent and Tardieu, 2012).

3. Results and Discussion

3.1 Regional scale maize yield-climate relationships

At a regional scale, the maize yield over NEC showed large year-to-year variations (the SD for *Δyield* is 946 kg ha^{-1}). The variations in maize yield were significantly negatively correlated with *ΔTmax* (R=-0.35, P=0.07), but only weakly correlated with *ΔPre* (R=0.24, P=0.21) and *ΔTmin* (R=-0.004, P=0.99) (Figure 3). Previous studies have shown the importance of understanding the correlation structure among climate variables in order to avoid misinterpretation of the yield-climate relationship (Sheehy et al., 2006; Welch et al., 2010). To minimize the influence of the covariation between climate variables, partial correlations and multiple regressions were applied in the following analyses (see Methods; Lobell and Field, 2007).

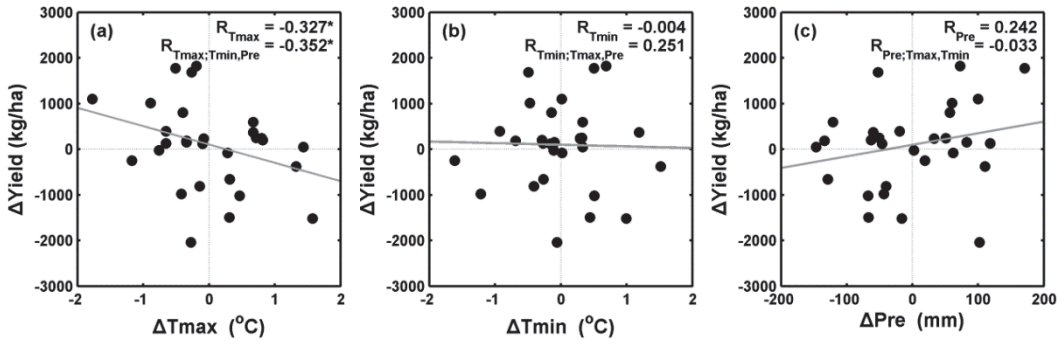

Figure 3. Relationship of variations in maize yield (*Δyield*) with variations in (a) growing season mean daily maximum temperature (*ΔTmax*), (b) growing season mean daily minimum temperatures (*ΔTmin*), and (c) growing season precipitation (*ΔPre*) over NEC during 1980-2009. Labels within the panel show correlation and partial correlation coefficients. The asterisk indicates statistically significant correlation at the 0.10 level. Solid grey lines show least squares linear fits.

Partial correlation between *Δyield* and *ΔTmax* (statistically controlling variations in *ΔTmin* and *ΔPre*) (R=-0.35, P=0.07) was stronger than that between any other pairs of candidate climate variables, indicating that *Tmax* was the dominant climatic factor at the regional scale. The multiple regression analysis showed that maize yield will decrease by 13.4±7.1% in response to a 1 °C increase in *Tmax*, which is consistent with previous estimates at provincial scales of between -5% °C^{-1} and -15% °C^{-1} (Tao et al., 2008). At the

same time, the opposite response of *Δyield* to *ΔTmin* was found, with a magnitude of 8.6±9.2% $^{o}C^{-1}$.

It should be noted that variations in the climatic variables explained only ~20% of maize yield variations at the regional scale, which indicates that a substantial fraction of the yield variation was not explained by the multiple regression model with regional average climate variations. Those unexplained yield variations might have been associated with changes in socioeconomic conditions that could have influenced crop management (Lobell and Field, 2007) or with the spatial differences in yield response to climate variations, which are explored below.

3.2 Spatial patterns of climate-maize yield relationships

3.2.1 Spatial pattern of the Tmax-maize yield relationship

There were large spatial differences in the relationship between *Δyield* and *ΔTmax.* About 70% of the prefectures showed negative partial correlation between *Δyield* and *ΔTmax* (statistically controlling the variations in *ΔTmin* and *ΔPre*) (Figure 1; Figure 4a). The partial correlation between *Δyield* and *ΔTmax* weakened from south to north, and was strongest and most statistically significant ($P<0.10$) in the southern-most Liaohe Plain (including Anshan, Panjin, and Fuxin). In the mountainous area, maize yield generally showed a positive response to *ΔTmax*. The positive partial correlation between *Δyield* and *ΔTmax* was statistically significant ($P<0.10$) in Daxing'anling, Jixi and Qitaihe.

The response of *Δyield* to *ΔTmax*, derived from the multiple regression, ranged from -29.5±15.2 % $^{o}C^{-1}$ to 23.6±9.7 % $^{o}C^{-1}$ in different prefectures. In Figure 4a, we found that the regionally negative responses of *Δyield* to *ΔTmax* were mostly induced by the negative response of *Δyield* to *ΔTmax* over the plain area, since more than 60% of the maize growing area lies in those plains. The strongest negative response was found in Panjin, on the Liaohe Plain (-30% $^{o}C^{-1}$), while the negative response of *Δyield* to *ΔTmax* in the Songnen Plain and Sanjiang Plain was moderate (between -19.9 % $^{o}C^{-1}$ and -0.2 % $^{o}C^{-1}$). A positive response of *Δyield* to *ΔTmax* was found in mountainous areas (Changbai Mountain, Daxing'anling and the edge of the Mongolian Plateau), accounting for about 30% of the prefectures, with the highest response being found in Daxing'anling (23.6±9.7 % $^{o}C^{-1}$).

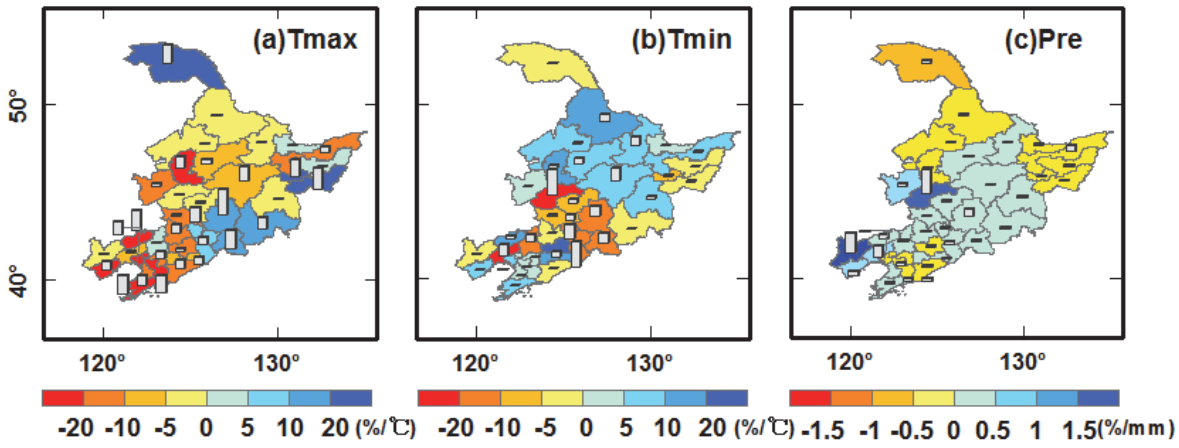

Figure 4. Spatial distribution of the response of *Δyield* to (a) *ΔTmax*, (b) *ΔTmin*, (c) *ΔPre* over each prefecture in NEC during the past three decades**.** The white bars show the coefficient of partial determination (R^2).

Since NEC is a cold temperate region, warming has been thought to reduce the cold damage and lengthen the thermal growing season, and thus benefit maize yield (Wang et al., 2007; Liu and Lin, 2007; IPCC, 2007; EBNCCAR, 2011). However, over the major maize production area in NEC, the prevailing negative response of *Δyield* to *ΔTmax*, which is consistent with previous studies at a provincial scale (Tao et al., 2008; Zhang and Huang, 2012), suggests that increasing daytime temperature has already negatively affected the maize yield. Some modeling studies have suggested that the decrease of maize yield in response to rising maximum temperature was primarily attributed to the acceleration of crop maturation and shortening of crop development duration (Wolf and Van Diepen, 1994; Lin et al., 2005; Xiong et al., 2007). If this was the primary reason for the negative impacts of *ΔTmax* on *Δyield*, we should expect a uniformly negative response of *Δyield* to *ΔTmax* rather than the opposite responses of *Δyield* to *ΔTmax* observed in the plain and in the mountainous areas. Alternatively, previous studies have indicated that maize yield will be lower if exposed more to extreme heat (temperature higher than 30 ºC) (Schlenker and Roberts, 2009; Lobell et al., 2013). We found that this hypothesis could explain the spatial differences in the response of *Δyield* to *ΔTmax*. Over the past three decades, maximum monthly mean *Tmax* in the plain area (such as Shenyang, Jinzhou and Fuxin) has exceeded 30 ºC in 23% of the years, while maximum monthly mean *Tmax* over some mountainous areas, such as Yanbian, Daxing'anling and Yichun, has never reached 30 ºC.

To further explore whether the spatial heterogeneity of the response of *Δyield* to *ΔTmax* could be explained by local climate conditions, we correlated the spatial variations in the response of *Δyield* to *ΔTmax* with spatial variations in mean growing season temperature (GST) and mean growing season precipitation (GSP) (Figures 5a and b). We found that while the spatial gradient of GSP could not explain the variations in the response of *Δyield* to *ΔTmax* (R=-0.01, P=0.95), there was significant negative correlation between GST and the response of *Δyield* to *ΔTmax* (R=-0.67, P<0.001). As GST increased, the response of *Δyield* to *ΔTmax* changed from positive to negative. The threshold of this positive-to-negative transition was about 17.9±0.2 ºC. It is projected that the temperature over NEC will have increased by more than 2ºC by the end of this century under the IPCC A2 scenario (EBNCCAR, 2011). If the relationship between GST and the response of *Δyield* to *ΔTmax* holds true in future, the negative response of *Δyield* to *ΔTmax* would be expected to occur over a larger spatial extent across NEC.

3.2.2 Spatial pattern of the Tmin-maize yield relationship

Figure 4b shows the spatial distribution of the relationship between *Δyield* and *ΔTmin*. In contrast to the relationship between *Δyield* and *ΔTmax*, we found positive partial correlation between *Δyield* and *ΔTmin* in 53% of the prefecture area, including most of the Liaohe Plain, Xiaoxing'anling and northern part of Sanjiang Plain (Figure 4b). The largest response of *Δyield* to *ΔTmin* was found in Fushun (26.6±15.9 % $^{o}C^{-1}$), which was about three times larger than the response of *Δyield* to *ΔTmin* at the regional scale. Such a spatial difference in the sign and magnitude of the response of *Δyield* to *ΔTmin* indicates that regional analyses could have hidden "winners" and "losers" under climate change (Godfray et al., 2010) even in a relatively small region, like NEC.

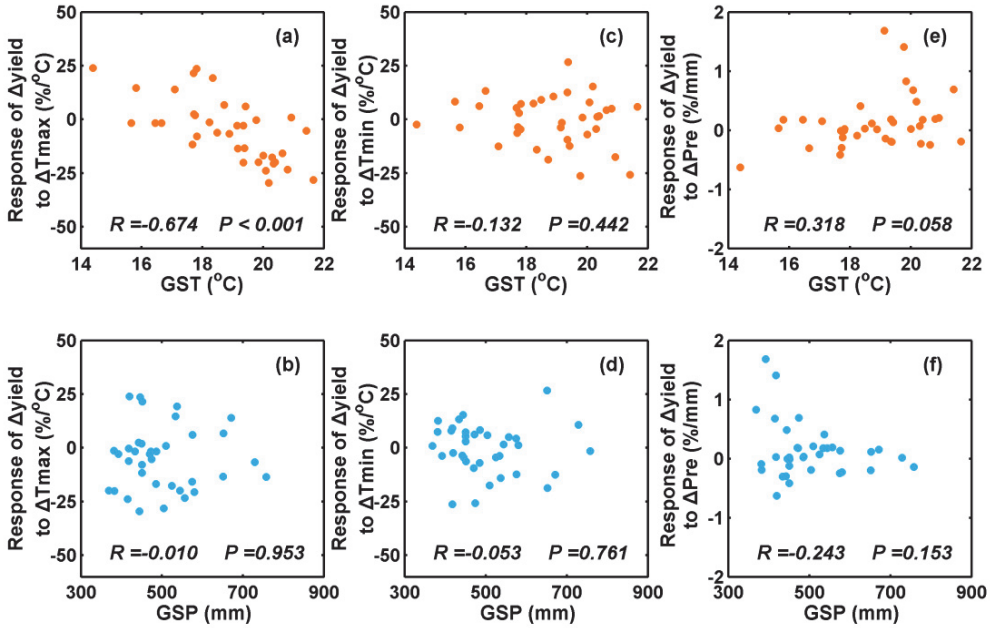

Figure 5. The response of *Δyield* to climate variations at the prefecture scale along the spatial gradient of mean growing season temperature (GST) (upper panels) and growing season precipitation (GSP) (lower panel) during the past three decades. The response of *Δyield* to *ΔTmax* with (a) GST and (b) GSP. The response of *Δyield* to *ΔTmin* with (c) GST and (d) GSP. The response of *Δyield* to *ΔPre* with (e) GST and (f) GSP. Texts show correlation coefficients (R) and their statistical significance (P).

A rising minimum temperature was found to negatively impact the crop yield in tropical and warm temperate regions (Peng et al., 2004; Welch et al., 2010) primarily due to increased respiration cost and reduced grain-filling duration caused by higher nighttime temperatures (Peng et al., 2004; Morita et al., 2005; Prasad et al., 2008; Mohammed and Tarpley, 2009). However, previous studies have shown that a rising minimum temperature could have benefited maize yield in NEC at provincial or regional scales (Tao et al., 2008; Chen et al., 2011; Liu et al., 2012). Such a positive response of maize yield to minimum temperature could be explained by two possible mechanisms. Firstly, although a warmer minimum temperature increases the respiration loss of carbohydrates during nighttime, this "starvation" of carbohydrate could stimulate photosynthesis during the following day (Paul and Foyer, 2001; McCormick et al., 2006). This stimulation of photosynthesis was found to exceed the carbon loss induced by higher nighttime temperatures, thus enhancing the productivity of cold temperate ecosystems (Wan et al., 2009). Secondly, warmer nighttime

temperatures could alleviate cold stress for germination and grain filling and reduce frost occurrence in NEC, where crop growth was thought to be limited by temperature (Chen et al., 2011). Therefore, the response of *Δyield* to *ΔTmin* should depend on the magnitudes of the opposing impacts exerted by rising minimum temperature. The contrary positive and negative impacts may also explain the generally small response of *Δyield* to *ΔTmin* (within ±10% $^{o}C^{-1}$ for 70% of the prefecture areas).

A previous study has indicated that the spatial variations in the sensitivity of *Δyield* to *ΔTmin* could be related to precipitation variations (Liu et al., 2012) at the provincial scale, but our spatial analyses indicated the response of *Δyield* to *ΔTmin* was not significantly correlated with either GST or GSP at prefecture scale (Figure 5c and d).

3.2.3 Spatial pattern of the precipitation-maize yield relationship

The spatial distribution of the relationship between variations in precipitation and variations in maize yield is shown in Figure 4c. Consistent with previous studies (Tao et al., 2008; Chen et al., 2011), variations in precipitation did not exert significant impacts on maize yield over most of NEC (89% of the prefectures). This is not surprising, since NEC in general received abundant precipitation and the evapotranspiration demand is lower than that in other parts of China due to the relatively low temperature (Ma, 1996). However, in the western part of NEC, where precipitation is lower than 400 mm (Figure 2b), there were significant positive correlations between *Δyield* and *ΔPre* in Jinzhou, Songyuan and Chaoyang ($R=0.54$, $P=0.04$, $R=0.73$, $P<0.01$, and $R=0.82$, $P<0.01$, respectively).

Spatial analyses revealed a significant positive correlation between GST and the response of *Δyield* to *ΔPre* ($R=0.32$, $P=0.06$; Figure 5e). This is probably because warmer temperatures could enhance the growth and evaporation demands on soil water (Breshears et al., 2005), and thus result in higher water stress during maize growth (Lobell et al., 2013). The warmer temperature induced water stress may have left precipitation as the limiting climatic factor for maize yield variations, as indicated by the observation that changes in *Δyield* have become more sensitive to changes in *ΔPre*. This highlights the interaction between temperature and precipitation in regulating variations in the maize yield.

As spatial variations in the demand for water could significantly influence the response

of *Δyield* to *ΔPre*, it may be hypothesized that changes in growing season precipitation, which is the major source of water supply to rainfed maize, should also influence the response of *Δyield* to *ΔPre*. Indeed, although the linear relationship between response of *Δyield* to *ΔPre* and GSP is statistically insignificant (P=0.15), there seems to be a nonlinear relationship between these variables (Figure 5e). Piecewise linear regression (Wang et al., 2011) indicated that a critical threshold occurred at about 442 mm. When GSP was below the threshold, the response of *Δyield* to *ΔPre* significantly decreased in response to an increase in GSP (P=0.07), while the response of *Δyield* to *ΔPre* became invariant to changes in GSP when GSP was larger than 442 mm (P=0.75). This critical threshold we detected was similar to that of a previous modeling study (Liu et al., 2012), which suggested that the water deficit should limit the potential yield of maize when precipitation is below 500 mm. It should be noted that our detection of the critical threshold between the response of *Δyield* to *ΔPre* and GSP was strongly affected by the few prefectures showing larger responses of *Δyield* to *ΔPre* than the rest of the study area (Figure 5e). In order to make more reliable projections, further studies based on finer scale data, which have a larger sample size, are needed to test whether the detected critical threshold is robust.

More than 90% of the maize growing area in the region is rainfed (Xiong et al., 2007; NBSC, 2011), and there was low correlation between *Δyield* and *ΔPre* over most of this region, thereby confirming that precipitation was not the limiting factor for maize production in this region over the past three decades. Nevertheless, this does not suggest that precipitation is a negligible factor in predicting future changes in maize yield. With the expansion of the maize growing area into northern and drier parts of this region (Zhang, 2004; Yun et al., 205; Xiong et al., 2007), and because warming induces an increase in drought stress (Breshears et al., 2005; Dai, 2011; Lobell et al., 2013), the role of precipitation could become more critical in the future.

3.2.5 Spatial pattern of the dominant climatic factor for maize yield variations

As shown in Figure 6, temperature variations (including variations in *Tmax* and *Tmin*) were the dominant or co-dominant climatic factors driving the variations in maize yield over most of the area in NEC (27 of 36 prefectures), which is broadly consistent with previous modeling and empirical studies (Tao et al., 2008; Chen et al., 2011; Liu et al., 2012). *Tmin* was the predominant climatic factor in 11 prefectures, mainly located in

Xiaoxing'anling Mountain and the Liaohe Plain, while *Tmax* was the predominant climatic factor in 16 prefectures mainly located in Liaodong Peninsula, Changbai Mountain and Daxing'anling Mountain. However, there were also some areas where temperature was less important than precipitation in driving variations of maize yield. Precipitation was found to be the dominant or co-dominant factor in 9 of the 36 prefectures (Figure 6), concentrated in areas with less precipitation during the growing season.

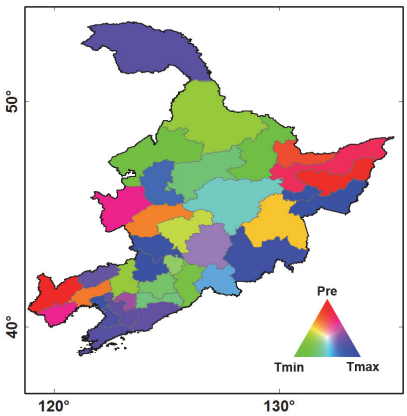

Figure 6. Spatial distributions of climatic controls on variations in maize yield. Coefficient of partial determination (R^2) between variations in maize yield and variations in the climate variables (*Tmax*, *Tmin* and *Pre*) were used to identify the dominant climate factor. Red indicates *Pre* was the primary climatic factor driving maize yield variations, green indicates *Tmin* was the primary climatic factor driving maize yield variations, and blue indicates *Tmax* was the primary climatic factor driving maize yield variations.

4. Implication for future research

Predicting the impacts of future climate change on crop yields heavily relies on the performance of process-based crop models (e.g. IPCC, 2007; Asseng et al., 2013) which, are typically developed and parameterized using a few sites of experimental trials (Xiong et al., 2008; Lobell et al., 2010). However, if failing to reproduce the spatial differences in the response of crop yield to climate change, models successful at just a few experiment sites may still produce biased estimates either at other sites with different climates or at larger spatial scales. Indeed, model inter-comparison results have shown that uncertainties in the model-predicted responses of crop yields to climate change are smaller at sites that may have been used for calibrations than those at sites that have not been used (Asseng et al.,

2013). This highlights the need to constrain the modeled response of crop yield to climate change by using more than just a few sites of experimental trials. Spatial variations of the observed yield response to climate variations provide a means of assessing the models, and this approach is thus recommended to be included in the crop model benchmarking efforts, in order to further understand and constrain the uncertainties in the predicted impacts of climate change on crop production at regional and global scales.

One of the limitations in our study was that we only considered growing season average climate variables (*Tmax, Tmin,* and *Pre*). Crop response to climate variations may differ among different phenophases (Kristensen *et al.*, 2011) and there is increasing evidence suggesting that climate extremes, such as droughts and extreme heat, have exerted significant influence on historical changes in crop yields (e.g. Asseng et al., 2011; Maltais-Landry and Lobell, 2012). Although these effects can be partially captured when using average climate variables (Lobell et al., 2008), further studies with high spatio-temporal resolution climate and crop development/phenology data in combination with crop models are needed to examine the effects more closely and to reduce the large uncertainties in the empirically-derived response of maize yield to climate change as presented in our study.

References

Asseng, S., Foster, I., and Turner, N.C., 2011. The impact of temperature variability on wheat yields. *Global Change Biology,* **17**: 997-1012.

Asseng, S., Ewert, F., Rosenzweig, C., Jones, J.W., Hatfield, J.L., Ruane, A.C., Boote, K.J., Thorburn, P.J., Rotter, R.P., Cammarano, D., Brisson, N., Basso, B., Martre, P., Aggarwal, P.K., Angulo, C., Bertuzzi, P., Biernath, C., Challinor, A.J., Doltra, J., Gayler, S., Goldberg, R., Grant, R., Heng, L., hooker, J., and Hunt, L.A., 2013. Uncertainty in simulating wheat yields under climate change. *Nature Climate Change,* doi: 10.1038/nclimate1916.

Breshears, D.D., Cobb, N.S., Rich, P.M., Price, K.P., Allen, C.D., Balice, R.G., Romme, W.H., Kastens, J.H., Floyd, M.L., Belnap, J., Anderson, J.J., Myers, O.B., and Meyer, C.W., 2005. Regional vegetation die-off in response to global-change-type drought. *Proceedings of the National Academy of Sciences of the United States of America,* **102**:15144-15148.

Chen, C., Lei, C., Deng, A., Qian, C., Hoogmoed, W., and Zhang, W., 2011. Will higher minimum temperatures increase corn production in Northeast China? An analysis of historical data over 1965–2008. *Agricultural and Forest Meteorology,* **151**:1580-1588.

Dai, A., 2011. Drought under global warming: a review. *Wiley Interdisciplinary Reviews: Climate Change,* **2**: 45-65.

Editorial Board of National Climate Change Assessment Report (EBNCCAR), 2011. *The 2nd National Climate Change Assessment Reports*, Science Press, Beijing.

Evans, L.T., and De Datta, S.K., 1979. The relation between irradiance and grain yield of irrigated rice in the tropics, as influenced by cultivar, nitrogen fertilizer application and month of planting. *Field Crops Research,* **2**: 1-17.

Godfray, H.C., Crute, I.R., Haddad, L., Lawrence, D., Muir, J.F., Nisbett, N., Pretty, J., Robinson, S., Toulmin, C., and Whiteley, R., 2010. The future of the global food system. *Philosophical Transaction of the Royal Society B - Biological Sciences,* **365**: 2769-2777.

Godfray, H.C., 2011. Food for thought. *Proceedings of the National Academy of Sciences of the United States of America,* **108**: 19845-19846.

IPCC, 2007. *Climate Change 2007: The Physical Science Basis. Contribution of Working Group I to the Fourth Assessment Report of the Intergovernmental Panel on Climate Change*. Cambridge University Press, Cambridge, United Kingdom and New York, NY, USA.

Jin, Z., Ge, D., Shi, C., and Gao, L., 2002. Several strategies of food crop production in the Northeast China Plain for adaptation to global climate change-a modeling study. *Acta Agronomica Sinica*, **28**: 24-31 (In Chinese with English abstract).

Kristensen, K., Schelde, K. and Olesen, J.E., 2011. Winter wheat yield response to climate variability in Denmark. The Journal of Agricultural Science, **149**: 33-47.

Lele, U., 2010. Food Security for a Billion Poor. *Science,* **327**:1554.

Liu, Y., and Lin, E., 2007. Effects of climate change on agriculture in different regions of China. *Advances in Climate Change Research*, **3**: 229-233 (In Chinese with English abstract).

Liu, Z., Yang, X., Hubbard, K.G., and Lin, X., 2012. Maize potential yields and yield gaps in the changing climate of northeast China. *Global Change Biology,* **18**: 3441-3454.

Lin, E., Xiong, W., Ju, H., Xu, Y., Li, Y., Bai, L., and Xie, L., 2005. Climate change impacts on crop yield and quality with CO2 fertilization in China. *Philosophical Transactions of the Royal Society B: Biological Sciences,* **360**:2149-2154.

Lobell, D.B., and Field, C.B., 2007. Global scale climate - crop yield relationships and the impacts of recent warming. *Environmental Research Letters,* **2**: 014002, doi:10.1088/1748-9326/2/1/014002.

Lobell, D.B., Burke, M.B., Tebaldi, C., Mastrandrea, M.D., Falcon, W.P., and Naylor, R.L., 2008. Prioritizing Climate Change Adaptation Needs for Food Security in 2030. *Science,* **319**: 607-610.

Lobell, D.B., and Burke, M.B., 2010. On the use of statistical models to predict crop yield responses to climate change. *Agricultural and Forest Meteorology,* **150**: 1443-1452.

Lobell, D.B., Schlenker, W., Costa-Roberts, J., 2011. Climate trends and global crop production since 1980. *Science,* **333**: 616-620.

Lobell, D.B., Hammer, G.L., Mclean, G., Messina, C., Roberts, M.J., and Schlenker, W., 2013. The critical role of extreme heat for maize production in the United States. *Nature Climate Change,* **3**: 497-501.

Ma, S., 1996. The estimation and application of agroclimate resources in Chang Bai Mountain region. *System Sciences and Comprehensive Studies in Agriculture*, **12**: 188-193.

Maltais-Landry, G., and Lobell, D.B., 2012. Evaluating the contribution of weather to maize and wheat yield trends in 12 US counties. *Agronomy Journal*, **104**: 301-311.

Mccormick, A.J., Cramer, M.D., and Watt, D.A., 2006. Sink strength regulates photosynthesis in sugarcane. *New Phytologist,* **171**:759-770.

Meng, E., Hu, R., Shi, X., and Zhang, S., 2006. *Maize in China: Production Systems, Constraints, and Research Priorities*. CIMMYT, Mexico.

Mohammed, A.R., and Tarpley, L., 2009. Impact of high nighttime temperature on respiration, membrane stability, antioxidant capacity, and yield of rice plants. *Crop Science,* **49**: 313-322.

Morita, S., Yonemaru, J., and Takanashi, 2005. Grain growth and endosperm cell size under high night temperatures in rice (*Oryza sativa L.*). *Annals of Botany*, **95**: 695-701.

National Bureau of Statistics of China (NBSC), 2011. *China statistics yearbook 2010*. China statistics press, Beijing.

Nicholls, N., 1997. Increased Australian wheat yield due to recent climate trends. *Nature,* **387**: 484-485.

Parent, B., and Tardieu, F., 2012. Temperature responses of developmental processes have not been affected by breeding in different ecological areas for 17 crop species. *New Phytologist,* **194**: 760-774.

Paul, M.J., and Foyer, C.H., 2001. Sink regulation of photosynthesis. *Journal of experimental botany*, **52**:1383-1400.

Peng, S.B., Huang, J.L., Sheehy, J.E., Laza, R.C., Visperas, R.M., Zhong, X.H., Centeno, G.S., Khush, G.S., and Cassman, K.G., 2004. Rice yields decline with higher night temperature from global warming. *Proceedings of the National Academy of Sciences of the United States of America,* **101**: 9971-9975.

Piao, S., Ciais, P., Huang, Y., Shen, Z., Peng, S., Li, J., Zhou, L., Liu, H., Ma, Y., Ding, Y., Friedlingstein, P., Liu, C., Tan, K., Yu, Y., Zhang. T., and Fang, J., 2010. The impacts of climate change on water resources and agriculture in China. *Nature,* **467**: 43-51.

Prasad, P.V.V., Pisipati, S.R., Ristic, Z., Bukovnik, U., and Fritz, A.K., 2008. Impact of Nighttime Temperature on Physiology and Growth of Spring Wheat. *Crop Science,* **48**:2372-2380.

Schlenker, W., and Roberts, M.J., 2009. Nonlinear temperature effects indicate severe damages to U.S. crop yields under climate change. *Proceedings of the National Academy of Sciences of the United States of America,* **106**:15594-15598.

Schmidhuber, J., and Tubiello, F.N., 2007. Global food security under climate change. *Proceedings of the National Academy of Sciences of the United States of America,* **104**:19703-19708.

Sheehy, J.E., Mitchell, P.L., and Ferrer, A.B., 2006. Decline in rice grain yields with temperature: Models and correlations can give different estimates. *Field Crops Research,* **98**: 151-156.

Tao, F., Yokozawa, M., Liu, J., and Zhang, Z., 2008. Climate-crop yield relationships at provincial scales in China and the impacts of recent climate trends. *Climate Research,* **38**:83-94.

Tao, F., and Zhang, Z., 2010. Adaptation of maize production to climate change in North China Plain: Quantify the relative contributions of adaptation options. *European Journal Of Agronomy,* **33**:103-116.

Tao, F., and Zhang, Z., 2011. Impacts of climate change as a function of global mean temperature: maize productivity and water use in China. *Climatic Change,* **105**:409-432.

Wan, S., Xia, J., Liu, W., and Niu, S., 2009. Photosynthetic overcompensation under nocturnal warming enhances grassland carbon sequestration. *Ecology,* **90**:2700-2710.

Wang, X., Piao, S., Ciais, P., Li, J., Friedlingstein, P., Koven, C., and Chen, A., 2011. Spring temperature change and its implication in the change of vegetation growth in North

America from 1982 to 2006. *Proceedings of the National Academy of Sciences,* **108**:1240-1245.

Wang, Z., Song, K., Li, X., Zhang, B., and Liu, D., 2007. Effects of climate change on yield of maize in maize zone of Songnen Plain in the past 40 years. *Journal of Arid Land Resources and Environment*, **21**: 112-117.

Welch, J.R., Vincent, J.R., Auffhammer, M., Moya, P.F., Dobermann, A., and Dawe, D., 2010. Rice yields in tropical/subtropical Asia exhibit large but opposing sensitivities to minimum and maximum temperatures. *Proceedings of the National Academy of Sciences of United States of America,* **107**: 14562-14567.

Wolf, J., and Van Diepen, C.A., 1994. Effects of climate change on silage maize production potential in the European community. *Agricultural and Forest Meteorology,* **71**: 33-60.

Xiong, W., Matthews, R., Holman, I., Lin, E., and Xu, Y., 2007. Modelling China's potential maize production at regional scale under climate change. *Climatic Change,* **85**:433-451.

Xiong, W., Holman, I., Conway, D., Lin, E., and Li, Y., 2008. A crop model cross calibration for use in regional climate impacts studies. *Ecological Modelling,* **213**:365-380.

Yun, Y., Fang, X., Wang, Y., Tao, J., and Qiao, D., 2005. Main grain crops structural change and its climate background in Heilongjiang Province during the past two decades. *Journal of Natural Resources*, **20**: 697-705.

Zhang, J., 2004. Risk assessment of drought disaster in the maize-growing region of Songliao Plain, China. *Agriculture, Ecosystems and Environment*, **102**: 133-153.

Zhang, T., Zhu, J., and Wassmann, R., 2010. Responses of rice yields to recent climate change in China: An empirical assessment based on long-term observations at different spatial scales (1981–2005). *Agricultural and Forest Meteorology,* **150**:1128-1137.

Zhang, T., and Huang, Y., 2012. Impacts of climate change and inter-annual variability on cereal crops in China from 1980 to 2008. *Journal of the Science of Food and Agriculture,* **92**:1643-1652.

Table S1. Correlations among variations in regional climate variables, including growing season mean daily maximum temperature (*Tmax*), growing season mean daily minimum temperature (*Tmin*) and growing season precipitation (*Pre*), during 1980-2009.

P / R	Tmax	Tmin	Pre
Tmax	-	<0.001	0.032
Tmin	0.633	-	0.463
Pre	-0.400	0.142	-

Figure S1. Spatial distribution of municipal administrations over NEC.

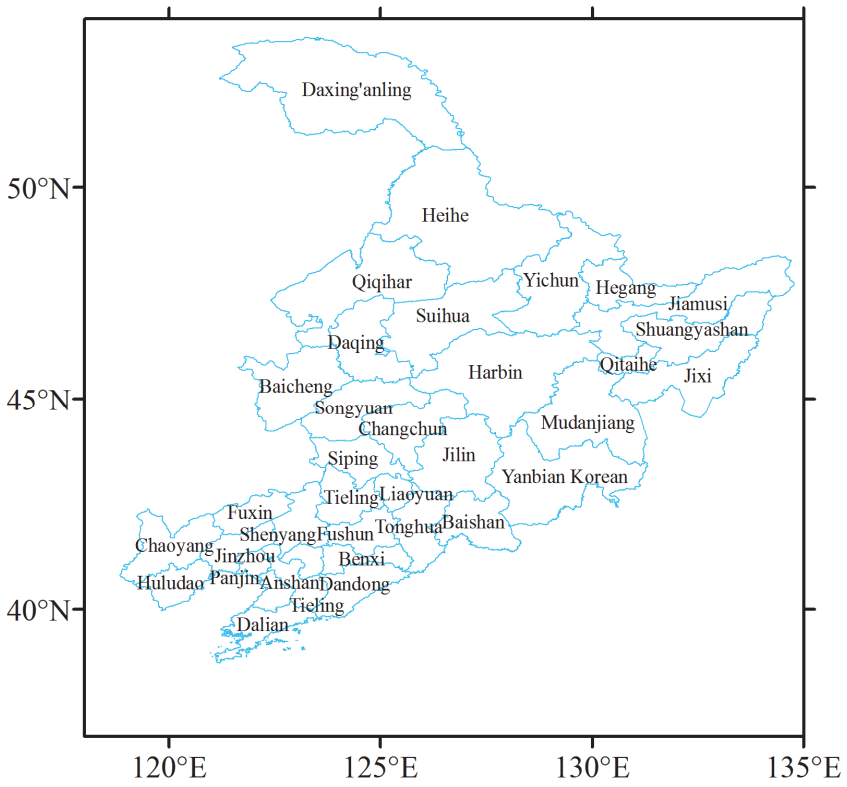

Figure S2. Spatial correlation between maize yield and growing season climate variables: (a) average daily maximum temperature (*Tmax*), (b) average daily minimum temperature (*Tmin*) and (c) precipitation (*Pre*)).

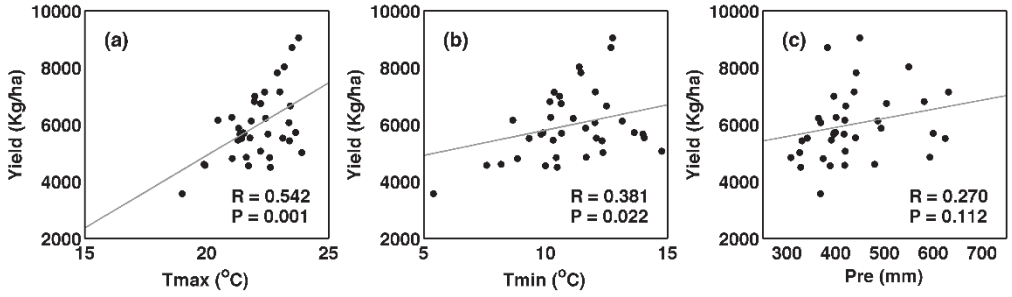

Chapter 3 Attributing historical trends in China's rice growing season based on calibrated ORCHIDEE-crop model

Summary

Whether crop phenology changes are caused by change in managements or by climate change belongs to the category of problems known as detection-attribution. Three type of rice (early, late and single rice) in China show an average increase in Length of Growing Period (LGP) during 1991-2012: 1.0±4.8 day/decade (±standard deviation across sites) for early rice, 0.2±4.5 day/decade for late rice and 2.0±6.0 day/decade for single rice, based on observations from 141 long-term monitoring stations. Positive LGP trends are widespread, but only significant ($P<0.05$) at 25% of early rice, 22% of late rice and 38% of single rice sites. We developed a Bayes-based optimization algorithm, and optimized five parameters controlling phenological development in a process-based crop model (ORCHIDEE-crop) for discriminating effects of managements from those of climate change on rice LGP. The results from the optimized ORCHIDEE-crop model suggest that climate change has an effect on LGP trends dependent on rice types. Climate trends have shortened LGP of early rice (-2.0±5.0 day/decade), lengthened LGP of late rice (1.1±5.4 day/decade) and have little impacts on LGP of single rice (-0.4±5.4 day/decade). ORCHIDEE-crop simulations further show that change in transplanting date caused widespread LGP change only for early rice sites, offsetting 65% of climate change induced LGP shortening. The primary drivers of LGP change are thus different among the three types of rice. Management are predominant

driver of LGP change for early and single rice. This study shows that complex regional variations of LGP can be reproduced with an optimized crop model. We further suggest that better documenting observational error and management practices can help reduce large uncertainties existed in attribution of LGP change, and future rice crop modeling in global/regional scales should consider different types of rice and variable transplanting dates in order to better account impacts of management and climate change. This chapter has been published as Wang X *et al.* (2017) Management outweighs climate change on affecting length of rice growing period for early rice and single rice in China during 1991–2012. *Agricultural And Forest Meteorology,* **233**, 1-11.

1. **Introduction**

The Length of the Growing Period (LGP), defined as the interval in days from the day of planting/transplanting to the day of maturity, is an integrated indicator of crop development that has been related to production (Bassu *et al.*, 2014, Zhang & Tao, 2013). Shortening LGP caused by warmer climate is recognized as a key emerging response through which climate change may impact agricultural production (Bassu *et al.*, 2014, Estrella *et al.*, 2007, Lin *et al.*, 2005, Porter *et al.*, 2014). However, historical change in LGP has been reported diversely across different crops and regions. Some studies found shortening LGP over the past decades (Chmielewski *et al.*, 2004, He *et al.*, 2015, Siebert & Ewert, 2012, Tao *et al.*, 2014b, Xiao *et al.*, 2013). For example, oat in Germany was found to have shorter LGP over the past five decade with rates of change ranging from -0.1 to -0.4 day/decade (Siebert & Ewert, 2012). On the other hand, there are also studies finding little change or even a lengthening in LGP (Liu *et al.*, 2012, Liu *et al.*, 2010, Sacks & Kucharik, 2011, Tao *et al.*, 2013, Zhang *et al.*, 2013). For example, maize in the US Corn Belt shows lengthening LGP during 1981-2005 with an average positive trend of 5 day/decade (Sacks & Kucharik, 2011).

The LGP change of China's rice (*Oryza sativa*), which is the staple food resource for more than half of Chinese population and the crop with the largest growing area in the country, has attracted research interest. Observed trends of rice LGP across different stations vary largely from -2 day/decade to more than 7 day/decade over the past 2-3 decades, the majority of the field-scale observations showing either non-significant change or a lengthening of LGP (Liu *et al.*, 2010, Tao *et al.*, 2006, Tao *et al.*, 2013). One hypothesis explaining the lack of evidence for shortening trend of rice LGP was that management practices has counterbalanced the effects of climate change (e.g. Liu *et al.*, 2012, Tao *et al.*,

2013, Zhang *et al.*, 2013). However, large uncertainties remain on the relative contributions of climate change, shifts in transplanting date and other management practices (e.g. use of longer-duration cultivar), which limits our ability to understand the past trends and project the near term evolution of LGP and its possible consequences for future crop production.

Attribution of the observed trend of LGP from past observations remains challenging because both changes in climate and in management practices have taken place simultaneously. Recent studies used statistical models to characterize the interannual sensitivity of rice LGP to temperature and to separate the contribution of the temperature trend to LGP trend for rice and maize crops over the period 1981-2009 (Tao *et al.*, 2014a, Tao *et al.*, 2013, Zhang *et al.*, 2013). This approach has some limitations: first, statistical models built from interannual LGP variations cannot isolate the impact of changing planting dates from the effects of climate change; second, statistical analyses usually assume linear and constant response to climatic variations (Zhang *et al.*, 2013), but several studies showed that the response is neither linear (Lobell *et al.*, 2013) nor constant with time (Lobell *et al.*, 2014; Burke & Emerick, 2015). On the other hand, crop models can provide an alternative mean to further understand mechanisms and quantify the attributions of different drivers (e.g. Lobell *et al.*, 2012). Therefore, a question to ask in complement of the statistical models is whether crop models can be used as an independent method to separate climate change impacts from management. Using crop models factorial simulations where each driver is varied at a time, or combined, instead of statistical models based on historical data can overcome the limitations by having mechanistic representation of climate change impacts (Gregory & Marshall, 2012), but earlier application of crop models for the attribution of rice LGP trends were criticized for lack of validation for the study region (Tao *et al.*, 2013).

The first objective of this study is to optimize a process-based crop model to represent rice phenology in China. The second objective is to run the optimized model for attributing LGP change to climate change and change in various management practices during the last two decades. To achieve these goals, we first collected and harmonized observations of the rice LGP during 1991-2012 from an extensive station network in China (287 sites). Then, a random set of 80% of the sites is used to optimize the process-based crop model (ORCHIDEE-crop) under a Bayesian framework, by calibration of the parameters controlling rice phenology. The optimized model results are then evaluated against the remaining 20% of the site observations. Finally, contributions to LGP trends from climate change, transplanting date change and other management practices (including cultivar change) are separated by comparing the LGP observations and simulations of the optimized model driven by observed and fixed transplanting date.

2. Methods

2.1 Rice phenology observations from Agrometeorological stations

Transplanting and maturity date of rice in China during 1991-2012 were recorded over 287 agro-meteorological field stations by the Chinese Meteorological Administration, covering the entire rice growing area, from the northeast to the southwest and Hainan Island (Fig. 1). The length of These observations were made following a standardized protocol across sites (CMA, 1993). The dataset includes single rice (177 stations), early rice (110 stations) and late rice (110 stations). Early rice and late rice have the same number of stations because they are two consecutive crops on the same site comprising the double rice cropping system (i.e. rotation between early rice and late rice (Tao et al., 2013)). 80% of the 287 stations are used to optimize ORCHIDEE-crop model parameters. Time coverage of the

stations ranges from few years to 21 years (Fig. 1) with 141 stations (88 for single rice and 53 for early/late rice) having records longer than 15 years, which are the long-term stations used for the detection and attribution of LGP trends (Figure S3).

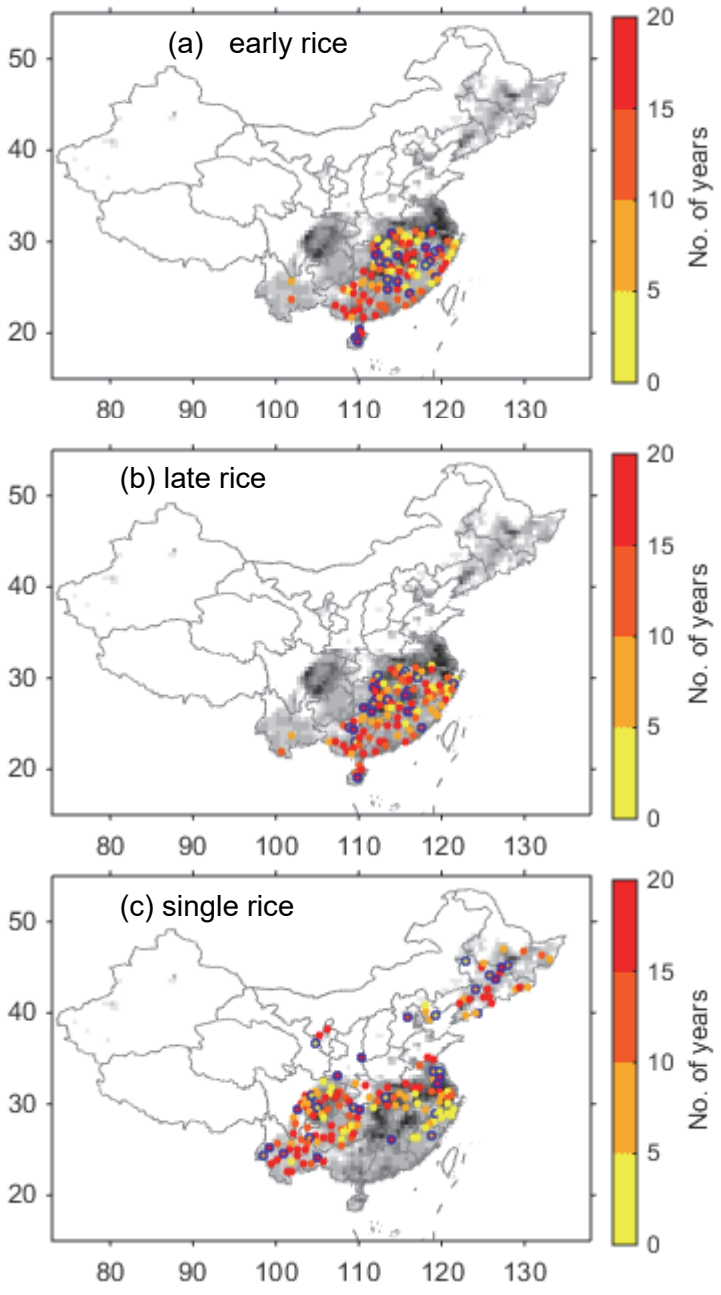

Fig. 1. *Spatial distribution of agrometeorological stations in China for (a) early rice, (b) late rice, and (c) single rice. Color shows the number of years of available observations in each station. Blue circle indicates stations randomly selected to cross-validate the model.*

Grey shading indicates the fraction of rice growing area (Frolking et al., 2002) that darker pixel has larger area of rice croplands.

2.2 Simulating rice phenology with ORCHIDEE-crop model

ORCHIDEE-crop model (svn version no. 2409) is a process-based crop model, which is based on the generic vegetation model ORCHIDEE (Krinner *et al.*, 2005), simulating carbon, water and energy fluxes (e.g. photosynthesis, respiration and evapotranspiration) and includes an agronomical module simulating crop phenology, leaf area dynamics, growth of reproductive organs, carbon allocations and management impacts (Wu et al. 2015). The formula for crop phenology, leaf area dynamics, growth of reproductive organs were originated from a generic crop model STICS (Brisson *et al.*, 2003). Compared with ORCHIDEE-STICS (Gervois *et al.*, 2004), an earlier version of the crop model, which chained the ORCHIDEE model with STICS only through leaf area dynamics, ORCHIDEE-crop has a complete coupling between crop growth and physiology of carbon and water exchanges in soil-vegetation-atmosphere continuum. ORCHIDEE-crop calculates thermal unit accumulation, photosynthesis and energy exchange on a half-hourly time step, while leaf area dynamics, carbon allocation and biomass and soil organic carbon change are simulated on a daily time step.

Like most crop models, the crop growth cycle in ORCHIDEE-crop is divided into several stages with the developments driven by accumulated thermal unit. Since simulation of rice growth starts from transplanting (LEV), the growth cycle is divided into only three phases, which are divided by the onset of grain filling (DRP) and the physiological maturity (MAT). The thermal unit (*gdd*) needed to grow from transplanting to maturity are prescribed parameters (GDD_{LEVDRP} and GDD_{DRPMAT}). Accumulation of thermal unit (*gdd*) is calculated

at each half-hourly time step following Eq. 1:

$$gdd = f(T) \times \delta_p \times \delta_v \times (\varepsilon \times \min(\delta_n, \delta_w) + 1 - \varepsilon) \quad (Eq.1)$$

Where f(t) is a tri-linear function of temperature (T) following Eq. 2, δ_p (δ_v, δ_n, δ_w) are crop-specific scalars for photo-period (vernalization, nitrogen, water) regulations respectively. ε is a scalar parameter describing the sensitivity of the crop to nitrogen and water stress.

$$f(t) = \begin{cases} 0, & t \leq T_{min} \text{ or } t \geq T_{max} \\ t - T_{min}, & T_{min} < t < T_{opt} \\ \frac{T_{opt} - T_{min}}{T_{opt} - T_{max}} \times (t - T_{max}), & T_{opt} < t < T_{max} \end{cases} \quad (Eq.2)$$

As described above, temperature change has a first-order control over *gdd* (Fig. S1). Therefore, the most important parameters for accumulations of *gdd* are GDD_{LEVDRP}, GDD_{DRPMAT}, T_{min}, T_{opt} and T_{max} (Table 1), which are to be optimized in the parameter optimization. Details of the regulation scalars can be found in Brisson *et al.* (2008). In our study, δ_v=1 because transplanted rice require no vernalization to develop; we assumed that δ_n=1 and δ_w = 1 because 93% of rice cropland in China is irrigated (http://www.knowledgebank.irri.org/country-specific/asia/rice-knowledge-for-china/2013-06-03-07-15-17, Salmon *et al.*, 2015), and the nitrogen fertilizer application rate is higher than 100 kgN ha^{-1} (Zhou *et al.*, 2014). In this study, we also assumed δ_p=1, which indicates that photoperiodic constraint on the phenology is minimal for rice. This is probably true for early and single rice, because varieties insensitive to day-length change are commonly used (Cao et al., 2011). There are, however, cases for late rice, where day-length sensitive varieties are used (Cao et al., 2011), but we cannot account it due to lake of information on the extent for application of day-length sensitive varieties. Further details on ORCHIDEE-crop structure and parameters can be found in Wu et al. (2015). It should be noted that rice phenology development is modelled mostly by temperature driven processes

in almost all rice models (Li et al., 2015), so the parameter we chose here represent the main processes driving the phenology development. Other parameters of ORCHIDEE-crop are not optimized here, because the phenology observations can provide loose constraint on them.

In this study, two types of simulation experiments were performed for each site: (1) For validation and comparison with observed LGP, simulation S0 was driven by observed variable climate and the observed variable transplanting date each year at each station; (2) For isolating the impact of transplanting date from that of climate change on LGP, simulations S1 was driven by a time-invariant (fixed) transplanting date defined as the average of the earliest three year of each record. Climate forcing for simulation S0 and S1 was obtained from CRU-NCEP dataset v5.2 (http://dods.extra.cea.fr/data/p529viov/cruncep/). The difference between S0 and S1 can be used to attribute the fraction of LGP trends explained by changes in transplanting dates. Assuming the model structure has no time-dependent systematic errors, the residual difference (Δ) between trends in observed LGP and in simulation S0 can be interpreted as reflecting the contribution of all other management operations not considered in S0, including change in the cultivars. Previous studies usually interpreted such a residual between observed and modelled LGP (either from statistical modelling or from process modelling) as being caused by change in the cultivars used over time (Liu et al., 2012, Tao et al., 2013, Zhang et al., 2013), but it could cover other changes in agronomic practice, such as fertilization change.

2.3 Parameter optimization with particle filter

We used a particle filter method with sequential importance resampling (PFSIR) to

optimize the ORCHIDEE-crop parameters for early, late and single rice phenology respectively over China. Particle filter is a Monte-Carlo implementation of recursive Bayesian theorem to estimate the posterior probability density of a state-space (here is the parameter set of the model) (van Leeuwen, 2009). A set of ensemble members of the parameter set called "particles" hereafter, are used as a discrete approximation of the multi-dimensional probability density function (PDF) of the model parameters. The PDF evolves by propagating all particles forward in space or time through the ORCHIDEE-crop model. Each step when observations become available, each particle is assigned a weight (or importance) according to the model-observation differences. A new set of particles is generated after each iteration by resampling the weighted particles (sequential importance resampling). The optimized parameter sets for early rice, late rice and single rice are obtained through applying PFSIR to ORCHIDEE-crop model respectively. Particle filters has been found to have broader suitability than traditional variational methods (Chorin & Morzfeld, 2013), in particular for non-linear cases. Thus, variant forms of particle filter have become growingly popular when applying in earth system models (e.g. Bilionis *et al.*, 2014, Yu *et al.*, 2014). Further details of PFSIR used in this study can be found in the Appendix.

Advantages of using the PFSIR method are multiple: First, unlike error minimization methods or manual adjustments previously adopted (e.g. Gregory & Marshall, 2012, Zhang *et al.*, 2014a), PFSIR not only provides a best (maximum likelihood) estimate, given an observation probability, according to the Bayes theorem, but also the uncertainties of the optimized parameters; Second, unlike variational methods (e.g. 4D-Var) assuming Gaussian distributions of the parameters, no assumptions are necessary for the posterior parameter distribution of the parameters in the particle filter, which makes it suitable for a model like

ORCHIDEE-crop that uses some non-Gaussian and threshold-like parameters; Third, particle filter does not assume linearity of the state-space, which overcomes some of the limitations of methods based upon linearization of the state-space such as ensemble Kalman filter (van Leeuwen, 2010); Fourth, when being fed with large dataset, the Bayes-based particle filter is less sensitive to data outliers than error minimization methods (e.g. Kersebaum *et al.*, 2015), which also make it suitable for application in crop models and over regional scale; Fifth, the particle filter does not require the effort of constructing the tangent linear model of the original model for calculating sensitivities of the model output to its parameters, and tends to have higher efficiency than other Monte-Carlo methods (Gaucherel *et al.*, 2008). The particle filter is thus recommended for non-linear data assimilation, though has limitations for high-dimensional system (van Leeuwen, 2009). With growing number of parameters (dimension of the parameter space), the filter may become less efficient and required a huge number of computing resources in order to obtain satisfactory estimates. Some improvements to the particle filter would be needed in such high-dimensional cases (e.g. van Leeuwen, 2010). Given the relatively small dimension of the parameter set (Table 1), this poses little threats to our study.

To evaluate the robustness of the optimized model, we randomly selected 20% of the sites (22 sites of early rice, 21 sites of late rice and 35 sites of single rice, see Fig. 1 for its spatial distribution) as validation sites. The validation sites are not used into the PFSIR, providing independent evaluation measurements of the performance for the optimized model. It should be noted that the probability of posterior parameter distribution usually reflects the strength of constraint from the observation data, thus the spread of posterior probability distribution is also a metric to evaluate the performance of the particle filter. Larger spread of posterior probability distribution would indicate loose constraint from the

observations.

It should be noted that we infer only one set of optimized parameter for each rice type over China, which is consistent with our intention to use a generic model across large regions, but could be a limitation in cases when local varieties within the same rice type have very different parameters. Separating the rice growing area into finer zones and producing multiple parameter sets for each rice type (Zhang *et al.*, 2014a) may yield smaller errors due to increased degree of freedom and a potentially better calibration reflecting the diversity of local varieties. But doing this would also increase the risk of over-fitting and would require a detailed zoning map of rice crop varieties instead of zoning map of climate. In addition, there are growing requests for assessing climate change impacts over regional and global scales (Rosenzweig *et al.*, 2014) asking for robust parameter sets representing a broad scale of the growing area.

2.4 Trend analyses

We calculated the trend of rice LGP from the observations, the simulations S0 and S1, and for the residual Δ by regressing time series of LGP at each station against year using least square regression. The trend estimates were compared with non-parametric test (Sen's slope) (Fig. S2). The similar estimates between least square regression slope and Sen's slope indicate robustness of the trend estimates to potential outliers. Statistical significance was reported based on two-tailed *t*-test. Only stations with more than 15 years of observations during 1991-2012 are used in the trend analyses (Fig. S3).

3. Results

3.1 Simulated LGP with prior and posterior parameters

Fig. 2 shows the histogram of the simulated bias of LGP (difference between observed LGP and simulated LGP) for simulation S0 before and after optimization, and for the three rice types. Over site-years used in optimization, the posterior model largely reduces the root mean square error (RMSE) from 32.7 days (prior) to 14.8 days for early rice (optimized) (Fig. 2a), from 108.9 days to 12.4 days for late rice (Fig. 2b), and from 73.7 days to 24.4 days for single rice (Fig. 2c). When we only look at spatial variations across sites (Fig. S4), we found that the posterior model not only reduces the absolute errors (indicated by the vicinity to 1:1 line), but also better reproduces the spatial LGP gradient among the sites used for optimization. The R^2 for the spatial gradient improves from 0.41 ($P<0.01$) to 0.55 ($P<0.01$) for early rice (Fig. S4a), from 0.00 ($P=0.91$) to 0.33 ($P<0.01$) for late rice (Fig. S4b), and from 0.21 ($P<0.01$) to 0.47 ($P<0.01$) for single rice (Fig. S4c). Interannual variations of LGP at the long-term sites used for optimization also show significant improvement for all three rice types ($P<0.05$) (Fig. S5). These show that given the structure of the ORCHIDEE-crop model, with the PFSIR optimization method, it is possible to find a set of parameters for each of the three rice types, which provides an improved fit to the LGP observations across sites and years.

To test whether the improvements due to optimization is limited to the sites chosen for optimization, we also use the prior and posterior model parameters in ORCHIDEE-crop runs at the cross-validation sites. The RMSE of LGP for the simulation S0 with prior parameters are 33.9 day for early rice, 113.0 day for late rice and 74.5 day for single rice, respectively. The RMSE of LGP with posterior parameters at the cross-validation sites are 16.3 day for early rice, 10.2 for late rice and 19.2 for single rice, which are close to that over the optimization sites (Fig. 2d-f). Therefore, the RMSE reduction over the validation sites is similar to that over the optimization sites (Fig. 2d-f). The improved spatial gradients (Fig.

S4d-f) and interannual correlation between observed and modeled LGP (Fig. S5d-f) also hold for the validation sites. Indeed, when we re-selected the sites used for optimization and running the particle filter once again for testing, we obtain a similar set of parameter set than the one presented in Table 1, further indicating the robustness of the optimized models in reproducing the spatiotemporal variations of rice LGP in China during 1990-2012, for the three rice types.

Table 1. Prior and posterior parameters for early rice, late rice and single rice.

	Prior	**Posterior**		
	Generic rice	Early rice	Late rice	Single rice
GDD_{LE}	895±115	860 ± 9	610±12	645±5
VDRP				
GDD_{DR}	554±115	322 ± 7	345±9	420±6
PMAT				
T_{min}	13.0±4.3	9.9 ± 0.5	9.2±1.1	9.4±0.5
T_{opt}	30.0±4.3	32.3 ± 1.9	23.4±0.6	22.8±0.5
T_{max}	40.0±4.3	36.5 ± 3.6	38.2±1.1	35.7±0.7

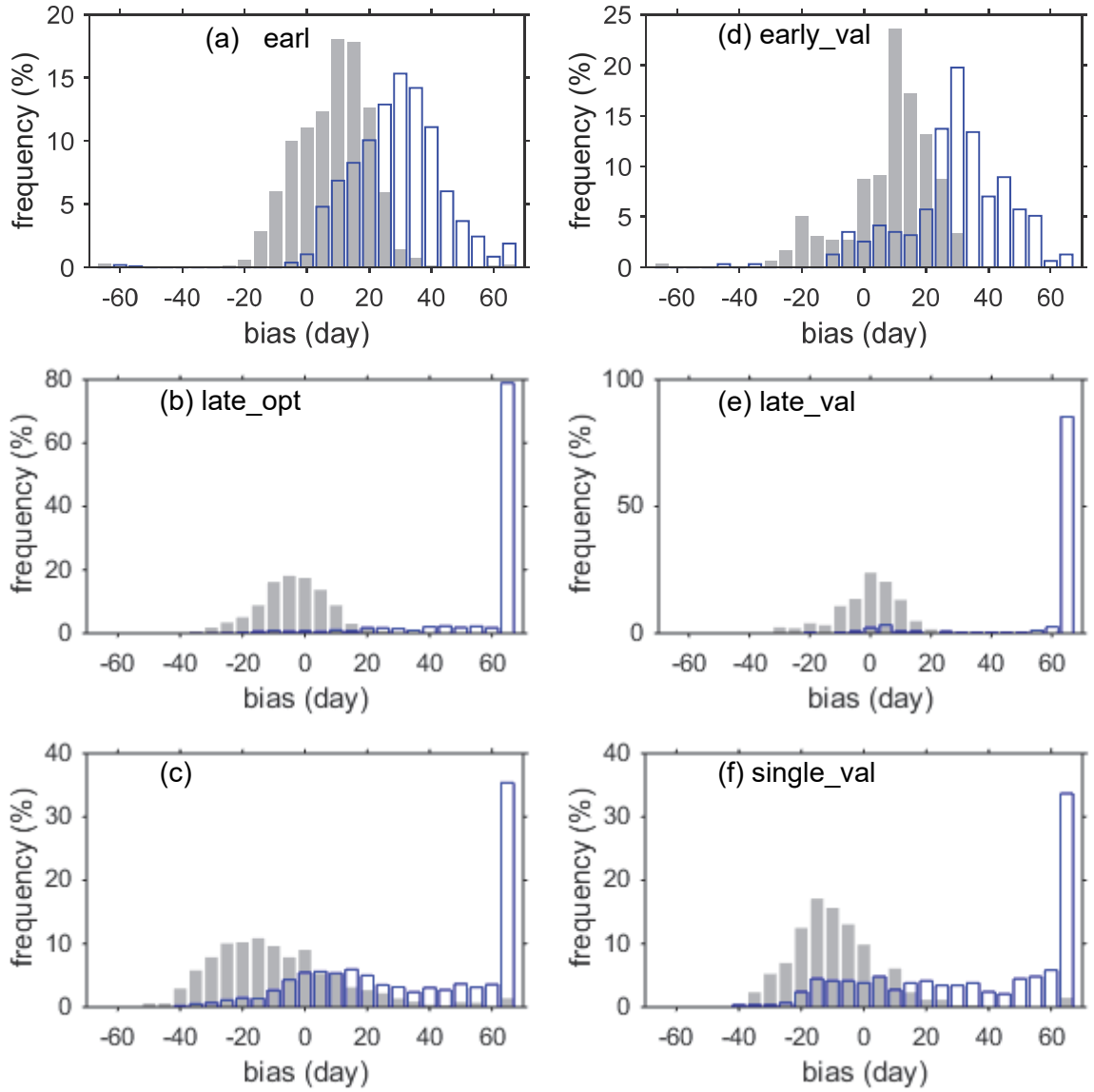

Fig. 2. *Histogram of the differences between observed length of rice growing period (LGP) and simulated LGP with prior parameters (blue-edged bars) and optimized parameters (grey bars) for (a) optimization sites of early rice, (b) optimization sites of late rice, (c) optimization sites of single rice, (d) validation sites of early rice, (e) validation sites of late rice, and (f) validation sites of single rice.*

The optimization of ORCHIDEE-crop parameters not only significantly reduced the misfit with site observations but also significantly changed the simulated trend in LGP (Fig S4). For early and single rice, the trend in optimized LGP (-0.7±2.7 day/decade (mean ±

standard deviation across sites) for early rice and -0.5±5.2 day/decade for single rice) differs by more than 60% ($P<0.01$) from the prior modeled LGP trend (-1.7±4.8 day/decade for early rice and -1.5±18.4 day/decade for single rice)(Fig. S6a and c). For late rice, the optimization even changes the sign of the simulated LGP trend and largely reduced the spatial variations of the trend (Fig. S6b). The average LGP trend for late rice is changed from -7.5±16.7 day/decade to 1.0±3.0 day/decade (Fig. S6b). The optimized model thus produces lengthening instead of shortening LGP for late rice. The LGP trend simulated by the optimized model is further analyzed in the section "*attribution of LGP trends to climate change, transplanting date change and other management factors"*.

3.2 Optimized parameter sets

Fig. 3 shows the probability distribution of the five optimized parameters (see Methods section for descriptions of the parameters) of the ORCHIDEE-crop simulation for LGP before (prior) and after (posterior) optimization for early rice, late rice and single rice, respectively. Optimized (posterior) parameters of thermal unit requirements (GDD_{LEVDRP} and GDD_{DRPMAT}) show largest uncertainty reduction (UR) with a 90% error reduction in the standard deviation after optimization (Fig. 3a and b, Table 1), indicating strong observational constraints on these parameter values. Early, late and single rice have their posterior thermal unit requirements (GDD_{LEVDRP} and GDD_{DRPMAT}) concentrated in a narrow range of values, which are significantly different from each other ($P<0.05$). On the other hand, the temperature threshold parameters regulating phenological development (T_{min}, T_{opt}, and T_{max} in Eq. 2) show different values after optimization among the three rice types. For early rice, T_{min} for phenology development is well constrained with a UR of 78% (9.9±0.5 ^{o}C, Fig. 3d), while T_{opt} has a large posterior range between 29 ^{o}C and 35 ^{o}C (32.3±1.9 ^{o}C, Fig. 3c) and a UR of 55%. For late and single rice, optimized T_{min} are slightly lower than

early rice (9.2±1.1 ºC for late rice and 9.4±0.5 ºC for single rice, Fig. 3d) and UR of 52% and 78%. On the contrary, optimized T_{opt} for late and single rice are much lower than early rice (23.4±0.6 ºC for late rice and 22.8±0.5 ºC for single rice, Fig. 3c) with UR ~85%. The higher optimal T_{opt} and T_{min} values found for early rice, compared to single and late rice suggest that early rice must be more acclimated to the high temperature in spring and summer over southern China, which matches its geographical distributions (Fig. 1) and was not accounted in the prior values of these parameters. For all the three rice types, the posterior probability distribution of T_{max} shows a large range (Fig. 3e) indicating that this temperature threshold that corresponds to the stop of phenology development is less well constrained from the LGP observations, likely because T_{max} is a high-end threshold, which is not frequently reached in the historical period 1991-2012 (4 site-days for early rice, no site-day for late rice and 7 site-days for single rice).

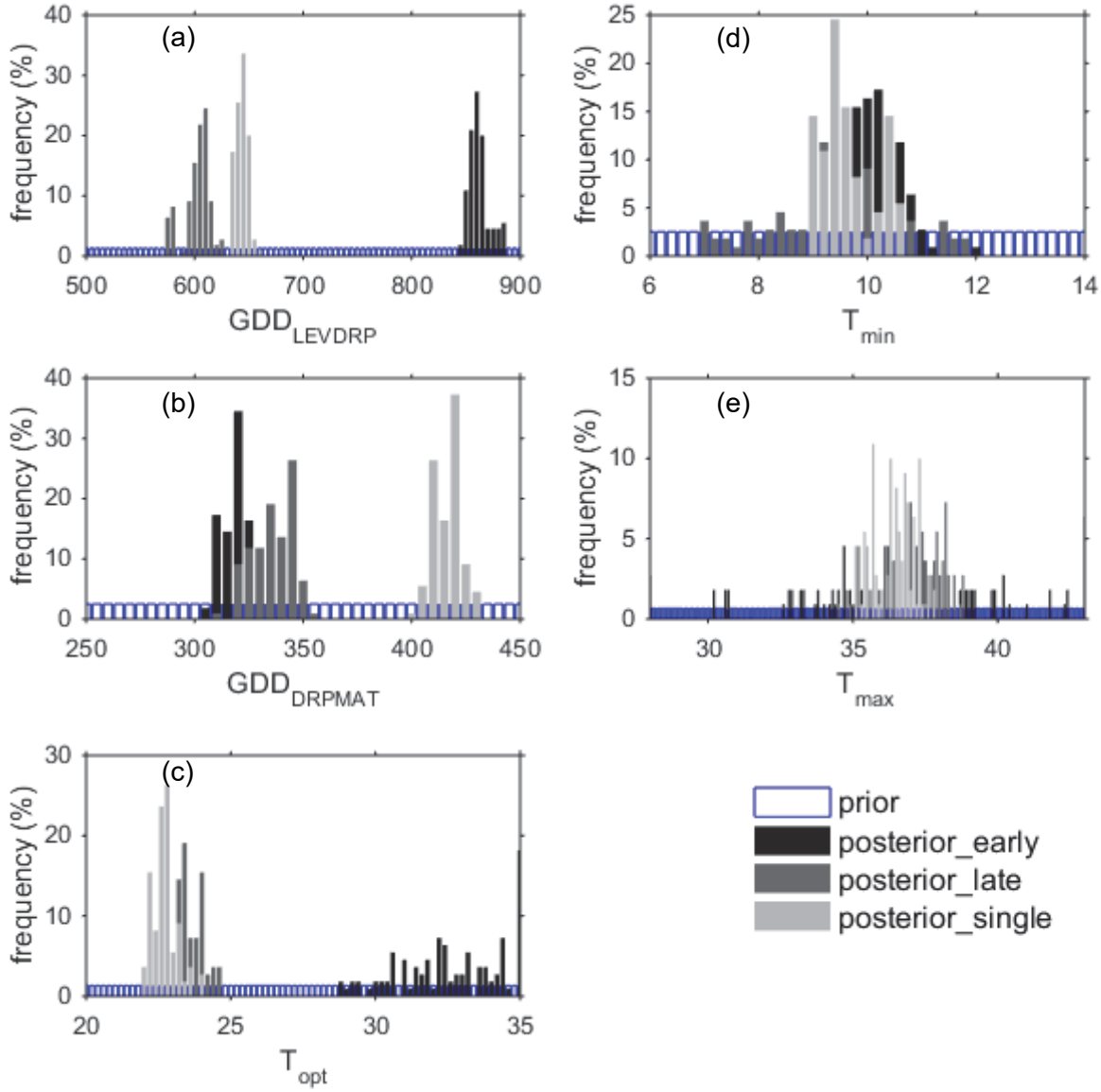

Fig. 3. *Histogram of the prior and posterior parameter distribution for early rice, late rice and single rice. The optimized parameters include (a) GDD$_{LEVDRP}$, (b) GDD$_{DRPMAT}$, (c) T_{opt}, (d) T_{min}, and (e) T_{max} (see Methods section for definitions and descriptions of the parameters).*

3.3 Attribution of LGP trends to climate change, transplanting date change and other management factors

At country scale, observations show an average lengthening of LGP for all three types

of rice (Fig. 4). Single rice sites show the largest lengthening rate of 2.0±6.0 day/decade (mean ± standard deviation in spatial variations), followed by early rice (1.0±4.8 day/decade) and late rice (0.2±4.5 day/decade). But there are large site-to-site variations in the observed LGP trend (Fig. S7). For single rice, 61% of the sites show a trend towards longer LGP, 50% of which are statistically significant (Fig. S7c). For early and late rice, the percentage of sites showing longer LGP is similar (58% and 55% for early and late rice respectively), but the percentage of significant positive trends was smaller than that for single rice (27% and 19% for early and late rice respectively). There is a large proportion of sites showing no significant change of LGP (more than 50% for all three types of rice), indicating that LGP change is either weakly sensitive to climate change or compensated by effects of change in climate and managements. To further understand the drivers of the LGP trends, we estimated the contribution of climate change alone from simulation S1, the contribution of transplanting date from the difference between simulation S0 and S1, and interpreted the contribution of all other management (OM) as being caused by a non-modeled residual term Δ, as explained in the Method section.

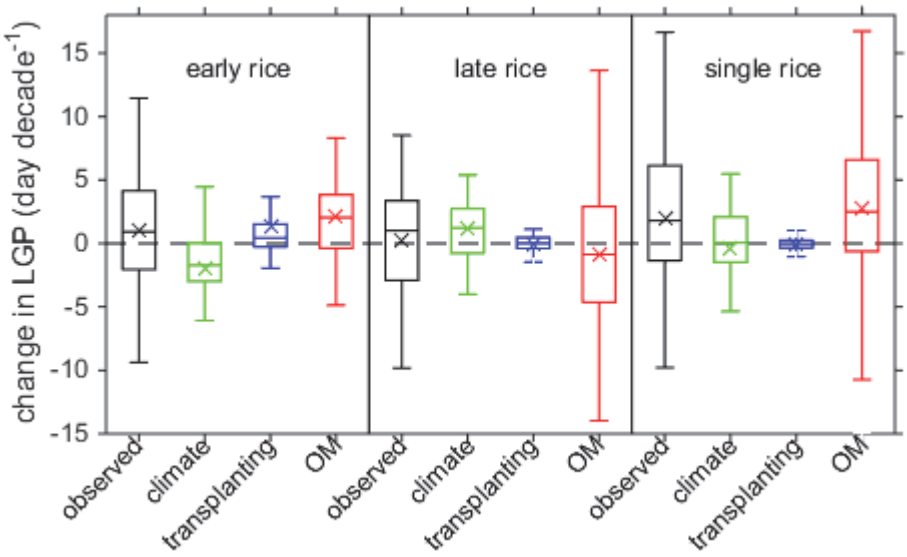

Fig. 4. *Box plot of change in the length of rice growing period length (LGP) over the past two decades derived from observations and simulations for the three rice types. The LGP change due to climate change is obtained from simulation S1; The LGP change due to change of transplanting date is obtained by the difference between simulation S0 and simulation S1; The LGP change due to other management (OM) is obtained by the difference between observations and simulation S0. The lower and upper edge of the box indicate 25th and 75th percentile of the trends. The line and cross inside the box indicate the median and the mean of the trends, respectively.*

As Fig. 4 and Fig. 5 shows, the impacts of climate change on LGP change differs between the three rice types. For early rice sites using the simulation S1 with the optimized model, we infer an average shortening of LGP induced by climate change alone of -2.0±5.0 day/decade (Fig. 4). Except for sites in Hainan and Guangxi, the shortening of LGP in simulation S1 is widespread (71%) and significant at 41% of the early rice sites (Fig. S7j). However, for late rice, climate change alone leads to an average lengthening of the LGP of 1.1±5.4 day/decade, with 16% of the sites having a significant lengthening mostly in Hunan, Jiangxi and Fujian provinces (Fig. S7k). This positive LGP trend for late rice in response to

climate change occurs in ORCHIDEE-crop because temperature during the growing season is reaching the optimum temperature of phenology development for late rice in southern China (Table 1). For single rice, the contribution of climate change to LGP trends shows regional differences. Climate change is modeled to shorten LGP over northeastern China and high-altitude Yungui plateau over southwestern China, but to lengthen LGP in the middle and lower reach of Yangtze River basin (Fig. S7l). These regional contrasts for single rice LGP trends leads to a near neutral average impact of climate change on LGP trend across China (-0.4±5.4 day/decade, Fig. 4). Among all the sites, climate change is the dominant factor contributing to the observed LGP trend for 26% of early rice sites, 28% of late rice sites and 19% of single rice sites (Fig. 5).

We found that 66% of the early rice sites experienced earlier transplanting date during 1991-2012 (Fig. S8). From the difference between modeled LGP in simulation S0 and S1, we infer that the earlier shift of the transplanting date (-2.0±4.8 day/decade) alone, has lengthened the LGP of early rice by 1.3±5.5 day/decade (Fig. 4). But earlier transplanting practice have not been adopted widely for late rice and single rice sites, and the observation sites showing positive and negative trends in transplanting dates are of similar proportion for late rice and single rice (Fig. S8b and c). The magnitude of the average trend in transplanting date is also small for these two types of rice (-0.3±3.4 day/decade for late rice and 0.1±4.1 day/decade for single rice), which has minor impacts on the simulated LGP change in the S0-S1 difference (-0.1±5.0 day/decade for late rice and -0.1±1.7 day/decade for single rice, Fig. 4). Therefore, the earlier shift of transplanting date is the dominant factor contributing to the trend of LGP at 17% of early rice sites (Fig. 5a), and a minor driver of LGP trends for other rice types, being dominant at only 7% of the late rice sites (Fig. 5b) and 2% of the single rice sites (Fig. 5c).

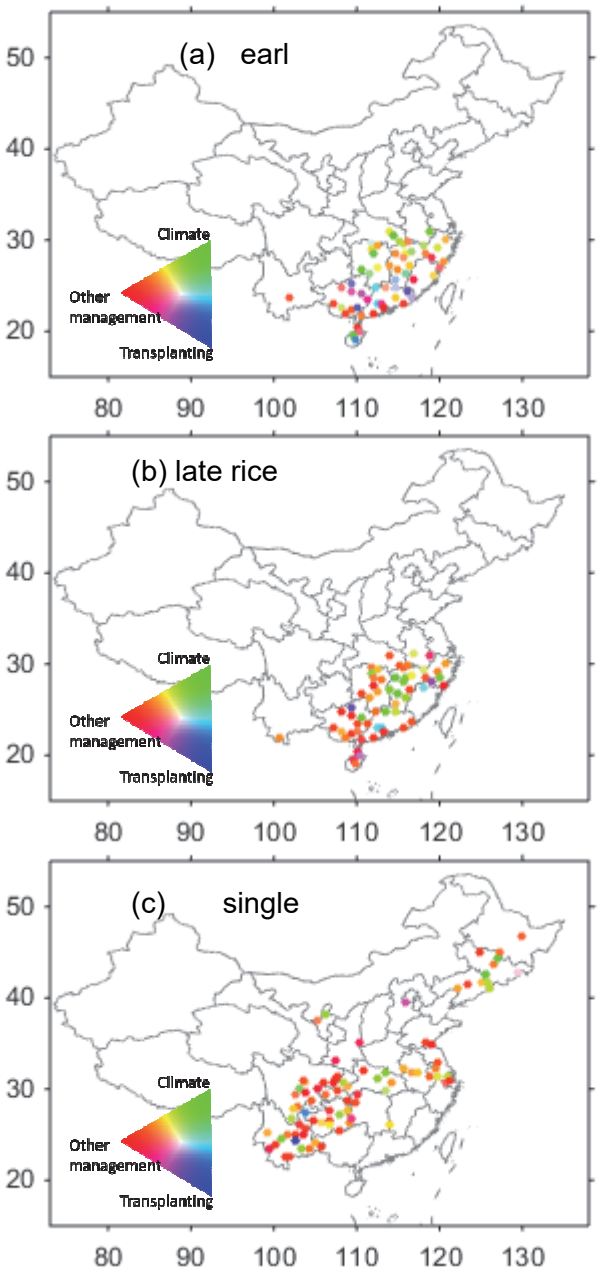

Fig. 5. *Spatial distribution of the controlling factors on change in the length of growing period (LGP) for (a) early rice, (b) late rice, and (c) single rice. Green color indicates LGP change is primarily driven by climate change, blue color indicates LGP change is primarily driven by transplanting date change, and red color indicates LGP change is primarily driven by other management. Intermediate colors indicate co-dominance by more than one factor.*

On average across sites, the role of other management practices (OM), inferred from the residual trend not explained by transplanting date and climate change, is found to be the predominant factor for LGP change for early and single rice. OM are identified to be responsible for a lengthening of LGP by 2.1±3.9 day/decade for early rice and 2.8±7.6 day/decade for single rice (Fig. 4). A great majority of the early rice sites (71%) and single rice sites (64%) show positive contributions of OM trends. Over 20% of early rice sites sand 27% of single rice sites, the OM induced LGP trend is statistically significant ($P<0.05$, Fig. S7d-f). On the contrary, OM contributes to a shortening of LGP for late rice by -0.8±5.8 day/decade (Fig. 4), with a significant LGP shortening in Hunan, Jiangxi, Guangdong and Fujian provinces (Fig. S7e). The dominant role of OM is prevalent in southern China provinces, such as Guangdong, Guangxi and Yunnan for both early rice and late rice (Fig. 5a-b). For single rice sites, OM is the predominant driver of the LGP trend from the northeast to the southwest at 78% of the sites (Fig. 5c).

4. Discussion

Our analyses of a large network of rice phenological observations with more than 100 long-term stations across rice growing area in China indicate that the LGP of single rice has become longer over the past two decades, which is consistent with a recent study focused on Northeast China and Yangtze River basin during 1980-2009 (Tao *et al.*, 2013). Although site-to-site variations are large, all three rice types exhibit an average trend towards longer LGP. The ORCHIDEE-crop model optimized upon observed LGP was run using factorial simulations, with either climatological (fixed) or observed transplanting dates, and variable climate. The results suggest that the primary factors driving the LGP trends are not the same among the three rice types.

We found that recent climate change considered as a single driver in the model, shortened the LGP of early rice (Fig. 4 & Fig. S7j), which is consistent with previous statistical modelling (Zhang *et al.*, 2013) and process modeling based on four sites (Liu *et al.*, 2012). For late rice, climate change appears to have induced little change or a lengthening of LGP, which is different from early rice (Liu *et al.*, 2012, Tao *et al.*, 2013) and from some other temperate crops (Lobell *et al.*, 2012). This is because the optimized parameter values indicate a lower optimum temperature (23.4 ± 0.6 ^{o}C) for phenology development of late rice than for early rice. Late rice sites are mainly located in southern China where temperature after transplanting (around July and August) is higher than this optimal temperature of phenology development of late rice (Li et al., 2010). Thus, further warming beyond the temperature optimum will not accelerate the phenology development and cause a lengthening of LGP (Fig. S1, Yin, 1994). It should be noted that the optimum temperature that we determined from PFSIR is consistent with statistical analyses of rice phenology observations in southern China (Xie *et al.*, 2008) and with the incubation study (Summerfield *et al.*, 1992), but lower than that used in previous models (Liu *et al.*, 2012, Zhang *et al.*, 2014b), parameters of which may have originally derived from earlier studies based on assumptions or rice varieties in Southeast Asia (e.g. Kropff *et al.*, 1993). Our capability to further assess this parameter is rather limited since field trials determining the optimum temperature of phenology development are rarely available, requiring more data and future studies to refine this key parameter in order to more accurately project climate change impacts on LGP change. It should also be noted that, although high temperature stress did not necessarily shorten LGP, it may still adversely affect rice yields as it stresses photosynthesis (Yin & Struik, 2009), and thus reduce biomass accumulation for the harvest.

By comparing the simulations driven by fixed transplanting dates (S1) and by variable transplanting dates (S0), we can separate the contribution of transplanting date trends on LGP trends. Although an earlier transplanting date is a pragmatic autonomous adaptation through which farmers adapt to climate change (Olesen *et al.*, 2011), its effect on the regional trends of LGP was not separated by previous statistical models (Tao *et al.*, 2013, Zhang *et al.*, 2013), probably due to its co-variations with climate (Tao *et al.*, 2006). It may also be related with the linear assumption of previous statistical analyses (e.g. Tao *et al.*, 2013; Zhang *et al.*, 2013), which can be improved using recent progresses in statistical analyses including non-linear or threshold like equation (e.g. Burke & Emerick, 2015; Solomon, 2016). We found that changes in transplanting date were widespread over the last 20 years for early rice sites in southern China, and that they contributed to lengthen LGP, whereas climate change has the opposing effect of shortening LGP. This suggests that the adoption of earlier transplanting date has partly mitigated climate change impacts on early rice growth over the past two decades. However, the same adaptation strategy is probably not possible for late rice because earlier transplanting and lengthening of LGP nearly compensate for each other for early rice, leaving no more time during the season available for earlier transplanting of late rice (MOA, 2014). In addition, advancing transplanting dates for late rice to mitigate climate change will have limitation due to frost risk and photo-period constraints in the autumn. The same reason may also explain why single rice sites show large site-to-site variations on the sign of change in transplanting date (Fig. S8).

Other management practices were found to be the dominant driver of LGP trends for early rice and single rice across the country (Fig. 5), which is about one magnitude larger than the contribution of transplanting date and climate trends for early rice and single rice, though with large site-to-site variations (Fig. 4). Previous studies usually interpreted this

residual contribution not explained by climate change as the contribution of cultivar change, in particular the adoption of long-duration cultivars (Liu *et al.*, 2012, Tao *et al.*, 2013, Zhang *et al.*, 2013), which was supported by the empirical assessment of change in thermal requirements (Zhang *et al.*, 2014b). This hypothesis is reasonable, since use of longer-duration cultivars is one of the most commonly used practices to achieve higher yields and mitigate the impacts of climate change (Aggarwal & Mall, 2002, Porter *et al.*, 2014). However, there are other management practices that could also impact LGP trends. For example, foliage nitrogen fertilizer spraying on leaf in the late growing season, can also lead to increase of leaf longevity and the growing season (Russell *et al.*, 1990). Future studies should account for these effects with spatially and temporally explicit datasets in order to more accurately attribute and project LGP change. In addition, OM trends may not necessarily induce longer LGP. Local agronomists in China have been studying and recommending the combination of rice varieties with shorter-duration and longer-duration cultivars in order to improve yield and to minimize risk of exposure to climate extremes (e.g. Ai *et al.*, 2010; Mao *et al.*, 2015; Li *et al.*, 2016) Shorter-LGP induced by OM seems to be widespread for late rice in southern China. These efforts were taken likely because shorter LGP for late rice can have the advantage to avoid the damage induced by cold weather events during anthesis and grain filling, known as the "cold dew wind" (Huo & Wang, 2009, Wu *et al.*, 2014). The risk of late rice exposure to cold damage can be more than 30% for some regions in southern China according to (Wu *et al.*, 2014), and warming over past decades does not alleviate the risk of the weather events and reduce late rice production when it occurs (Huo & Wang, 2009, Ministry Of Agriculture, 2014).

Unlike previous studies identifying climate change as the dominant driver of rice phenology change, using field trials (De Vries *et al.*, 2011), statistical models (Zhang *et al.*,

2013) or crop model simulation (Yao *et al.*, 2007), our analyses combining phenology observations and optimized crop model simulations indicate that management practices (including both change in transplanting date and changes of OM) probably outweigh the impact of climate change on LGP change for early rice and single rice in China during the past two decades. However, we are only able to separate the effects on LGP trends of trends transplanting date from other management practices, such as cultivar change, due to limited data on spatio-temporal variations of other management practices. On the other hand, attribution of LGP trends to OM has the largest uncertainty in this analysis since the role of OM is inferred from the misfit of model runs driven by climate change and observed transplanting date and the observations. Errors in the attribution of LGP trends to climate or transplant date trends, depends largely on the crop model used, a structural bias in this model, and non-unified observational error across sites and years will translate into an erroneous attribution to OM. Through the Bayesian optimization framework (particle filter with sequential importance resampling), we optimized the ORCHIDEE-crop model to fit the spatio-temporal variations of LGP for the three rice types across China. The optimized model not only can reproduce the phenology of the sites used for optimization, but also remains robust when applied to validation sites (Fig. 3). Therefore, the optimized model provides some confidence in the attribution, compared to models not optimized for rice croplands in China (e.g. Liu *et al.*, 2012). Indeed, the posterior model largely differs from the prior model in the estimated climate change impacts on LGP change (Fig. S6), further highlighting the necessity of optimizing crop models for regional studies. Admittedly, the optimized model simulations still cannot perfectly reproduce spatiotemporal variations in LGP, which may introduce uncertainties in the attribution of LGP trends to climate trends, but this should not largely impact our conclusions because we found no significant correlation between trend in the residual LGP (difference between observations and

simulation S0) and the trend in growing season temperature (Fig. S9). This indicates that the trend attributed to OM is probably not biased by climate trend unexplained by ORCHIDEE-crop. On the other hand, in addition to optimizing the parameters of a single model against observations to reduce parameter uncertainties, recent studies indicate that multiple models can perform better than one model (Li *et al.*, 2015, Martre *et al.*, 2015), due to the consideration of structural uncertainties. Although there are many difficulties in coordinating multiple models, promising future studies using model ensembles with the same protocol can improve our understanding regarding the structural uncertainties (e.g. Elliott *et al.*, 2015). It should also be noted that almost all current rice models, including ORCHIDEE-crop predict phenology development based on variations in temperature. The physiological impacts of non-temperature drivers should be further explored in future studies. Finally, observational error may also play an important role in the attribution to OM, which have largely been neglected both in our modelling study and previous statistical attribution (e.g. Zhang et al., 2013). Since the observation over all the stations followed the same protocol (CMA, 1993), it is often assumed that the observational error is uniform across sites and years. Thus, it would not impact the trend estimates and therefore attribution of the LGP trends. Although the assumption is reasonable, the reliability of this assumption remains uncertain. For better data-model integration, we recommend future data collection efforts to further report the error term together with the observations, which will help minimize potential biases in model parameterization and attribution efforts.

Conclusions

In this study, we calibrated ORCHIDEE-crop model to represent spatio-temporal variations of rice LGP for three different types of rice in China, and applied this model forced by historical change in climate and transplanting date to attribute the trend in rice

LGP. On one hand, we showed that, technically, 1) using Bayes-based particle filter, a generic process-based crop model can be objectively parameterized to represent spatio-temporal variations in rice LGP over China and 2) attribution of LGP trend based on calibrated model provides an alternative to statistical attribution previously used. On the other hand, through factorial simulations, we found that LGP change for different rice types show contrasting dominant drivers. Managements outweighs climate change in affecting LGP of early and single rice, but not for late rice. This suggests that future modelling efforts at global and regional scale should consider various types of rice grown and time-varying management practices. Since large uncertainties still remain in understanding change in LGP, improving documentation of management practices in addition to transplanting date, better description of observational error and ensemble crop modelling can further reduce uncertainties in attributing climate change impacts in future studies.

Appendix: Particle filter with sequential importance resampling

The basic idea of the particle filter is to represent the probability distribution function (PDF) of the parameters through an ensemble of parameters, each set of which is called a particle. At each step of the particle filter, the relative importance of the particle, or weight (w) is given by Eq. A1:

$$w_i = \frac{p(y|x_i)}{\sum_{i=1}^{N} p(y|x_i)} \qquad (Eq.A1)$$

where N is the number of particles, y is the observation and $p(y|x_i)$ is probability density of the observations given the simulation with the particle x_i ($M(x_i)$) following Eq. A2:

$$p(y|x) = e^{-\frac{(y-M(x))^2}{2\delta^2}} \qquad (Eq.A2)$$

where δ is the observation error. In this study, we assume observational error is

uniform across sites and years, since the observations over the network were made by trained staff following the same protocol (CMA, 1993), which are designed to unify and minimize the observational error across the network. Theoretically, it is possible to analytically have the PDF of the particles by putting all observations into the equation in one time. However, in practice, over a large number of sites/time steps, it requires a large number of particles to well sample the entire parameter space and computationally inefficient by wasting time in barely possible particles. Therefore, the Markov process (filter) to realize recursive Bayesian theorem is applied here (Eq. A3):

$$p(x^{1:N}) = p(x^N|x^{N-1})\ p(x^{N-1}|x^{N-2})\ldots p(x^2|x^1) \qquad \textbf{(Eq.A3)}$$

where $x^{1:N}$ is the particle after N iterations. This Markov process makes the entire calculation iterative. When there is no observation in site i, the Markov process can still evolve by adding a random term to the particle in site i-1, but what we aim is to obtain final posterior PDF of the parameters given the observations over N sites ($y^{1:N}$):

$$p(x^{1:N}|y^{1:N}) = \frac{p(y^{1:N}|x^{1:N})p(x^{1:N})}{p(y^{1:N})} \qquad (Eq.\ A4)$$

Using Eq. A3 to further break down Eq. A4, we obtain Eq. A5:

$$p(x^{1:N}|y^{1:N}) = \frac{p(y^N|x^N)p(x^N)}{p(y^N)}\ \frac{p(y^{N-1}|x^{N-1})p(x^{N-1})}{p(y^{N-1})}\ldots\frac{p(y^1|x^1)p(x^1)}{p(y^1)} \qquad (Eq.\ A5)$$

Applying Eq. A2 to Eq. A5, we obtained the numerical solution for all terms from 1 to N. For each step i, importance resampling is taking place to randomly redraw a new ensemble of particles from the weighted old ensemble to represent $p(x^i)$, which leads to disregard particles that have very small weights and thus refine the ensemble. Sometimes the importance resampling may disregard some locally low probably particles but having global significance. Therefore, we usually perform twice of the entire PFSIR process with different re-order observations to test its convergence in order to minimize the potential

error due to this. More details and illustration of the particle filter can be found in van Leeuwen (2010). To adapt ORCHIDEE-crop model to different cropping systems, single rice and double rice (early rice and late rice) in China, we adapted particle filter with sequential importance resampling (van Leeuwen, 2009) separately for the three rice types (Table 1).

Prior parameters of the ORCHIDEE-crop was obtained from (Irfan, 2013). The range of prior parameters were obtained from Sanchez et al. (2014), which synthesized experiment knowledge on the range of basal, optimal and maximum temperature thresholds of rice development, and Valade et al. (2014), which contains modeller's prior knowledge for the range of the parameters. Since we knew little about the prior probability distribution of the parameters, we assumed the prior parameter equally distributed within its range in order to guarantee a well sampling of the entire parameter space. Another issue may limit the capability of PFSIR is the error in the observation data. Unfortunately, accuracy description of the phenology observations are not available except that observations were made following the same standard protocol. However, the dataset is being treated as reliable data source without the need to do further filtering (e.g. Tao et al., 2013; Zhang et al., 2013).

References

Aggarwal PK, Mall RK (2002) Climate change and rice yields in diverse agro-environments of India. II. Effect of uncertainties in scenarios and crop models on impact assessment. *Climatic Change,* **52**, 331-343.

Ai Z, Qing X, Peng J (2010) Ecological suitability of different combinations of hybrid rice varieties for

double rice cropping in Hunan province. *Hybrid Rice,* **S1**, 371-377

Bassu S, Brisson N, Durand J-L *et al.* (2014) How do various maize crop models vary in their responses to climate change factors? *Global Change Biology,* **20**, 2301-2320.

Bilionis I, Drewniak BA, Constantinescu EM (2014) Crop physiology calibration in CLM. *Geoscientific Model Development Discussions,* **7**, 6733-6771.

Brisson N, Gary C, Justes E *et al.* (2003) An overview of the crop model stics. *European Journal Of Agronomy,* **18**, 309-332.

Burke M, Emerick K (2015) *Adaptation to climate change: evidence from US agriculture* Stanford University SSRN 2144928.

China Meteorological Administration (1993) Agro-meteorological Observation Standard. China meteorological press, Beijing.

Chmielewski F-M, Müller A, Bruns E (2004) Climate changes and trends in phenology of fruit trees and field crops in Germany, 1961-2000. *Agricultural And Forest Meteorology,* **121**, 69-78.

Chorin AJ, Morzfeld M (2013) Conditions for successful data assimilation. *Journal of Geophysical Research: Atmospheres,* **118**, 11,522-511,533.

De Vries ME, Leffelaar PA, Sakan N, Bado BV, Giller KE (2011) Adaptability of irrigated rice to temperature change in sahelian environments. *Experimental Agriculture,* **47**, 69-87.

Elliott J, Müller C, Deryng D *et al.* (2015) The Global Gridded Crop Model Intercomparison: data and modeling protocols for Phase 1 (v1.0). *Geosci. Model Dev.,* **8**, 261-277.

Estrella N, Sparks TH, Menzel A (2007) Trends and temperature response in the phenology of crops in Germany. *Global Change Biology,* **13**, 1737-1747.

Gaucherel C, Campillo F, Misson L, Guiot J, Boreux JJ (2008) Parameterization of a process-based tree-growth model: Comparison of optimization, MCMC and Particle Filtering algorithms. *Environmental Modelling & Software,* **23**, 1280-1288.

Gervois S, De Noblet-Ducoudré N, Viovy N, Ciais P, Brisson N, Seguin B, Perrier A (2004) Including Croplands in a Global Biosphere Model: Methodology and Evaluation at Specific Sites. *Earth Interactions,* **8**, 1-25.

Gregory PJ, Marshall B (2012) Attribution of climate change: a methodology to estimate the potential contribution to increases in potato yield in Scotland since 1960. *Global Change Biology,* **18**, 1372-1388.

He L, Asseng S, Zhao G *et al.* (2015) Impacts of recent climate warming, cultivar changes, and crop management on winter wheat phenology across the Loess Plateau of China. *Agricultural And Forest Meteorology,* **200**, 135-143.

Huo Z, Wang S (2009) *Agriculture and Meteorological Disasters*, China Meteorological Press.

Irfan K (2013) Adaptation of the generic crop model STICS for rice (*Oryza sativa L.*) using farm data in Camargue. PhD Thesis, Universite Aix-Marseille, France.

Kersebaum KC, Boote KJ, Jorgenson JS *et al.* (2015) Analysis and classification of data sets for calibration and validation of agro-ecosystem models. *Environmental Modelling & Software,* **72**, 402-417.

Krinner G, Viovy N, De Noblet-Ducoudré N *et al.* (2005) A dynamic global vegetation model for studies of the coupled atmosphere-biosphere system. *Global Biogeochem. Cycles,* **19**, GB1015.

Kropff M, Van Laar H, Matthews R, Ten Berge H (1993) *ORYZA1, a basic model for irrigated lowland rice production,* Manila, Philippines, International Rice Research Institute.

Li Q, Ye X, Yang Z (2010) Impacts of climatic condition and its change on the temperature suitability and potential productivity of rice in the Yangtze River delta of China. *Journal of Zhejiang University – Agriculture & Life Sciences*, **26**, 39-45.

Li R, Zhang K, Gan Y, Ren B, Huang W (2016) Adaptability test report of different double-cropping late Japonica varieties and their sowing dates in Miluo. *Hunan Agricultural Sciences*, **3**, 18-20.

Li T, Hasegawa T, Yin X *et al.* (2015) Uncertainties in predicting rice yield by current crop models under a wide range of climatic conditions. *Global Change Biology,* **21**, 1328-1341.

Lin E, Xiong W, Ju H, Xu Y, Li Y, Bai L, Xie L (2005) Climate change impacts on crop yield and quality with CO2 fertilization in China. *Philosophical Transactions of the Royal Society B: Biological Sciences,* **360**, 2149-2154.

Liu L, Wang E, Zhu Y, Tang L (2012) Contrasting effects of warming and autonomous breeding on single-rice productivity in China. *Agriculture, Ecosystems & Environment,* **149**, 20-29.

Liu Y, Wang E, Yang X, Wang J (2010) Contributions of climatic and crop varietal changes to crop production in the North China Plain, since 1980s. *Global Change Biology,* **16**, 2287-2299.

Lobell DB, Hammer GL, Mclean G, Messina C, Roberts MJ, Schlenker W (2013) The critical role of extreme heat for maize production in the United States. *Nature Clim. Change,* **3**, 497-501.

Lobell DB, Roberts MJ, Schlenker W, Braun N, Little BB, Rejesus RM, Hammer GL (2014) Greater Sensitivity to Drought Accompanies Maize Yield Increase in the U.S. Midwest. *Science,* **344**, 516-519.

Lobell DB, Sibley A, Ivan Ortiz-Monasterio J (2012) Extreme heat effects on wheat senescence in India. *Nature Clim. Change,* **2**, 186-189.

Mao Y, Xiong Y, Zeng T *et al.* (2015) Effects of different ecological conditions on yield of different high quality rice varieties. *Seed*, 34, 92-95.

Martre P, Wallach D, Asseng S *et al.* (2015) Multimodel ensembles of wheat growth: many models are better than one. *Global Change Biology,* **21**, 911-925.

Ministryofagriculture (2014) Technical advices for protecting late rice in southern China from the cold dew wind http://www.moa.gov.cn/fwllm/nszd/2014nszd/201407/t20140731_3985986.htm (ed rice expert team of Ministry of Agriculture).

Olesen JE, Trnka M, Kersebaum KC *et al.* (2011) Impacts and adaptation of European crop production systems to climate change. *European Journal Of Agronomy,* **34**, 96-112.

Porter JR, Xie L, Challinor AJ *et al.* (2014) Food security and food production systems. In: *Climate Change 2014: Impacts, Adaptation, and Vulnerability. Part A: Global and Sectoral Aspects. Contribution of Working Group II to the Fifth Assessment Report of the Intergovernmental Panel of Climate Change.* (eds Field CB, Barros VR, Dokken DJ, Mach KJ, Mastrandrea MD, Bilir TE, Chatterjee M, Ebi KL, Estrada YO, Genova RC, Girma B, Kissel ES, Levy AN, Maccracken S, Mastrandrea PR, White LL) pp Page. Cambridge, United Kingdom and New York, NY, USA, Cambridge University Press.

Rosenzweig C, Elliott J, Deryng D *et al.* (2014) Assessing agricultural risks of climate change in the 21st century in a global gridded crop model intercomparison. *Proc Natl Acad Sci U S A,* **111**, 3268-3273.

Russell G, Marshall B, Jarvis PG (1990) *Plant Canopies: Their Growth, Form and Function*, Cambridge University Press.

Sacks WJ, Kucharik CJ (2011) Crop management and phenology trends in the U.S. Corn Belt: Impacts

on yields, evapotranspiration and energy balance. *Agricultural And Forest Meteorology,* **151**, 882-894.

Sánchez B, Rasmussen A, Porter JR (2014) Temperatures and the growth and development of maize and rice: a review. *Global Change Biology,* **20**, 408-417.

Salmon JM, Friedl MA, Frolking S, Wisser D, Douglas EM (2015) Global rain-fed, irrigated, and paddy croplands: A new high resolution map derived from remote sensing, crop inventories and climate data. *International Journal of Applied Earth Observation and Geoinformation,* **38**, 321-334.

Siebert S, Ewert F (2012) Spatio-temporal patterns of phenological development in Germany in relation to temperature and day length. *Agricultural And Forest Meteorology,* **152**, 44-57.

Solomon (2016) *Climate econometrics*, NBER Working Paper 22181(http://www.nber.org/papers/w22181)

Summerfield RJ, Collinson ST, Ellis RH, Roberts EH, De Vries FWTP (1992) Photothermal Responses of Flowering in Rice (Oryza sativa). *Annals Of Botany,* **69**, 101-112.

Tao F, Yokozawa M, Xu Y, Hayashi Y, Zhang Z (2006) Climate changes and trends in phenology and yields of field crops in China, 1981-2000. *Agricultural And Forest Meteorology,* **138**, 82-92.

Tao F, Zhang S, Zhang Z, Rötter RP (2014a) Maize growing duration was prolonged across China in the past three decades under the combined effects of temperature, agronomic management, and cultivar shift. *Global Change Biology,* **20**, 3686-3699.

Tao F, Zhang Z, Shi W *et al.* (2013) Single rice growth period was prolonged by cultivars shifts, but yield was damaged by climate change during 1981-2009 in China, and late rice was just opposite. *Glob Chang Biol,* **19**, 3200-3209.

Tao F, Zhang Z, Xiao D *et al.* (2014b) Responses of wheat growth and yield to climate change in

different climate zones of China, 1981–2009. *Agricultural And Forest Meteorology,* **189–190**, 91-104.

Valade A, Ciais P, Vuichard N *et al.* (2014) Modeling sugarcane yield with a process-based model from site to continental scale: uncertainties arising from model structure and parameter values. *Geosci. Model Dev.,* **7**, 1225-1245.

Van Leeuwen PJ (2009) Particle Filtering in Geophysical Systems. *Monthly Weather Review,* **137**, 4089-4114.

Van Leeuwen PJ (2010) Nonlinear data assimilation in geosciences: an extremely efficient particle filter. *Quarterly Journal Of The Royal Meteorological Society,* **136**, 1991-1999.

Wu L, Huo Z, Jiang Y, Zhang L, Yu C (2014) Geographical distribution of risk factors on cold dew wind of late rice in southern China. *Chinese Journal of Ecology,* **33**, 2817-2823.

Wu X, Vuichard N, Ciais P et al. (2015) ORCHIDEE-CROP (v0), a new process based Agro-Land Surface Model: model description and evaluation over Europe. *Geosci. Model Dev. Discuss*., **8**, 4653-4696.

Xiao D, Tao F, Liu Y *et al.* (2013) Observed changes in winter wheat phenology in the North China Plain for 1981-2009. *International Journal Of Biometeorology,* **57**, 275-285.

Xie B, Luo B, Yin J, Song Z, Li Y (2008) Index Identification of Suitable Temperature at the Booting Stage and Accumulated Temperature over 10℃ during the Whole Growth Period in Rice in South China. *Journal of Anhui Agricultural Sciences,* **32**, 044.

Yao F, Xu Y, Lin E, Yokozawa M, Zhang J (2007) Assessing the impacts of climate change on rice yields in the main rice areas of China. *Climatic Change,* **80**, 395-409.

Yin X (1994) A Nonlinear Model to Quantify Temperature Effect on Rice Phenology and It's Application.

Acta Agronomica Sinica, **6**, 007.

Yin X, Struik PC (2009) C3 and C4 photosynthesis models: An overview from the perspective of crop modelling. *NJAS - Wageningen Journal of Life Sciences,* **57**, 27-38.

Yu Z, Fu X, Lü H *et al.* (2014) Evaluating Ensemble Kalman, Particle, and Ensemble Particle Filters through Soil Temperature Prediction. *Journal of Hydrologic Engineering,* **19**, 04014027.

Zhang S, Tao F (2013) Modeling the response of rice phenology to climate change and variability in different climatic zones: Comparisons of five models. *European Journal Of Agronomy,* **45**, 165-176.

Zhang S, Tao F, Shi R (2014a) Modeling the rice phenology and production in China with SIMRIW: sensitivity analysis and parameter estimation. *Frontiers of Earth Science,* **8**, 505-511.

Zhang S, Tao F, Zhang Z (2014b) Rice reproductive growth duration increased despite of negative impacts of climate warming across China during 1981–2009. *European Journal Of Agronomy,* **54**, 70-83.

Zhang T, Huang Y, Yang X (2013) Climate warming over the past three decades has shortened rice growth duration in China and cultivar shifts have further accelerated the process for late rice. *Global Change Biology,* **19**, 563-570.

Zhou F, Shang Z, Ciais P *et al.* (2014) A New High-Resolution N2O Emission Inventory for China in 2008. *Environmental Science & Technology,* **48**, 8538-8547.

Supplementary Information

Figure S1. Response of phenology development to temperature based on the prior parameters. See Methods section and Eq. 2 for detail explanations for the parameters (T_{min}, T_{opt} and T_{max}).

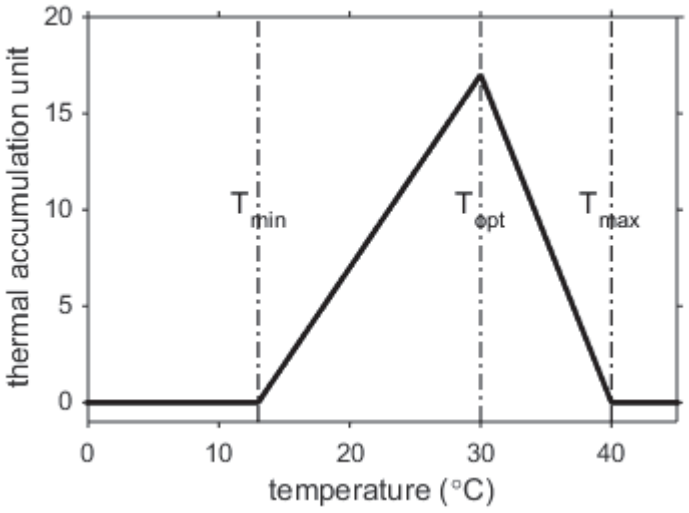

Figure S2. Comparison of trend estimates by parametric tests (linear regression slope) and non-parametric tests (Sen's slope). Different colors indicate sites of different rice types (early rice, late rice and single rice). The dash line indicates 1:1 ratio.

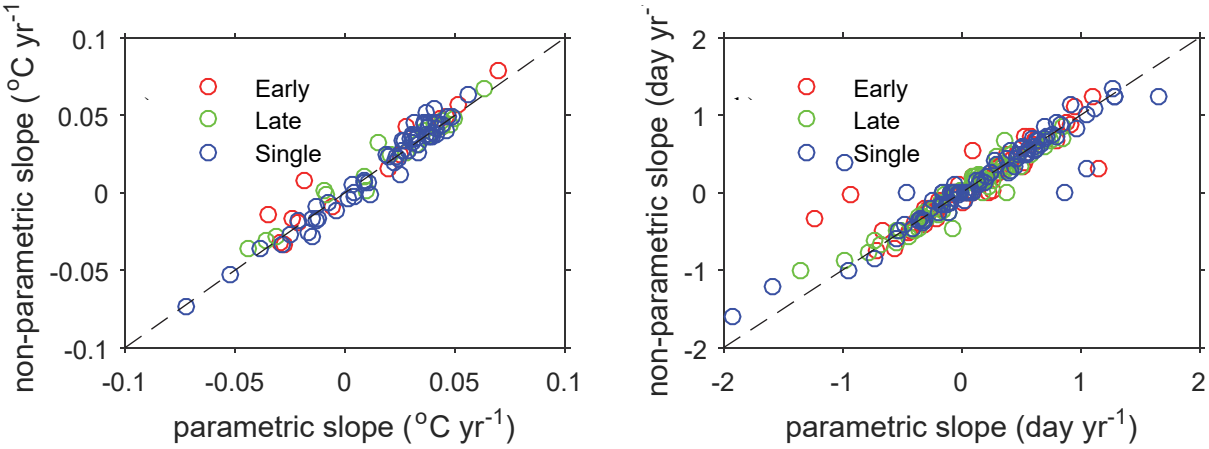

Figure S3. Spatial distribution of long-term (>15 years) rice phenology observation sites. Shaded area indicates the rice growing area with darker pixels having larger growing area.

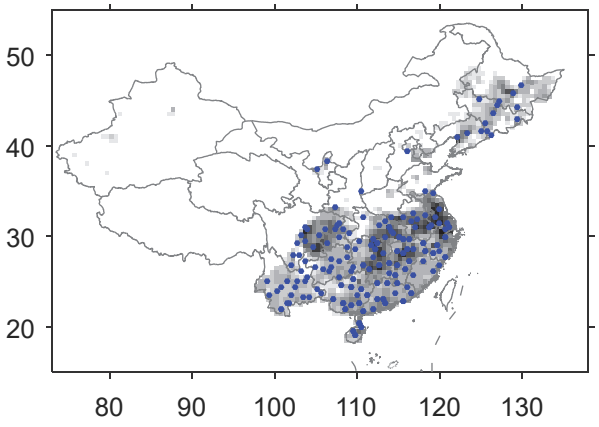

Figure S4. Spatial relationship between observed length of rice growing period length (LGP) and simulated LGP for (a) optimization sites of early rice, (b) optimization sites of late rice, (c) optimization sites of single rice, (d) validation sites of early rice, (e) validation sites of late rice, and (f) validation sites of single rice.

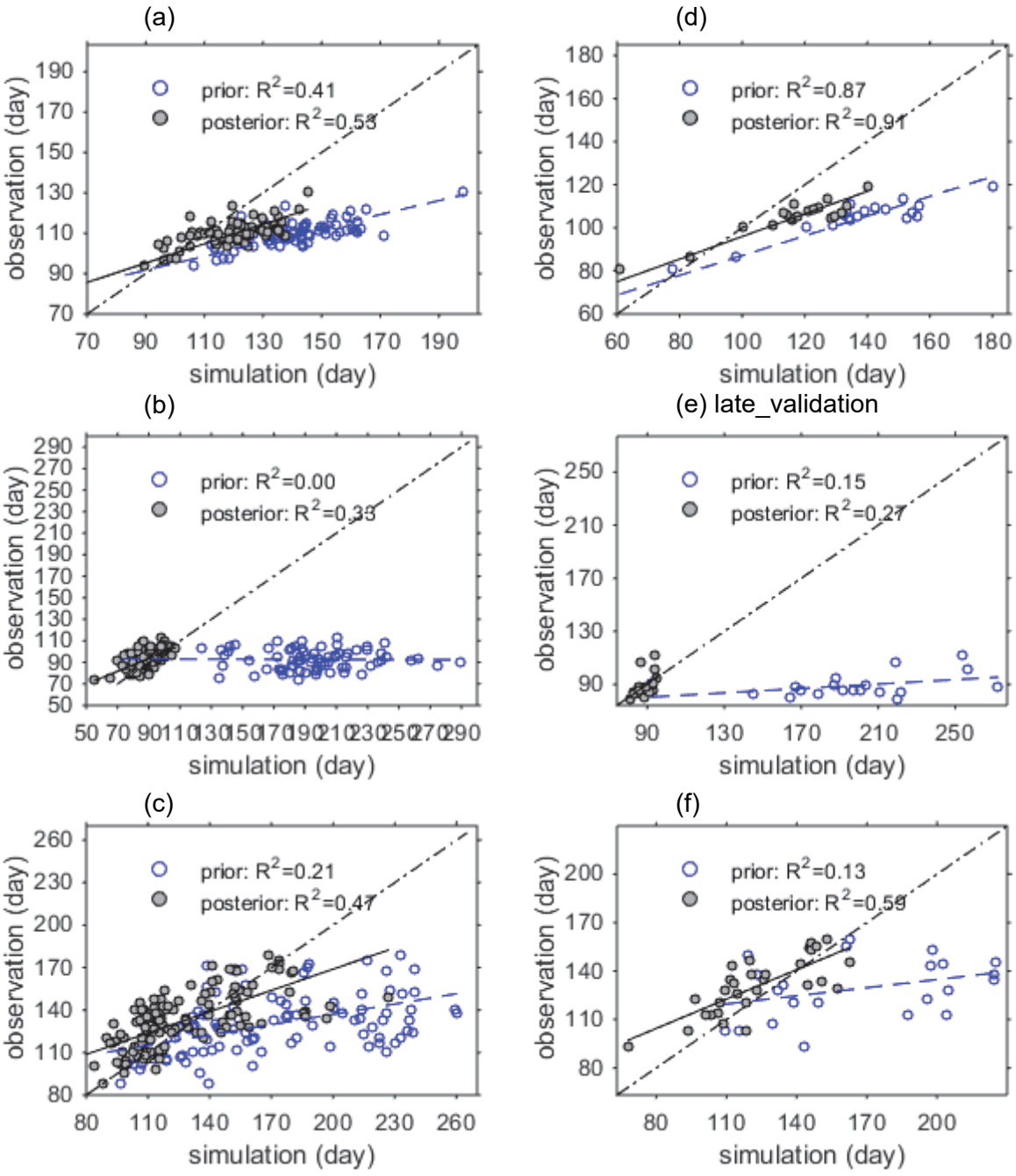

Figure S5. Inter-annual relationship between observed length of rice growing period (LGP) and simulated LGP for (a) optimization sites of early rice, (b) optimization sites of late rice, (c) optimization sites of single rice, (d) validation sites of early rice, (e) validation sites of late rice, and (f) validation sites of single rice. Blue-edge bars indicate simulation results with prior parameters, and grey bars indicate simulation results with posterior parameters.

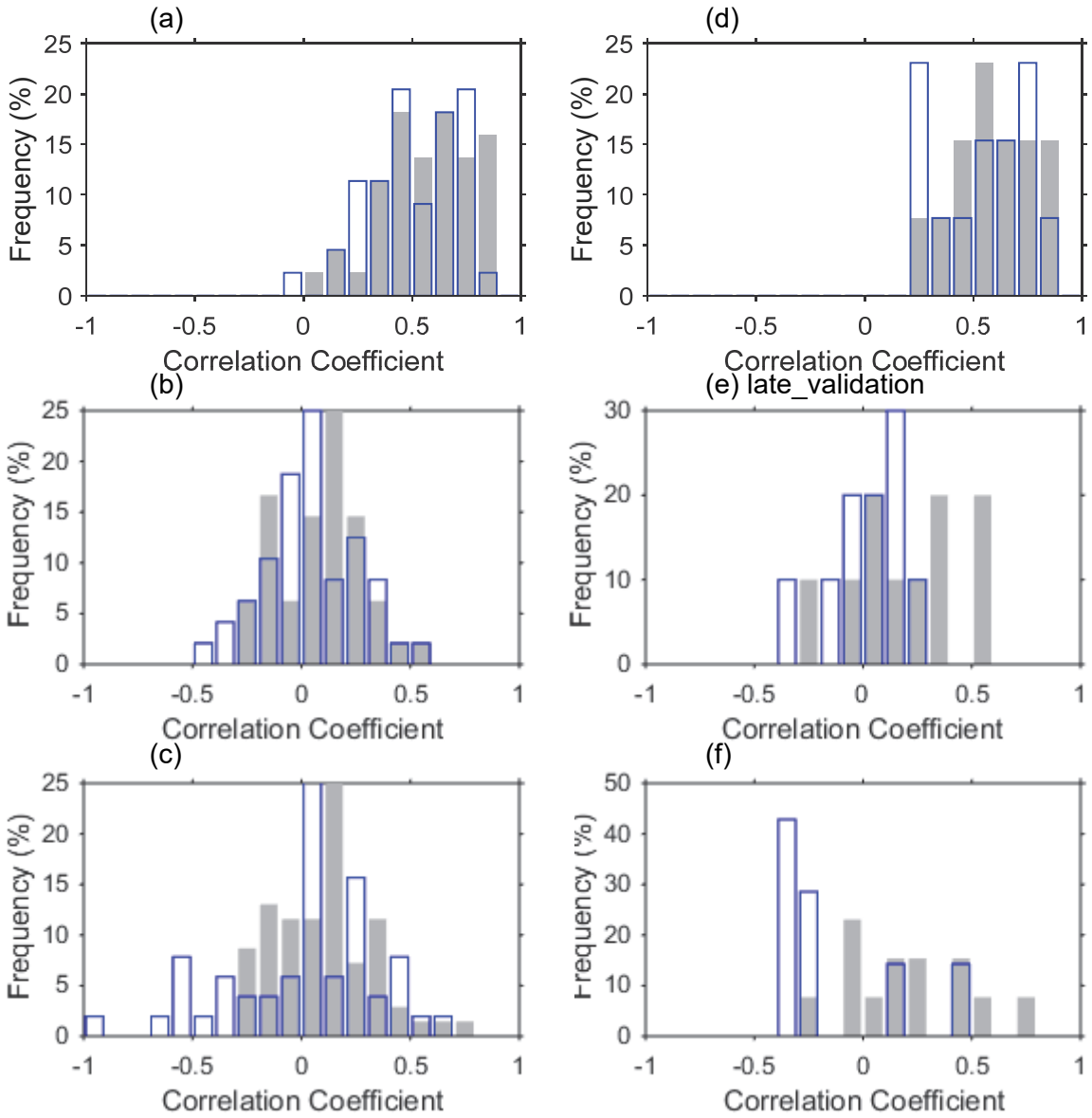

Figure S6. Histogram of change in length of rice growing period (LGP) estimated by ORCHIDEE-crop model for (a) early rice sites, (b) late rice sites and (c) single rice sites. Blue-edge bars indicate simulations with prior parameters, and grey bar indicate simulations with posterior parameters.

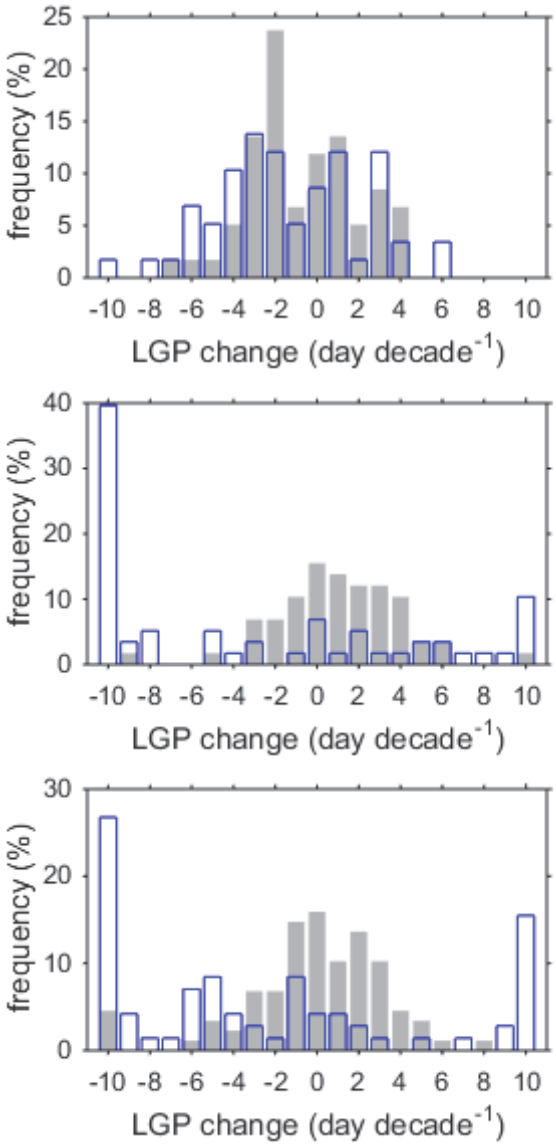

Figure S7. Spatial distribution of change in length of rice growth period (LGP) over the past two decades derived from (a-c) observations, (d-f) the difference of observations and simulation S0 (driven by observed transplanting date, see Methods section), (g-i) the difference of simulation S0 and simulation S1 (driven by fixed transplanting date, see Methods section) and (j-l) simulation S1 for (left panel) early rice sites, (central panel) late rice sites and (right panel)single rice sites. Black square indicates statistically significant (P<0.05) trend.

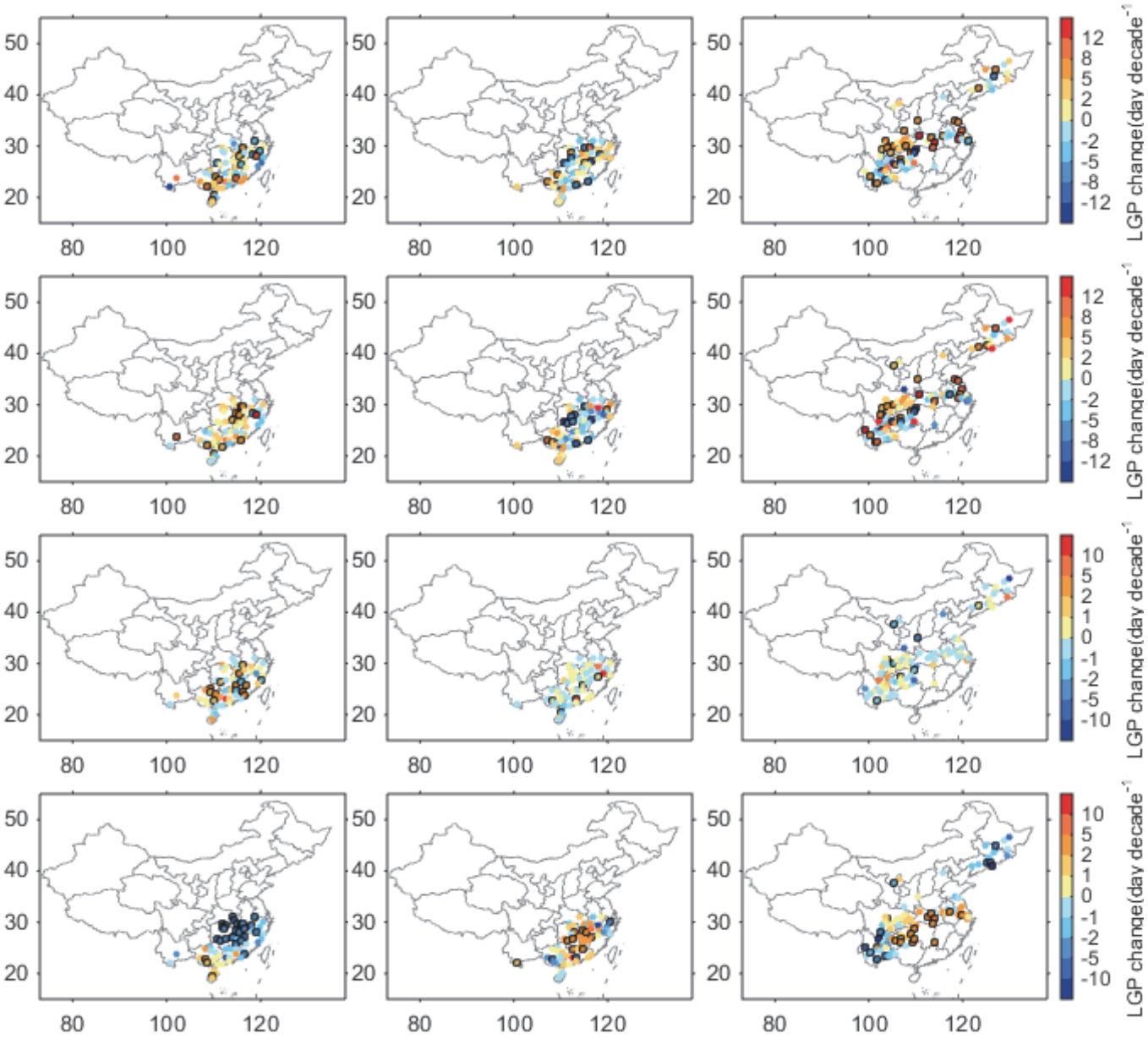

Figure S8. Spatial pattern of change in transplanting date over the past two decades for (a) early rice sites, (b) late rice sites and (c) single rice sites.

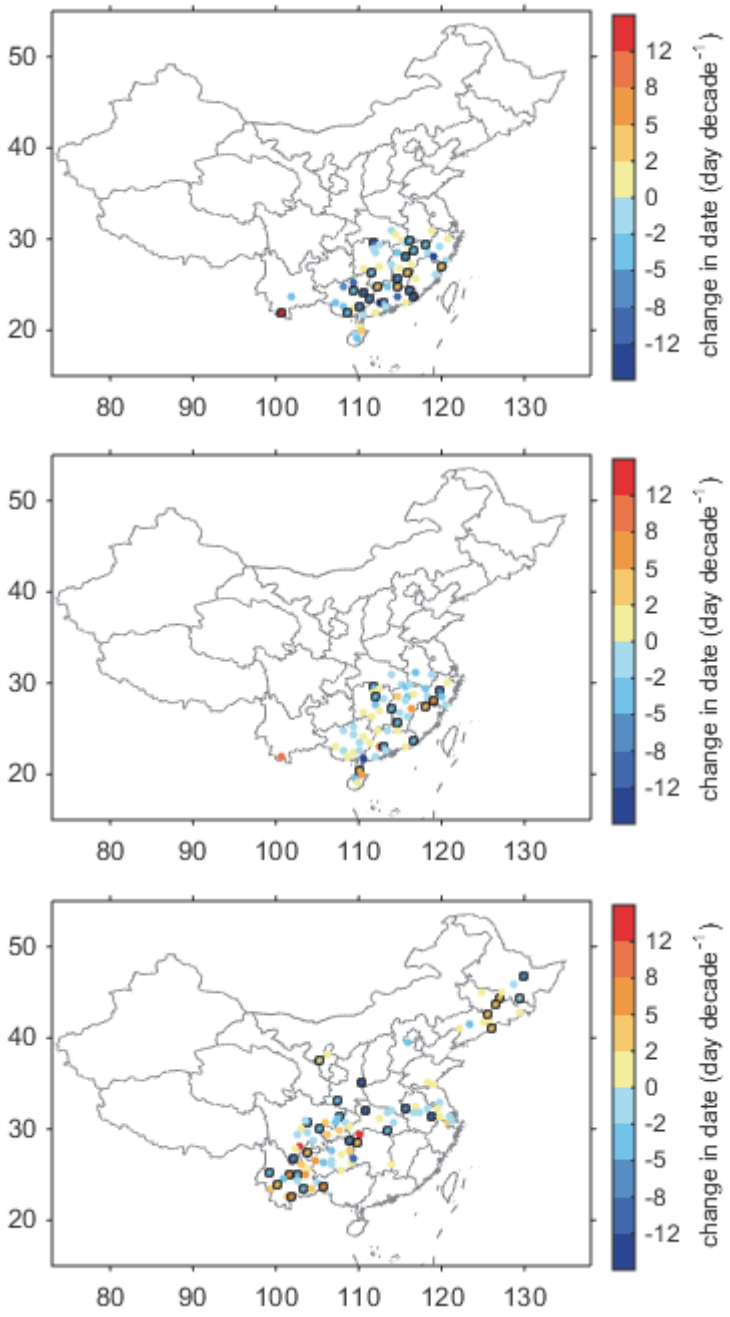

Figure S9. Relationship between trend in growing season temperature and trend in LGP residual (the difference between observed LGP and simulated LGP after optimization) for (a) early rice sites, (b) late rice sites and (c) single rice sites.

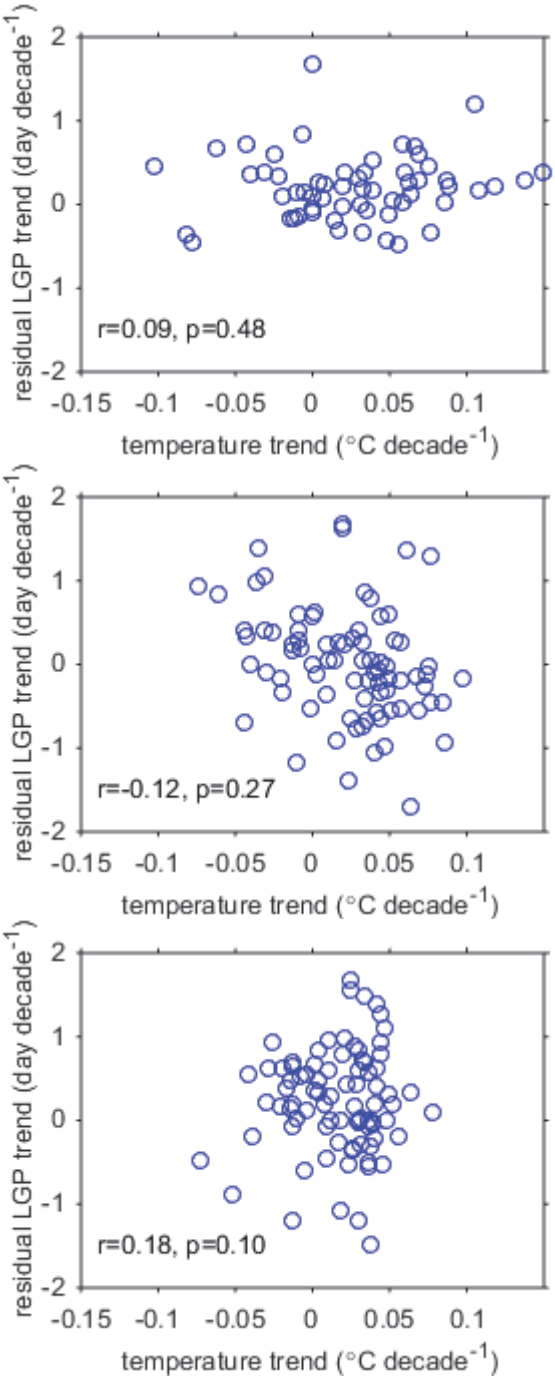

Figure S10. Spatial pattern of change in growing season temperature over the past two decades for (a) early rice sites, (b) late rice sites and (c) single rice sites.

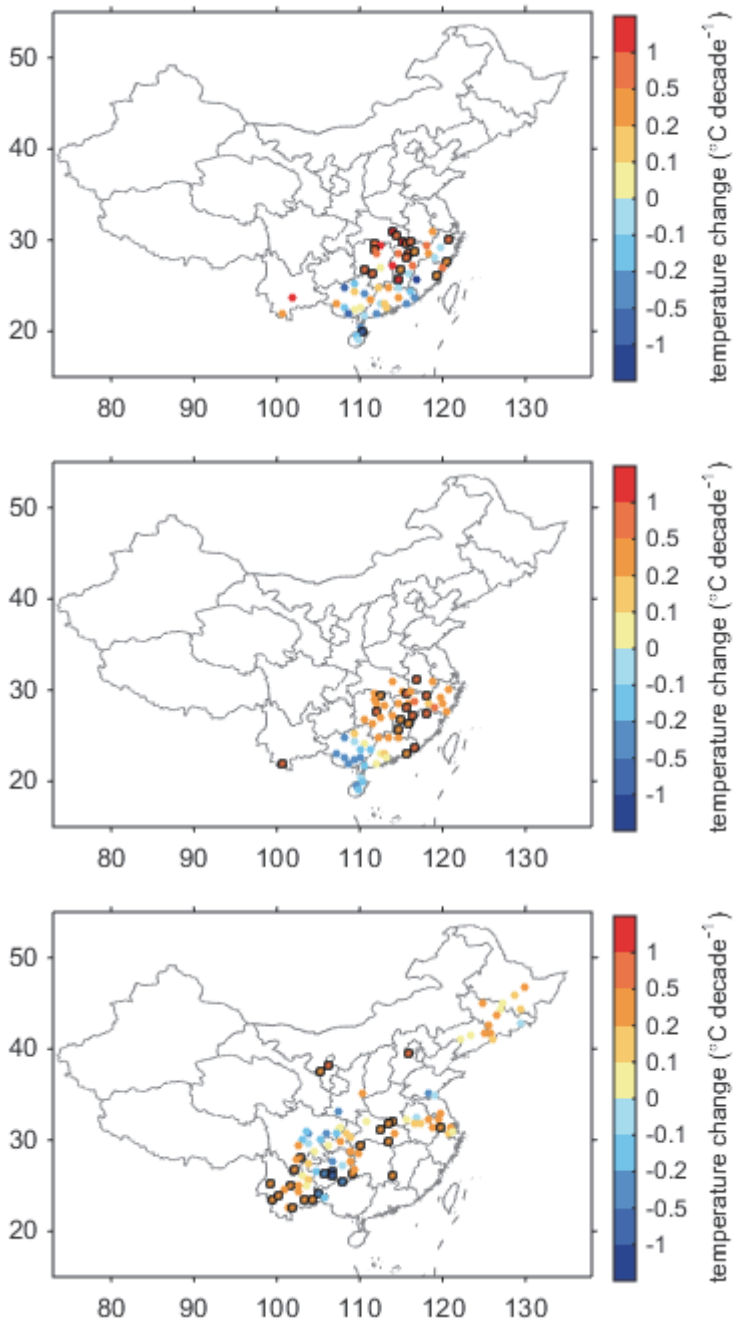

Chapter 4 Reanalyzing global crop yield response to warmer temperature using manipulation experiments and global crop models

Summary

Response of global crop yield to warmer temperature is fundamental to food security under climate change, but its magnitude remains uncertain and largely relies on crop modeling (Challinor et al., 2014; IPCC AR5). Here, we harmonized a global dataset of field warming experiments comprised of 48 sites for the big four crops (wheat, maize, rice and soybean), and utilized the ensemble of gridded global crop models (Rosenzweig et al., 2014) together to perform data-constraint estimates of crop yield response to change in temperature (S_T). Compared with warming experiments, ensemble mean of crop models tends to overestimate the magnitude of S_T for wheat, but underestimate S_T for other crops. Through emergent constraint at global scale, we have more than 90% confidence that warmer temperature will reduce yield for maize (-7.1±2.8% K^{-1}), rice (-5.6±2.0% K^{-1}) and soybean (-10.6±5.8% K^{-1}), while S_T for wheat is also likely to be negative (-2.9±2.3% K^{-1}). The data-based constraint reduces uncertainties associated with crop model estimates by 12%-54% for different crops. At country scale, the best estimates of S_T for the top five producers of each crop are prevalently negative. Considering different climate change scenarios (1.5 K, 2.0 K, RCP2.6 & RCP6.0 at the end of this century), yield loss due to

warming ranges from 2% to 24% among these major producers, and the maximum yield loss becomes 12%, if global warming can be limited by 2.0K. Even with the lowest warming scenario (1.5 K), none of major producers for the studied crops is likely to benefit from warmer temperature without effective adaptation, though yield vulnerabilities may differ by one magnitude across crops and countries. At the time of preparation, this chapter is going to be submitted as Wang X *et al.* Field warming experiments constrain global crop yield reductions under Paris' global warming targets.

Rapid warming over the past decades have significant impacts on crop yield (Lobell et al., 2011). The severity of this issue has been masked by yield increment through green revolution. With exhaustion of technological potential (Brisson et al., 2010) and expected increase in climate change impacts (Tubiello et al., 2007), our society is facing a great challenge: Can we ensure food security for the ever-growing global population under climate change? The first step to adapt for expected warmer climate is to understand how crop yield response to temperature change. It was generally believed that warmer temperature negatively affects crop yield when baseline temperature is about or above the optimum, while it could positively affect crop yield in cool region where temperature is well below the optimum (Porter et al., 1999; IPCC AR4; Sanchez et al., 2014). However, recent studies show that higher temperature in cool climate can also reduce crop yields (Semenov et al., 2012; Teixeira et al., 2013; Asseng et al., 2015). Despite our growing knowledge that the yield response to temperature change is crop and region specific (e.g. Zhao et al., 2016ab; Asseng et al., 2016), the global picture of crop yield respond to warmer temperature is still quite vague. The winners and losers of crop production due to warmer temperature remains largely uncertain either.

Crop models are the widely used tools in predicting yield response to warming (Wheeler et al., 2013; Challinor et al., 2014). These process-based models simulate how temperature affect crop growth dynamics at daily or sub-daily time-steps, though models may vary in the formula, in the way of model tuning, and thus in parameter values. Contemporary assessment of crop response to warmer climate largely relies on crop simulations performed with different models, settings and locations (Challinor et al., 2014;

Asseng et al., 2014; IPCC AR5). The ensemble of gridded crop models (Rosenzweig et al., 2014) provides us a set of global simulations driven by consistent climate and management forcing. Recent studies show that model ensemble may have smaller biases in simulated yield than the individual model over the multi-site tests (Asseng et al., 2014; Bassu et al., 2014; Martre et al., 2015; Li et al., 2015), but the structure and parameter differences in the models still result in large uncertainties in the yield response to temperature change (Asseng et al., 2013; Asseng et al., 2014; Bassu et al., 2014; Martre et al., 2015; Li et al., 2015; Muller et al., 2016). On the other hand, by exposing crops to artificial warming, field warming experiments provide direct estimates on yield response to warmer temperature, without hypotheses on the processes. For decades, scientists have performed warming experiment for various crops around the world (Van et al., 1999; Ottman et al., 2012; Tian et al., 2012), comprising a rich mine to dig for exploring warming impacts. However, these experiments have largely been neglected in current global assessments (e.g. Challinor et al., 2014; IPCC AR5; Liu et al., 2016) due to the challenge to scale up from field to regions and the globe. In this study, we address this challenge with the emergent constraint approach (Cox et al., 2013), through which we reassess global and regional crop yield response to warmer temperature jointly using field warming experiments and crop models. We focus on the big four crops (wheat, maize, rice and soybean), which accounts for more than 60% of global caloric production.

First, we harmonized a global field warming experiment dataset comprised of 48 sites (Fig 1) coming from 46 peer-reviewed literatures (see Methods). Wheat is the mostly studied crop with 25 sites, which distribute over the top four wheat producers (European Union, China, India and US). If we assume pixels with similar baseline climate (difference

in mean annual temperature less than 1ºC and difference in annual precipitation less than 150mm) to the sites can be well represented by the sites, 70% of the wheat cropping area is well represented (Fig 1a). The less represented area mostly locates in northern high latitude, such as central Canada and Russian Siberia. Rice has the second most sites spreading among the top-two rice producing countries (China and India) and others (Fig 1b). Although cropping area of wheat and rice are on the same magnitude, the extents of rice cropping area are much more concentrated than that of wheat. The 15 sites (60% of wheat sites) still well represent 60% of rice cropping area. The less represented area has very humid climate, like that around the equator. There are five maize sites in four countries including top two maize producers (US and China), which account 60% of global maize production. 30% of maize cropping area is well represented, but hot climate zones (e.g. Africa and South America) are not (Fig 1c). Soybean has the least number of sites among them. The three sites locate in US and Japan, well representing 15% of global soybean croplands. Though soybean production of the two countries accounts for 35% of global production, major data gaps exist for other large soybean producers, such as Brazil, Argentina and China (Fig 1d).

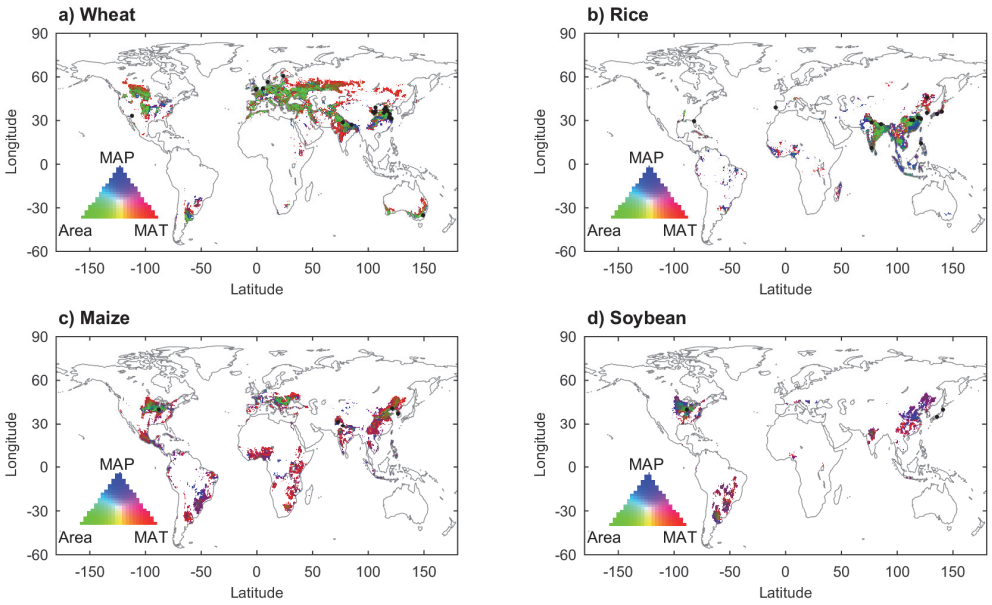

Figure 1 Spatial pattern of experiment sites and its representativeness for (a) wheat, (b) rice, (c) maize and (d) soybean. Black dots show the location of experiment sites. Representativeness is measured according to the difference between the grid and the site with most similar climate in mean annual temperature (MAT) and mean annual precipitation (MAP). Well represented area (see Methods) is shown in green, with brighter green color indicate closer climate resemblance to experiment sites and larger harvest area. Blue and red color gradient is proportional to the difference between grids and sites in MAT and MAP. Blue colors indicate larger difference in MAP, while red color indicate larger difference in MAT. Magenta colors indicate the differences in both MAT and MAT are large. Only contemporary crop harvest area is shown for each crop according to Chad et al., 2008.

As the field warming sites are not evenly distributed over the cropping area and crop yield response to warming varied largely with background climate (Ruiz-Vera et al., 2014; Zhao et al., 2016), statistics (e.g. mean or median) of the sites cannot be directly interpreted as regional/global values. However, we found that crop models simulating larger negative warming impacts on the experiment sites also predict larger yield loss in response to

warmer temperature globally (Fig 3a-d). This strong relationship (R^2=0.46-0.87 for different crops) between site-scale yield response to warmer temperature (S_T) and global-scale S_T enables us to use observations at field experiment sites to constraint the probability distribution of global yield response to change in temperature. At the experiment sites, the observed S_T are largely within the range of S_T simulated by seven models, but difference between observed S_T and model mean S_T have different signs among different crops. For wheat, the observed site-mean S_T (-1.6±1.2% K^{-1}) is close to the upper end of simulated site-mean S_T (Fig 2a), while the observed site-mean S_T for maize (-10.3±1.0% K^{-1}) and soybean (-7.4±2.9% K^{-1}) are at the lower end of simulated site-mean S_T (Fig 2c-d). For rice, the observed site-mean S_T (-7.4±2.9%K^{-1}) relatively close to the model mean.

Fig 2e shows the probability density function (PDF) of global S_T predicted by ensemble crop models before constraint (assuming each crop model is equally likely to correctly estimate S_T) and that by emergent constraint with observations from field warming sites. The emergent constraint both changes the best estimates of global S_T and narrows the associated uncertainties (s.d. of the PDF) by 12% - 54% for different crops studied. For wheat, the best estimate of global S_T reduces to -2.9±2.3% K^{-1} from -3.8±2.6% K^{-1}. On the contrary, global S_T for the other crops become more negative (-7.1±2.8% K^{-1} for maize, -5.6±2.0% K^{-1} for rice, and -10.6±5.8% K^{-1} for soybean respectively) than the prior model estimates (-2.9±6.1% K^{-1} for maize, -4.6±2.8% K^{-1} for rice, and -4.2±6.6% K^{-1} for soybean respectively). Among the four crops, largest correction of global S_T occurred in soybean (150%), but the uncertainties of global S_T of soybean is at least two times than the other crops, due to very limited number of warming experiment sites for soybean (Fig 1c) and large discrepancies across the sites on the warming impacts (Fig 2d; Tacarindua et al., 2013;

Kumagai & Sameshima, 2014; Ruiz-Vera et al., 2015). The prior model spread in S_T for maize is similar to that for soybean (Fig 2e). However, the high confidence of warming impacts over the experiment sites results in tripled estimates of global S_T and largest error reduction (54%) through observational constraint. The constraint leads to relatively smaller change in best estimates of S_T for rice (22%) and wheat (14%), as the prior spread of crop model estimates on wheat and rice yield response to warming are about 40% to that of maize and soybean (Fig 2a-b) and relatively more consistent with the field warming experiments. Previous studies for wheat reporting widespread negative impacts of warming on wheat yield has already raised alerts on global food security (e.g. Zhao et al., 2016; Liu et al., 2016). However, the magnitude of wheat yield loss in response to warming is much less than that of maize and rice, which are the staple food resources for developing countries in Africa and Asia, highlighting a potentially larger susceptibility of the less developed countries to climatic change.

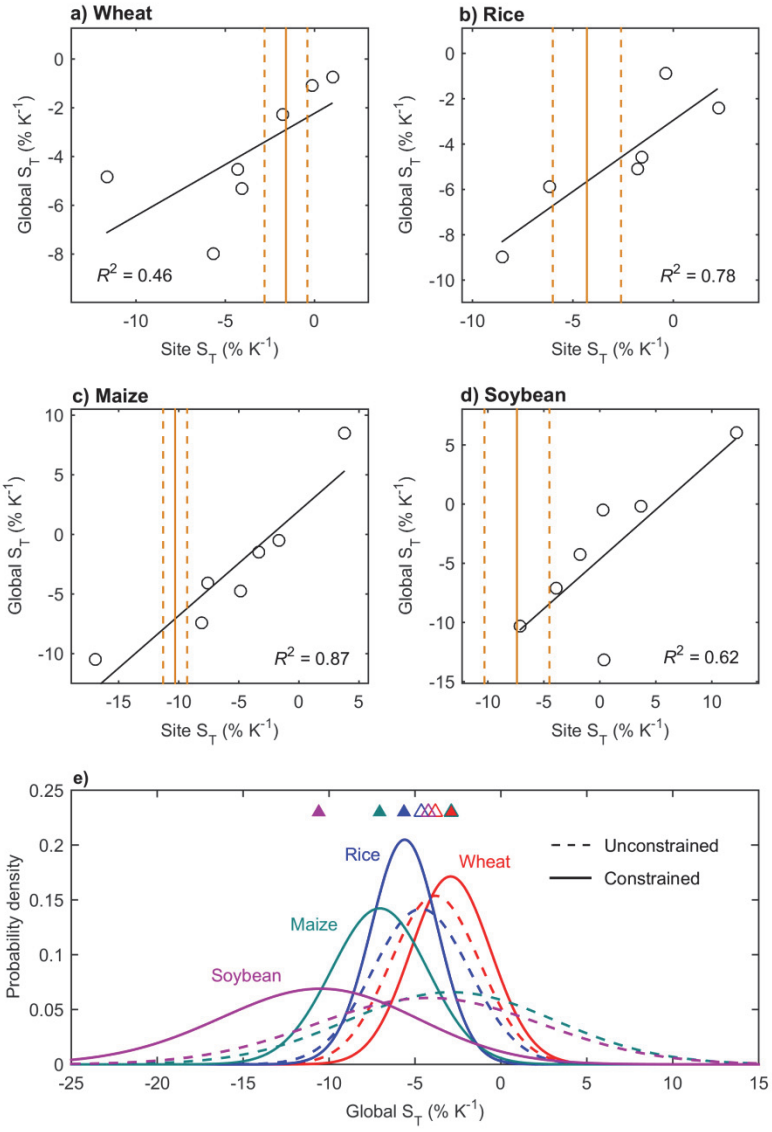

Figure 2 Emergent constraint of crop yield response to temperature change (S_T) based on experiment data. (a-d) Relationship between S_T over the field warming experiment sites and S_T over the globe simulated by global gridded crop models for (a) wheat, (b) rice, (c) maize and (d) soybean. Orange lines shows the best estimates of S_T (Solid lines) and associated uncertainties (Dashed lines) derived from the experiments. (e) probability density function of global S_T before (dashed lines) and after constraint by experiment data (solid lines) for the four crops. The empty triangles show the ensemble model mean of S_T before

constraint, while the filled triangles show the best estimate of S_T after constraint.

To distinguish potential winners and losers due to warming, we further constraint country-wide S_T over top five producers of each crop, which represent 35% - 59% of global production of that crop (FAO, 2014). The relationship between simulated global S_T and country-wide S_T across the models are used in this constraint (see Methods; Extended Data Fig 1). For major producers of wheat, S_T over India, USA and France are larger than global S_T (Fig 3a), which is less than half of S_T over India (-7.0±4.5% K^{-1}). S_T over China (-2.6±4.8% K^{-1}) and Russia (-2.6±4.3% K^{-1}) are similar and slightly lower than global S_T, though prior model estimates show larger S_T over China than that over Russia (Fig 3a). Data-based multi-regional analyses that can be compared with our study is still lacking, but recent hotspot analysis of warming impacts on wheat yield seems supporting our finding that India may be one of the most susceptible wheat producer to warmer temperature (Asseng et al., 2016), suggesting our country-based constraint approach is quite robust though still with large uncertainties. Indeed, the uncertainties of wheat S_T after constraint at the country scale are 2-3 times than that of global wheat S_T (Fig 3a). The country-scale S_T for wheat may be even slightly larger than the prior model ensemble, because models disagree largely on regional differences in S_T (Extended Data Fig 2). Similar lack of error reduction applies to country-scale S_T for soybean (Fig 3g), but not for rice (Fig 3c) and maize (Fig 3e), where observational constraint reduces uncertainties for country-scale S_T by 4% - 44% for different countries (Fig 3c & e). For rice, the difference in S_T among countries are relatively small. China, the largest rice producer, has the least negative rice S_T of -4.3±3.1% K^{-1}, while Bangladesh, one of the least developed countries, may suffer most from warming (-6.8±2.9% K^{-1}). For maize, S_T across countries differ more than two times.

Maize yield of its largest producer, USA, is probably mostly affected by warming ($-10.9\pm6.0\%\ K^{-1}$). Although the prior model ensemble shows some major producers (maize over France and soybean over Argentina) might have slight yield increment in response to warming, however, the observational constraint shows that none of the major producers for the studied crops is likely going to benefit from warming (Fig 3).

The expected warming may not be unanimous globally that lower latitudes and coastal area may experience smaller magnitude or warming than the rest land area (IPCC AR5). Therefore, in addition to spatial variations in S_T, the projected spatial pattern of warming may also affect the vulnerability and uncertainties in crop yield responses to projected global warming. For wheat and rice, the difference in yield response is dominantly explained by the difference in S_T across countries (Fig 3b,d). It is less so for maize and soybean as the predicted yield responses of different countries deviate from the gradient of S_T (Fig 3f,h). This is mostly related to that the magnitude of warming over US corn belt is much lower than other major maize producing area (Extended Data Fig 6). In spite of uncertainties in spatial variations of S_T and warming magnitude, the overall picture is quite clear. Even with the 1.5 degree scenario, which is the target set in Paris agreement and has the lowest magnitude of warming, the yield loss in response to warming can still be substantial ranging from 1.6% to 6.6% among major cereal producers (Fig 3b,d,f,h). If anthropogenic CO_2 emission follows voluntary nationally determined contributions, the track of emission will lie between RCP 2.6 and RCP 6.0 (Hempel et al., 2013). Accordingly, at the end of this century, warming induced yield loss may range from 1.8% to 9.6% for major cereal producers under RCP 2.6, and it is between 7.2% and 24.2% under RCP 6.0 (Fig 3b,d,f,h). If we successfully limited global warming by 2.0 K as agreed in the Paris

agreement, the warming induced yield loss can be limited by 2.9-12.5% (Fig 3b,d,f,h).

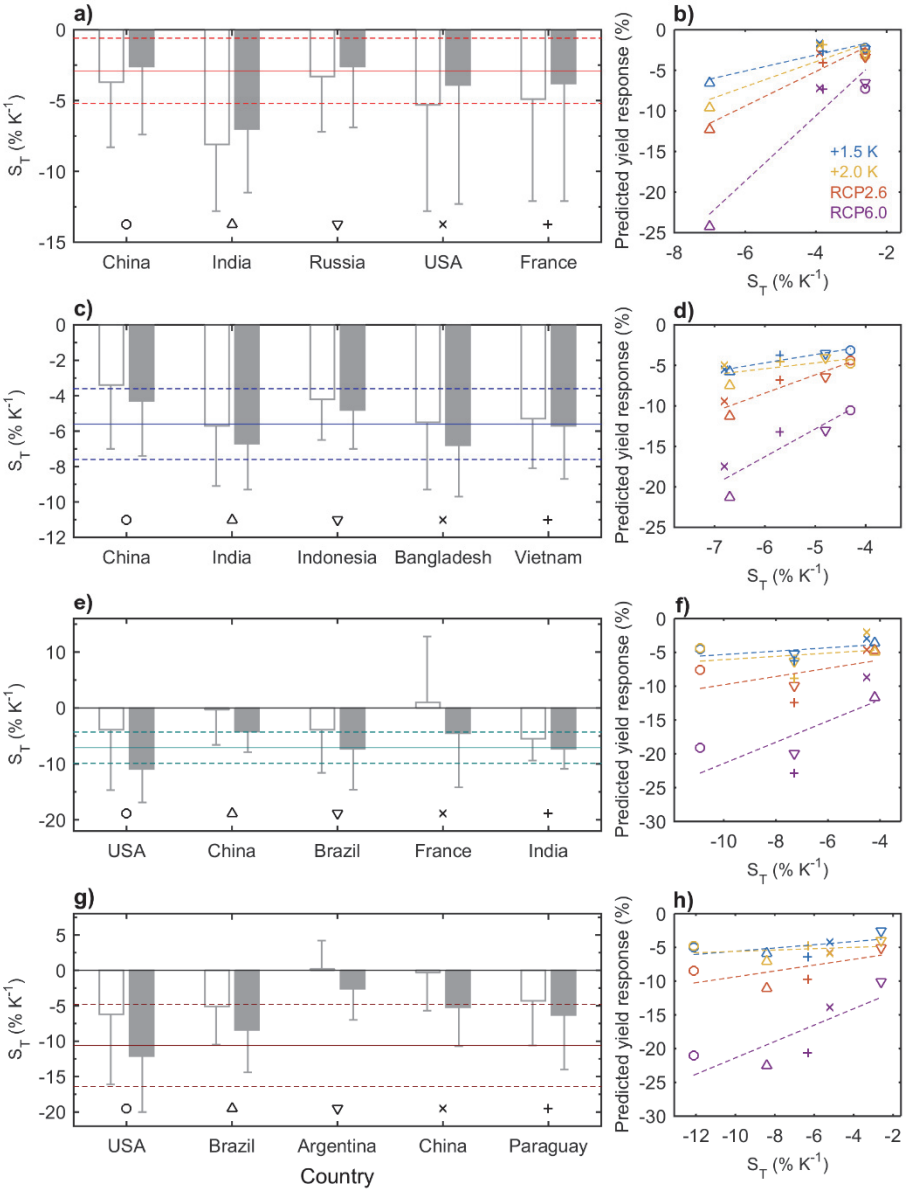

Figure 3 Yield response to temperature change (S_T) and its vulnerability under different climate change scenarios (1.5 K, 2.0 K, RCP2.6 and RCP6.0) over top five producers of (a-b) wheat, (c-d) rice, (e-f) maize and (g-h) soybean. Bars on the left panels show country-scale S_T before (empty bars) and after (filled bars) emergent constraint. Colored

lines show the global-scale S_T and uncertainties after constraint. Right panels show the relationship between S_T and yield loss due to global warming projected by the climate model under different scenarios (1.5 K, 2.0 K, RCP 2.6 and RCP 6.0 at the end of this century).

To summarize, our approach scales up the field warming experiment results to the globe and reduce uncertainties in projected warming impacts on global crop yield. While we have more than 90% confidence that global S_T for maize, rice and soybean is negative, the global S_T for wheat is only likely to be negative because of smaller magnitude of negative response and existence of positive S_T over some experiment sites. With more clear global pictures of S_T, the remaining main uncertainties in projecting warming impacts on crop yield lie in three aspects. First, our constraint approach only slightly reduced uncertainties in regional S_T mainly due to limited number and uneven distribution of available experiment sites. This is particularly the case for latitudes northern than 45°N (Fig 1), which could be substantial with the prospects of northward expansion of croplands (Pugh et al., 2016). Second, the interactive effects of warming and simultaneous change in atmospheric CO_2, moisture supply and adaptation measures are yet well understood and quantified (e.g. Ruiz-Vera et al., 2015; Schauberger et al., 2017; Tack et al., 2016; Usui et al., 2016). For example, FACE experiments show that the interactive effects of warming and atmospheric CO_2 can be either insignificant for rice (Usui et al., 2016) or changing soybean yield by up to 33% (Ruiz-Vera et al., 2013), but extrapolating the few FACE sites to wider regions are still challenging. Finally, spatial pattern, magnitude and seasonality of warming is also a substantial source of uncertainties (e.g. Osborne et al., 2013), which requires joint inter-sectoral modelling efforts (Rosenzweig et al., 2017) by climate and crop modellers.

Methods

Field warming experiments

A literature search was performed on studies that applied artificial warming on wheat, rice, maize or soybean through Web of Science, Google Scholar and China National Knowledge Infrastructure (CNKI; http://www.cnki.net). We considered all peer-reviewed studies published between January 1990 and February 2016 from which the yield changes and warming magnitude were reported. To avoid the confounding effects of methodological difference between field studies and in-door incubations, we restricted the database to field-scale experiments, and no laboratory or controlled condition experiments are included. To avoid short-term noise, we only considered experiments that last more than two months and include reproduction stage of growing season. Following the above criteria, a total of 48 sites (Fig. 1) from 46 literatures were found and included in the analysis. The sensitivity of crop yield to global temperature change, S_T (% K^{-1}), was used to represent the response of crop yield to temperature change. The studies with local temperature change (ΔT) unequal to +1 K were firstly adjusted to +1 K impact by dividing the impact value by ΔT, which assumed a quasi-linear relationship between impacts and ΔT.

$$S_T = \frac{\Delta yield}{\Delta T}$$

Global gridded crop models (GGCMs)

The Inter-Sectoral Impact Model Intercomparison Project 1 (ISI-MIP-1; Warszawski et

al., 2014) started a fast-track global climate impact assessment for the main global crops in 2012, including wheat, rice, maize and soybean. Seven global gridded crop models (EPIC, GEPIC, IMAGE, LPJ-GUESS, LPJmL, pDSSAT and PEGASUS) were used to simulate crop yield in $0.5^o \times 0.5^o$ grid cells over the globe, forced with climate reconstruction for 1980-2099 (Extended Data Figure 2-5). The simulations were carried out under a scenario of constant CO_2 concentration (380 ppm in 2000) and full irrigation, to avoid confusion of covariance with CO_2 and precipitation. More detailed information about the simulations can be found in Rosenzweig et al., 2014. S_T values simulated by global crop models were calculated from yield changes between 2029-2058 (+2 K of global mean temperature) and 1981-2010 (baseline) which were then divided by change in local temperature. For global or country-scale S_T, all the grids were averaged by weighting the corresponding growing area of each crop (Chad et al., 2008).

Emergent Constraint at global and country scale

Emergent constraint is an approach to bridge two diagnostic variables, where one can be confronted with experimental or observed data, the others cannot, across an ensemble of models. Its efficiency has been proved by recent earth system studies in correcting biases and reduce uncertainties (e.g. Cox et al., 2013; Sherwood et al., 2014).The theoretical details of the emergent constraint are explained in Cox et al., 2013. In our study, we applied emergent constraint approach to bridge the S_T at field sites and S_T at global and country scale. For the constraint at global scale, the uncertainties in S_T estimates come from three sources: uncertainties in observed site scale S_T, uncertainties in simulated site scale S_T, and uncertainties in the relationship between site scale S_T and global scale S_T (Fig 2) For the constraint at country scale, it includes an additional source of uncertainties in the

relationship between global scale S_T and country scale S_T simulated by the crop models (Extended Data Fig 6).

Climate change projection under various scenarios

Four climate change scenarios (+1.5 K, +2.0 K, RCP2.6 and RCP8.5) were considered in this study because +1.5 K and +2.0 K are the agreed target by Paris agreement in limiting the degree of global warming (UNFCCC, 2015). RCP2.6 and RCP6.0 represents the lower bounds and higher bounds of emission pathways if anthropogenic CO_2 emission follows INDCs (intended nationally determined contribution; IEA, 2016). The spatial pattern of global warming was deduced from the bias-corrected climate change projection by IPSL-CM5A-LR (Hempel et al., 2013). We used this model result because it is the only available bias-corrected climate projection available for impact studies at the time of preparation of this manuscript. Although a large ensemble of CMIP5 climate model projections are available, it is difficult to extract the scenarios of 1.5 K and 2.0 K (Frieler et al., 2016), mostly because the simulation length did not extended back to pre-industrial period. We defined the period of +1.5 K (+2.0 K) as the 30-year running mean of global temperature exceeding 1.5 K (2.0 K) warmer than the pre-industrial period in RCP2.6 (RCP6.0), following the impact model protocol providing results for the IPCC "special report in 2018 on the impacts of global warming of 1.5 °C above pre-industrial levels and related global greenhouse gas emission pathways" (Frieler et al., 2016). At the end of this century (2070-2099), the global warming projected by the bias-corrected IPSL-CM5A-LR represent 1.7 K (RCP2.6) and 3.2 K (RCP6.0) warmer global temperature than the pre-industrial period (1860-1889). The vulnerability of crop yield of major cereal producers was calculated as the products of S_T and projected temperature change over the country.

References

Asseng, S. *et al*. Uncertainty in simulating wheat yield under climate change. *Nature Clim. Change* **3,** 827–832 (2013).

Asseng, S. *et al*. Rising temperatures reduce global wheat production. *Nature Clim. Change* **5,** 143–147 (2015).

Asseng, S. *et al*. Hot spots of wheat yield decline with rising temperatures. *Global change boil.* (2016). Doi: 10.1111/gcb.13530

Bassu, S. *et al.* How do various maize crop models vary in their responses to climate change factors? *Global Change Biol.* **20**, 2301–2320 (2014).

Brisson, N. *et al*. Why are wheat yields stagnating in Europe? A comprehensive data analysis for France. *Field Crop. Res.* **119**, 201–212 (2010).

Cox, P. M. *et al*. Sensitivity of tropical carbon to climate change constrained by carbon dioxide variability. *Nature* **494,** 341–344 (2013).

Challinor, A. J. *et al*. A meta-analysis of crop yield under climate change and adaptation. *Nature Clim. Change* **4**, 287–291 (2014).

Easterling,W. *et al*. in Climate Change 2007: Impacts, Adaptation and Vulnerability (eds Parry, M. L., Canziani, O. F., Palutikof, J. P., van der Linden, P. J. & Hanson, C. E.) 273–313 (Cambridge Univ. Press, 2007).

FAO, *Food and Agriculture Organization of the United Nations*, http://faostat.fao.org (2014).

Hempel, S., Frieler, K., Warszawski, L., Schewe, J. & Piontek, F. A trend-preserving bias correction–the ISI-MIP approach. *Earth Syst. Dynam.* 4, 219–236 (2013).

Kumagai, E. & Sameshima, R. Genotypic differences in soybean yield responses to increasing temperature in a cool climate are related to maturity group. *Agric. For.*

Meteorol. **198**, 265-272 (2014).

Li, T. *et al*. Uncertainties in predicting rice yield by current crop models under a wide range of climatic conditions. *Global Change Biol.* **21,** 1328–1341 (2015).

Liu, B. *et al*. Similar estimates of temperature impacts on global wheat yield by three independent methods. *Nature Clim. Change* **6**, 1130–1136 (2016).

Lobell, D. B., Schlenker, W. & Costa-Roberts, J. Climate trends and global crop production since 1980. *Science* **333**, 616–620 (2011).

Martre, P. *et al*. Multimodel ensembles of wheat growth: many models are better than one. *Global change biol.* **21**, 911-925 (2015).

Müller, C. *et al*. Global Gridded Crop Model evaluation: benchmarking, skills, deficiencies and implications. *Geosci. Model Dev. Discuss.* (2016). Doi: 10.5194/gmd-2016-207

Osborne, T., Rose, G. & Wheeler, T. Variation in the global-scale impacts of climate change on crop productivity due to climate model uncertainty and adaptation. *Agric. For. Meteorol.* **170**, 183-194 (2013).

Ottman, M. J., Kimball, B. A., White, J. W. & Wall, G. W. Wheat growth response to increased temperature from varied planting dates and supplemental infrared heating. *Agron. J.* **104,** 7–16 (2012).

Porter, J. R. & Gawith, M. Temperatures and the growth and development of wheat: a review. *Eur. J. Agron.* **10**, 23-36 (1999).

Porter, J. R. *et al*. In *Climate Change 2014: Impacts, Adaptation and Vulnerability: Contribution of Working Group II to the Fifth Assessment Report of the Intergovernmental Panel on Climate Change*, Field, C. B. *et al.*, Eds. (Cambridge Univ. Press, Cambridge, 2014), pp. 485–533.

Pugh T. A. M. *et al*. Climate analogues suggest limited potential for intensification of production on current croplands under climate change. *Nature Commun*. **7**, 12608 (2016).

Rosenzweig, C. *et al*. Assessing agricultural risks of climate change in the 21st century in a global gridded crop model intercomparison. *Proc. Natl. Acad. Sci. U.S.A.* **111,** 3268–3273 (2014).

Rosenzweig, C. *et al*. Assessing inter-sectoral climate change risks: the role of ISIMIP. *Environ. Res. Lett.* **12**, 010301 (2017).

Ruiz-Vera, U. M. *et al.* Global Warming Can Negate the Expected CO_2 Stimulation in Photosynthesis and Productivity for Soybean Grown in the Midwestern United States. *Plant Physiol* **162**, 410-423 (2013). Doi:10.1104/pp.112.211938

Ruiz-Vera, U. M. *et al*. Global warming can negate the expected CO_2 stimulation in photosynthesis and productivity for soybean grown in the Midwestern United States. *Plant Physiol.* **162**, 410–423 (2015).

Sánchez, B., Rasmussen, A. & Porter, J. R. Temperatures and the growth and development of maize and rice: a review. *Global Change Boil.* **20**, 408-417 (2014).

Schauberger, B. *et al.* Consistent negative response of US crops to high temperatures in observations and crop models. *Nature Commun.* **8**, 13931 (2017). Doi:10.1038/ncomms13931

Semenov, M. A. *et al*. Shortcomings in wheat yield predictions. *Nature Clim. Change* **2**, 380-382 (2012).

Tacarindua, C. R. P. *et al*. The effects of increased temperature on crop growth and yield of soybean grown in a temperature gradient chamber. *Field Crops Res.* **154**, 74–81 (2013).

Tack, J., Barkley, A. & Nalley L. L. Effect of warming temperatures on US wheat yields. *Proc. Natl. Acad. Sci. USA* **112**, 6931–6936 (2015).

Tack, J. *et al.* Quantifying Variety-specific Heat Resistance and the Potential for Adaptation to Climate Change. *Global Change Boil*. **22**, 2904–2912 (2016).

Teixeira, E. I. *et al*. Global hot-spots of heat stress on agricultural crops due to climate change. *Agric. For. Meteorol.* **170**, 206-215 (2013).

Tian, Y. *et al.* Warming impacts on winter wheat phenophase and grain yield under field conditions in Yangtze Delta Plain, China. *Field Crop. Res.* **134**, 193–199 (2012).

Tubiello, F. N., Soussana, J. F. & Howden, S. M. Crop and pasture response to climate change. *Proc. Natl. Acad. Sci. USA* **104**, 19686-19690 (2007).

Usui, Y. et al. Rice grain yield and quality responses to free-air CO2 enrichment combined with soil and water warming. *Global Change Boil.* **22**, 1256-1270 (2016).

Van, O. M., Schapendonk, A. H. C. M., Jansen, M. J. H., Pot, C. S. & Maciorowski, R. Do open-top chambers overestimate the effects of rising CO_2 on plants? An analysis using spring wheat. *Global Change Biol.* **5**, 411–421 (1999).

Wheeler, T. & Von Braun J. Climate change impacts on global food security. *Science* **341**, 508-513 (2013).

Zhao, C. *et al*. Plausible rice yield losses under future warming. *Nature Plants* **3**, 16206 (2016).

Zhao, C. *et al*. Field warming experiments shed light on the wheat yield response to temperature in China. *Nature Commun.* **7**, 13530 (2016).

Extended Data Figure 1 Relationship between S_T over the globe and S_T over the five major producers simulated by global gridded crop models for (a-e) wheat, (f-j) rice, (k-o) maize and (p-t) soybean.

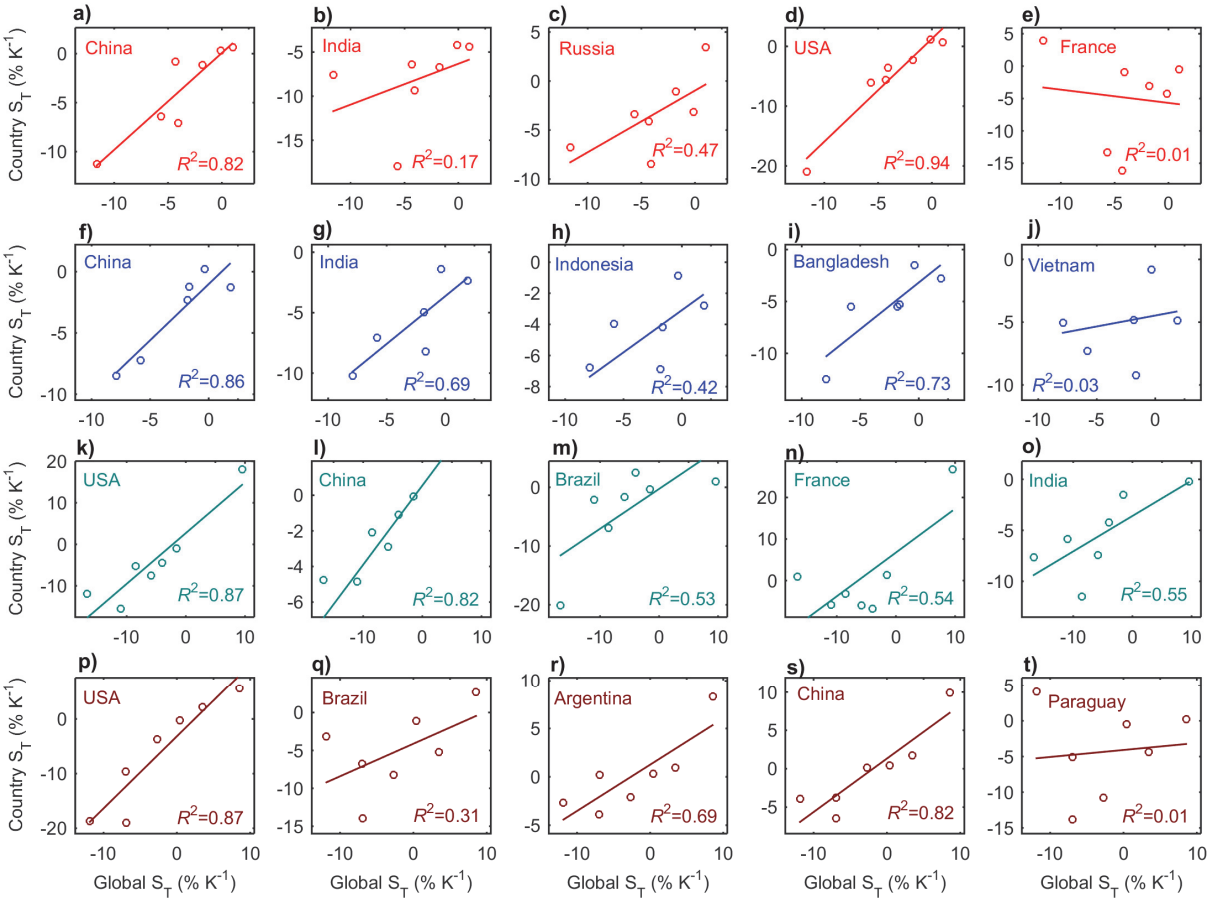

Extended Data Figure 2 Spatial patterns of S_T simulated from seven global gridded crop models (a-g) for wheat. The black dots represent the sites for field warming experiments.

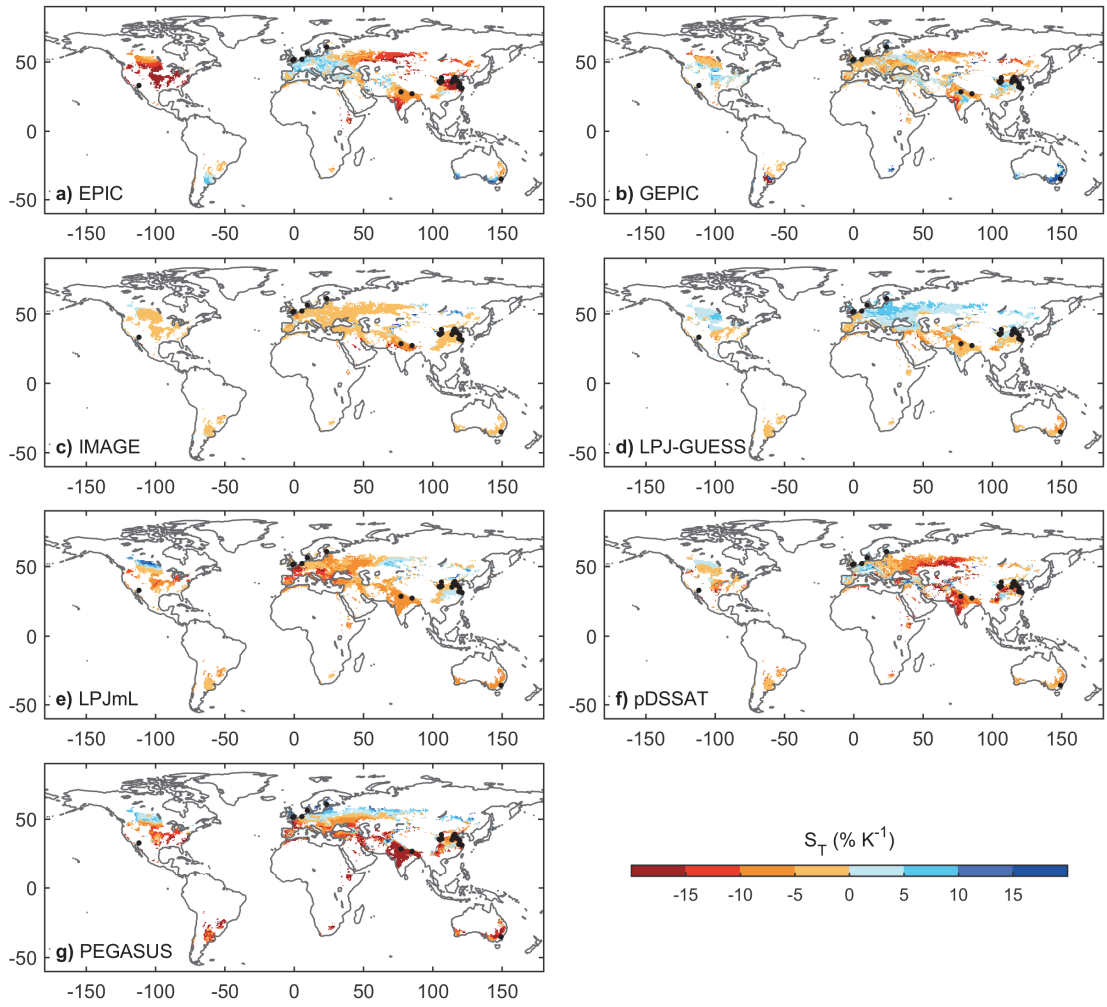

Extended Data Figure 3 Spatial patterns of S_T simulated from seven global gridded crop models (a-g) for rice. The black dots represent the sites for field warming experiments.

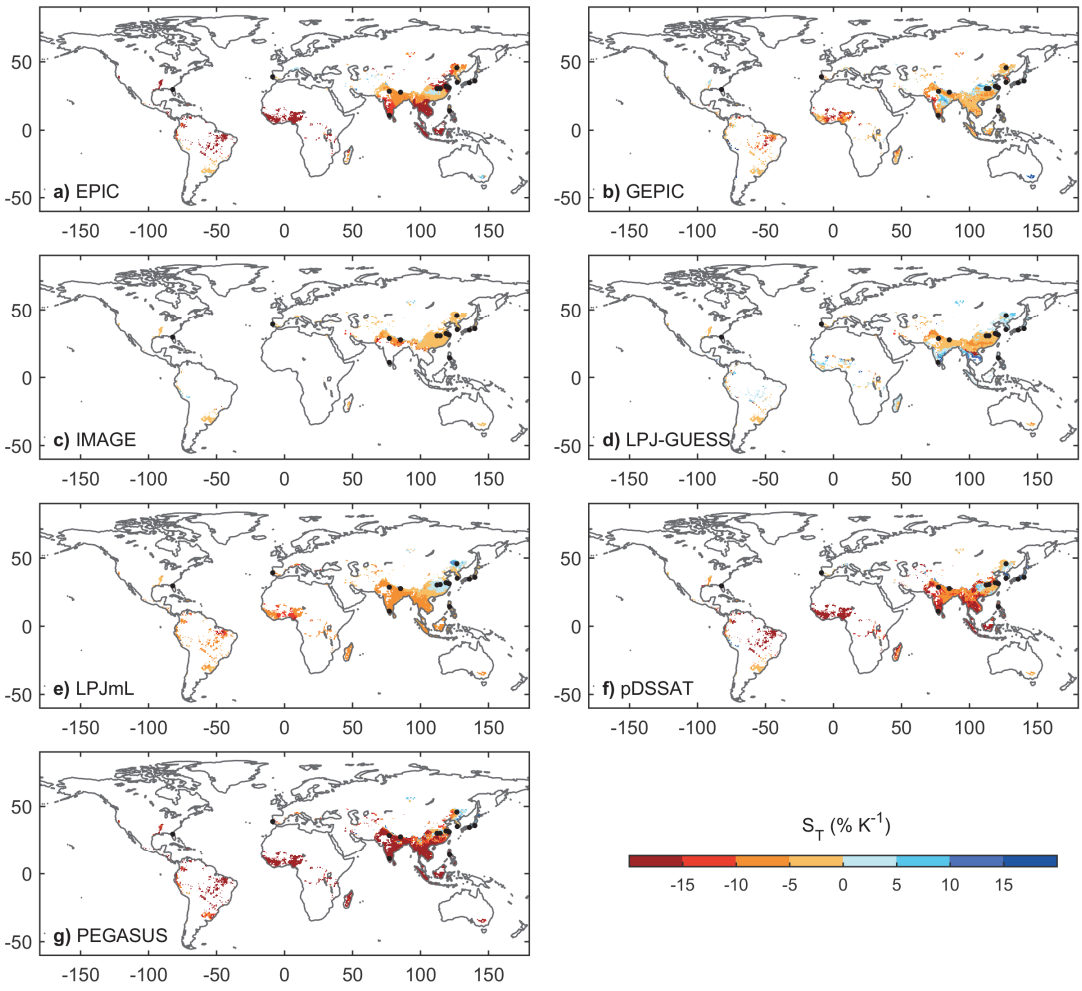

Extended Data Figure 4 Spatial patterns of S_T simulated from seven global gridded crop models (a-g) for maize. The black dots represent the sites for field warming experiments.

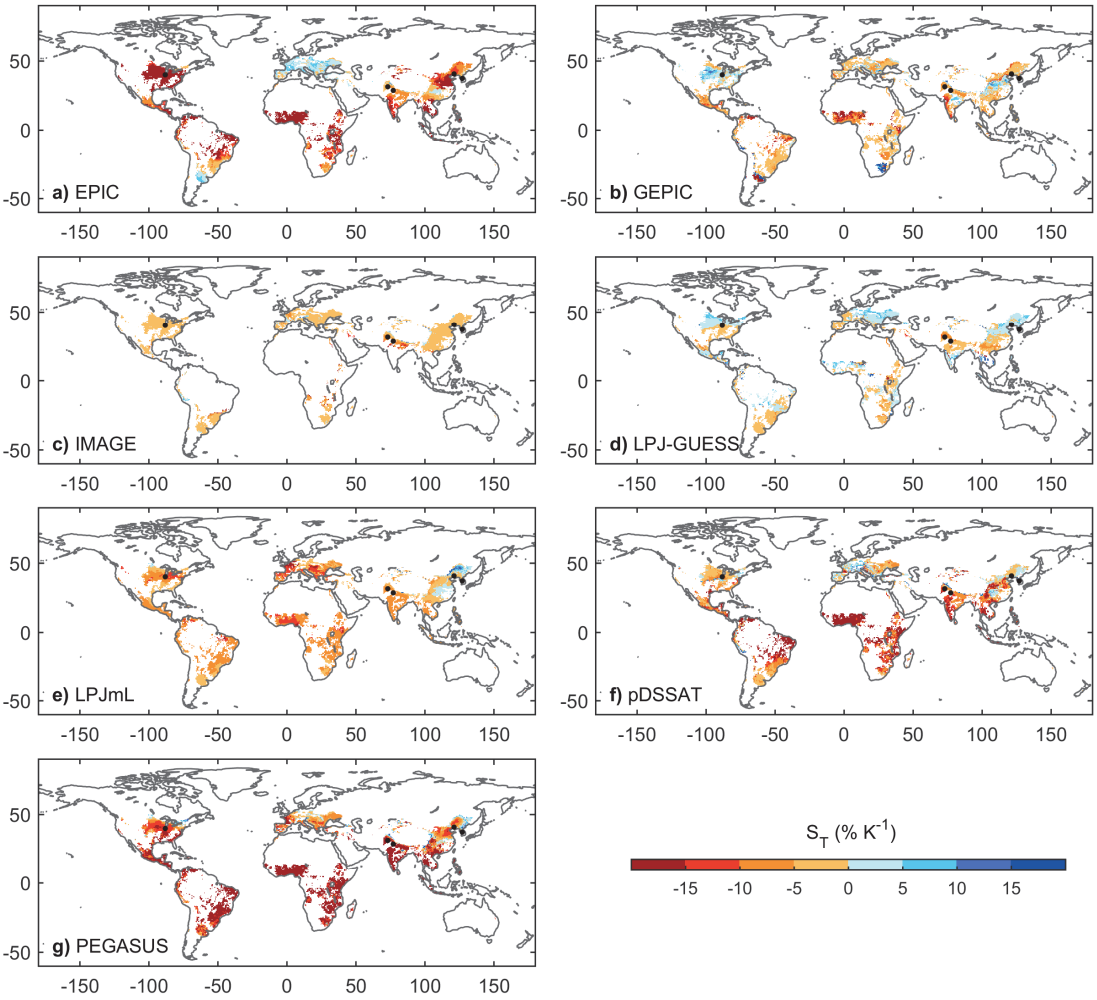

Extended Data Figure 5 Spatial patterns of S_T simulated from seven global gridded crop models (a-g) for soybean. The black dots represent the sites for field warming experiments.

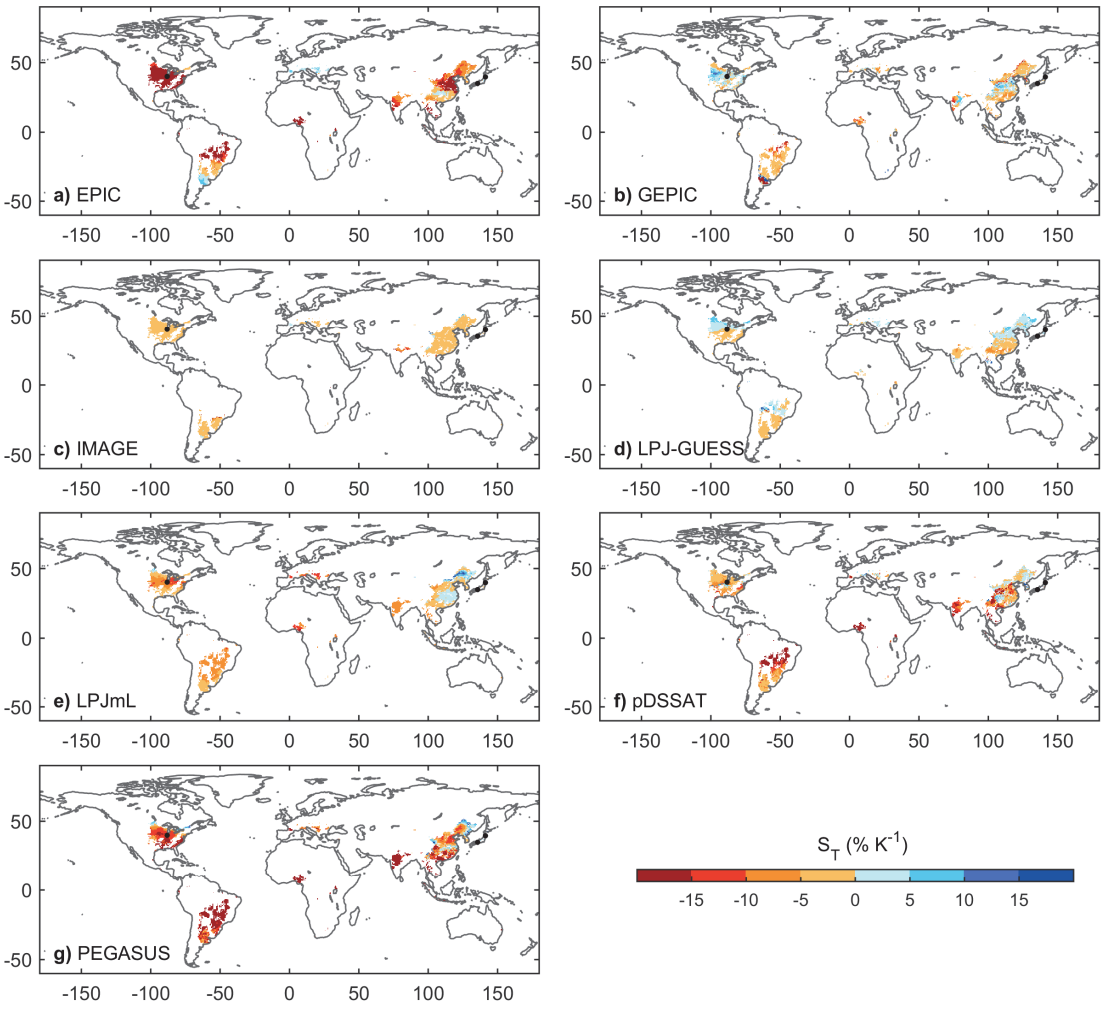

Extended Data Figure 6 The predicted changes of mean annual temperature (MAT) over contemporary growing areas for wheat (a-c), rice (d-f), maize (g-i) and soybean (j-l) under different climate change scenarios (+1.5 K, +2.0K, RCP2.6 and RCP6.0).

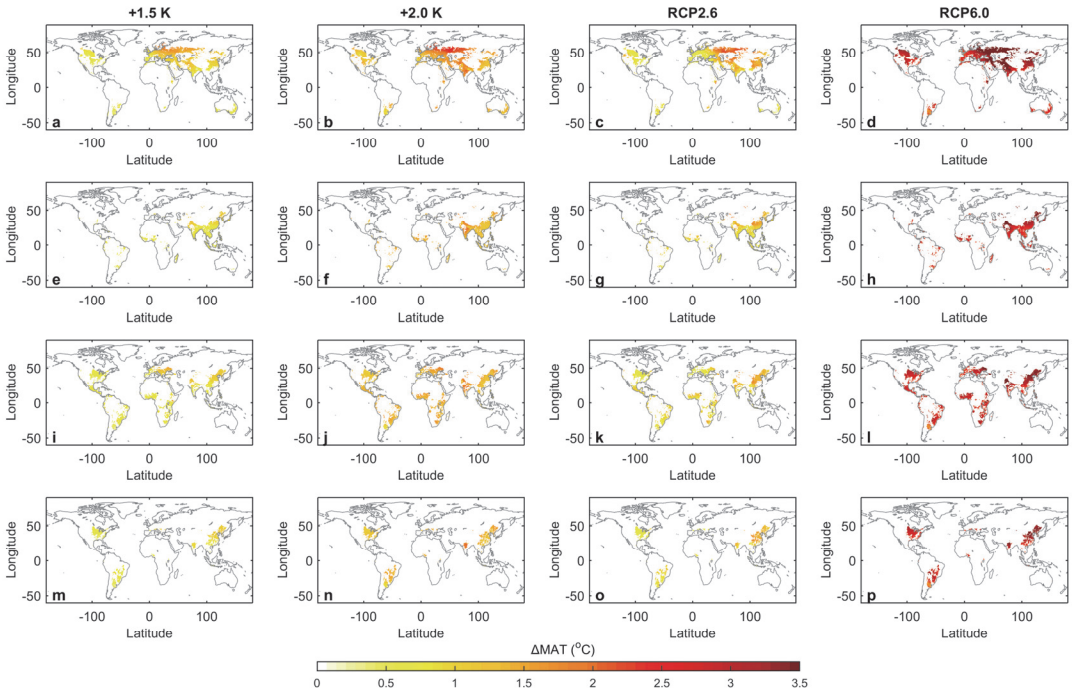

Chapter 5 Global irrigation contribution to wheat and maize yield

Summary

Irrigation is an important management option for increasing crop productivity and adapting for adverse climate change impacts. However, the irrigation contribution to global crop yields remains unclear, in particular because direct observations are scarce. Here, we provide such estimates for wheat and maize at global scale by developing a Bayesian framework integrating estimates from both climate analogue approach and global crop modelling on the relative difference between attainable rainfed and irrigated yield (Δyield). The resulted reanalysis outperform initial sources when confronted against independent US statistical survey data. Our results show that, at global scale, Δyield is 34% (±25%) for wheat and 22% (±23%) for maize. Spatial variation in Δyield are several folds, driven more by gradients in precipitation than by evaporative demand. Moreover, 30–47% of contemporary rainfed areas would not have sufficient local runoff resources to fulfill the potential irrigation demand. The tension between irrigation demand and available water resources at local and river basin scales suggest that engineering efforts such as trans-basin water diversion would be needed to expand irrigation on a sustainable basis. Considering reanalyzed Δyield was about half than ensemble model estimates, hydro-economic and agro-economic studies based on simulated effect of irrigation on yield improvement would have to be revisited. At the time of thesis preparation, this chapter is going to be submitted as Wang X *et al.* Global irrigation contribution to wheat and maize yield

Over the next several decades, the projected increase in global population and increasing demand for animal products will require substantial increases in global crop production (Tilman et al., 2011; FAO, 2012). Because cropland expansion is limited by availability of land, negative implications for greenhouse gas emissions (Houghton et al., 2012; Carlson et al., 2017), and severe ecological consequences (Cassman et al., 2003; Laurance et al., 2014) via removal of forests and grasslands, much attention has been devoted to the intensification of crop production systems in ways that minimize environmental impacts. The challenge of increasing crop yields is further enhanced by climate change, which is expected to result in substantial net declines in regional to global crop yields (Lobell et al., 2011; Asseng et al., 2015; Rosenzweig et al 2014). Improving and expanding current irrigation is seen as a possible measure to achieve higher yield levels in water-limited regions while also improving the resilience of cropping systems to climate variability (Mueller et al., 2012; Jägermeyer et al. 2017; Schauberger et al., 2017).

Despite recognizing the importance of irrigation to increasing yield (Mueller et al., 2012; Jägermeyer et al. 2016), the contribution of irrigation to yield increment at regional to global scales remains uncertain. The classical methods assumed one/two coefficient of evapotranspiration for each crop, which dismiss climatic and varietal variability. Different assumptions taken by different researcher based on this line of methods can result in estimates differed by two times (40% of production in Rosegrant et al. 2009 vs. 20% of production in Siebert and Döll 2010). More recent studies (e.g. Mueller et al., 2012, 2013; Jägermeyer 2016, 2017; Neverre et al. 2016) generally take two more complex methods: the

climate analogue (CA) and process based crop modeling.

The CA approaches are based on global datasets of census and survey-derived yield data, combined with classification of climatic growing zones and irrigation extent. Attainable yields are defined as the 95th percentile yields within a climate zone, and these are calculated including and excluding irrigated areas to define rainfed and irrigated attainable yields (Mueller et al., 2012; Mueller et al. 2013; see Methods). With this approach, the contribution of irrigation to yield under current technology can be estimated because it implicitly accounts for factors (e.g. climate and crop varieties) interacting with irrigation. However, spatial extrapolation of the derived attainable yields relies upon relatively simple climate indices (growing degree days and precipitation). These indexes do not account for intra-seasonal weather variations and the disproportionate effects of short-duration weather events during sensitive periods of the growing season (e.g. episodes of dry periods (Lesk et al., 2016), hot extremes (Lobell et al., 2012; Gourdji et al., 2013) and low temperature stress (Espe et al., 2017) during reproductive growth period). As an alternative to up-scaling farm-level data, gridded crop models provide spatially explicit simulations of irrigated and rainfed yield over the globe. Due to mechanistic representations of crop growth dynamics, daily or sub-daily temporal resolution and efforts put to improve and evaluate simulated crop response to climate variations (Martre et al., 2015; Li et al., 2015; Muller et al., 2016), the ensemble of these models was shown to robustly representing impacts of spatial variations in climate on yield (e.g. Asseng et al., 2015; Liu et al., 2016).

However, such models also have limitations in representing the diversity of crop varieties, management practices, irrigation technology and soil properties (e.g. Folberth et al., 2016), which may lead to biases in estimating the magnitude of irrigation contribution to the yield in a specific location.

As the advantages of CA and gridded crop model approaches are complementary, we hypothesize that integrating their results in a single coherent framework may overcome their respective limitations and lead to more precise estimates of the role of irrigation on regional and global crop yield. Here we use the climate analogue (CA) attainable yield dataset from Mueller et al. (2013) (see Methods) and the crop model simulations from the Global Gridded Crop Model (GGCM) inter-comparison project (Elliott et al., 2015; see Methods), with 10 state-of-the-art gridded crop models. These crop models also provided results for the latest assessment report of the Inter-governmental Panel on Climate Change (IPCC). We reanalyze the above data streams with Bayesian Model Averaging (see Methods; Raftery et al., 2005), focusing here on wheat and maize due to their large-scale geographic coverage, dominant role in global crop production and data availability.

First, we examine the performance of our reanalysis against an independent dataset of irrigated and rainfed yield over the US based on county yield surveys from the US Department of Agriculture that differentiate rainfed from irrigated yields (referred to as gridded-USDA in the following). We compare Δyield (the ratio of the difference between

irrigated and rainfed yield to irrigated yield; see Methods) in the gridded-USDA dataset to Δyield estimated by CA (Fig 1a), by GGCMs (Fig 1b) and by the combined Bayesian reanalysis of both (Fig 1c). Δyield from CA is less biased than that from GGCMs as Δyield from CA distributed on both side of 1:1 line (Fig. 1a), while Δyield from GGCMs is almost always higher than Δyield from gridded-USDA and on average more than twice than gridded-USDA (Fig. 1b). However, the correlation between Δyield from gridded-USDA and Δyield from GGCMs (r=0.67 for wheat, r=0.72 for maize; Fig 1b) are larger than that between gridded-USDA and Δyield from CA (r=0.49 for wheat, r=0.59 for maize; Fig 1a). This suggests a better representation of spatial variations in Δyield by the GGCMs. The Bayesian fusion reanalysis integrating CA and GGCMs provides a more precise estimate of Δyield than either of the methods taken separately, by preserving good spatial variations (r=0.69 for wheat, r=0.76 for maize) and reducing the large biases in Δyield from GGCMs (Fig 1c).

Based on our reanalysis, global mean Δyield for wheat is 0.34±0.25 (mean ± standard deviation over contemporary harvested area (Monfreda et al., 2008)) and for maize is 0.22±0.23. This suggest that full irrigation may increase wheat yield (52%) more than maize yield (28%) in relative terms at global scale. However, the contribution of irrigation to crop yields has large spatial differences (Fig 2). For wheat (Fig 2a), Δyield varies by an order of magnitude across latitudes. Wheat yields benefit more from irrigation in semi-arid and subtropical regions (between latitudes 15ºN and 23ºN Δyield >50%, i.e. irrigated yield is

double of rainfed yield) compared to higher latitudes (Δyield <10%). In some major wheat producing regions, such as the US, eastern Europe (Ukraine and western Russia) and the lower reach of the Yangtze river basin, yield increases from irrigation are limited **(**<10%), probably due to sufficient precipitation during wheat growing seasons (Extended Data Fig 1). By contrast, in drier regions such as the US Great Plains, the Mediterranean, Central Asia, northern China and Australia, wheat yield is found to benefit largely from irrigation (Δyield >50%). There are, however, some "wet" region (where annual precipitation is larger than 1000mm) showing a large positive Δyield, such as southwestern China and India. This can be either related to a mismatch between wheat growing seasons and the wet season over these regions affected by South Asia monsoon or related to the larger evaporative demand induced by higher temperatures. The latitudinal differences in Δyield of maize are not as large as those of wheat (Fig 2b). Large Δyield of maize is found in semi-arid and summer dry regions around ~30ºN, such as the US Great Plains, southern Europe and northwestern China, with a few exceptions in Brazil (mainly the Cerrado area) and South Africa. Although the potential for yield increment over sub-Saharan Africa is generally high (Mueller et al., 2012), however, the Δyield of maize over this region is low due to coincidence between maize growing season here and the wet season.

Given that climate drivers for the spatial variations in Δyield may vary among different crops and regions, we perform partial correlation analyses between Δyield and various climate variables for 3.5º by 3.5º moving windows (Fig 3). We find that Δyield across about

half of the crop area (47% for wheat, 43% for maize) is significantly correlated ($P<0.05$) with mean annual temperature, whereas areas showing a significant correlation with annual precipitation are even larger (67% for wheat, 70% for maize). For both wheat and maize, the dominance or co-dominance of temperature in Δyield are only found in north of 40ºN, such as Canada, the Northeast US and Northeast China, while precipitation is dominant in spatial variations of Δyield over all other regions. This implies that spatial variations in Δyield are mostly determined by variations in climatic water supply, proxied by precipitations, rather than climatic water demand, proxied by temperature. The correlation between Δyield and precipitation is only weak for maize over western Africa, eastern India and southern China, suggesting that local maize yield is not primarily limited by water supply, which is consistent with the low Δyield over these regions (Fig 2). The above results remain robust when we change the proxy of climatic water demand from temperature to potential evapotranspiration (PET) (Extended Data Fig 2; See Methods).

Increasing crop yield through extension of irrigation to realize Δyield shown in Fig. 2 is limited by available water resource. We therefore compared reanalyzed irrigation requirement for wheat and maize (see Methods) with available runoff resources (Fekete et al., 2000), which provides a limit to surface water supply for irrigating contemporary rainfed wheat and maize croplands. We consider two parameters for irrigation practices in utilizing runoff: 1) the Δyield threshold, which determines the minimum irrigation benefit, above which we apply full irrigation and 2) maximum ratio of runoff that can be diverted

sustainably for irrigation while safeguarding the riverine ecosystems (Jägermeyr et al., 2017). When considering a reasonable range of the two parameters (Fig 4a; see Methods section), 80.2 million ha to 125.9 million ha of contemporary rainfed wheat and maize cropland do not have sufficient runoff to meet the full irrigation demand (Fig 4b; Extended Data Fig 3), which accounts for 30% - 47% of contemporary rainfed croplands of wheat and maize. Large area with water deficit concentrates around 30°N and 30°S, including western US and Canada, circ-Black Sea, Central Asia, North and Northeast China, Argentina, South Africa and Australia (Fig 4b; Extended Data Fig 3) with the largest deficit found in southwestern Australia exceeding 100 mm. When comparing the irrigation demand with river discharge (GRDC, 2007) at basin scale for major river basins growing wheat and maize (Extended Data Fig. 4), we also found large spatial heterogeneity in the balance between water supply and irrigation demand (Extended Data Table 1). The projected irrigation requirements of wheat and maize accounts for less than 0.1% of river discharge in Congo basin but more than three times than the river discharge of Murray basin (Extended Table 1). Irrigation requirements exceeds 20% of today's river discharge for one fifth of the basins (Don, Huai, Tigris & Euphrates, Yellow River, Ural), highlighting the grand challenge of fully realizing the potential of irrigation to increase crop yield globally for wheat and maize. If further considering today's water withdrawal may already be non-sustainable in some basins where demand-to-supply ratio is low (e.g. 4% for Indus), irrigating the crops in a sustainable way becomes even more challenging. Besides mining ground water for irrigation, the trans-basin water transfer program (e.g. the South-to-North

Water Diversion Project in China) can be a viable and sustainable alternative to mitigate the imbalance between water supply and demand, as the total irrigation demand over Yellow River basin and Yangtze River basin accounts for only 1.4% of river discharge of Yangtze River.

We note that the above analysis on the balance between irrigation supply and demand is subject to several uncertainties. In particular, on the supply side, the available runoff that can be used for irrigation varied substantially within the basin and across the seasons. We have also ignored elevation constraints that may determine whether hillside croplands can use runoff for irrigation. On the demand side, our approach likely underestimates irrigation demands for two reasons. We only consider wheat and maize, while other irrigation-demanding cereals (e.g. rice), cotton, vegetable and oil crops have not been included due to data limitations. We estimated rainfed cropland area as area without irrigation facilities (Siebert et al., 2013), which may underestimate the area of croplands needing additional irrigation as many croplands equipped with irrigation facilities today are still rainfed or applying deficit irrigation due to economic consideration or access to water resources (Siebert et al., 2013). With potentially smaller demand and larger supply than the reality, our estimates on the imbalance between projected irrigation demand and supply may still be quite conservative. At global scale, despite growing details of spatial distribution of irrigation facilities (Siebert et al., 2013), our knowledge on the amount and spatial and temporal distribution of irrigation water applied in croplands remains a data gap limiting

our analyses to realize the potential of irrigation for yield increment.

Overall, our integrated estimate combining empirical evidences and process modelling on irrigation contribution to yield provides new insights for interdisciplinary studies in agronomy, hydrology and economy. The reanalyzed Δyield can be used directly to provide yield difference between irrigated and rainfed crop to obtain the localized average irrigation water value when yield difference is the essential factor in determining water use decisions (Neverre et al., 2016). Since global Δyield estimated by crop models varied by a factor of 4 across themselves and was, on average, ~2 times larger than observations, previous hydrologic analyses rely upon one crop model or one simplified empirical model (one/two crop specific coefficient for evapotranspiration) to estimate the yield difference between irrigated and rainfed crop could have largely underestimated uncertainties in yield difference between rainfed and irrigated yield (e.g. Rosegrant and Cai, 2002; Siebert and Döll 2010; Jägermeyr et al., 2017).

Sustainably enhancing crop yield through expansion of irrigation could prove difficult. Improvement of irrigation practices could save water and allow to expand irrigation (Jägermeyer et al. 2016), as could long distance transfers between water rich basins and water poor basins such as the South-to-North Water Diversion Project in China (Berkoff, 2003). As a next step, the improved estimation of Δyield could be used to value more precisely irrigation water value and allow large scale hydroeconomic evaluations which also

represent other sectors to gain in better precision and thus decisions (Neverre et al. 2016).

Methods

Attainable yield estimates from climate analogues

The estimated rainfed and irrigated attainable yields are derived using a climate analogue approach, which is updated from Mueller et al. (2012) as described in Mueller et al. (2013). A series of climatic growing zones are defined based on increments of growing degree days and precipitation. Within each growing zone, "irrigated" attainable yields are calculated as the area-weighted 95th percentile of all yield observations (Monfreda et al. 2008) within the bin. The "rainfed" attainable yields are calculated from all yield observations within the bin that are located in a political unit with <10% of crop area irrigated, where crop-specific irrigation maps are from the MIRCA2000 irrigation dataset (Portmann et al. 2010). The rainfed and irrigated attainable yield estimates used for this analysis are grid cell averages derived from replicating this sampling procedure for varying numbers of climate zones, from 100 to 400 (10x10 to 20x20 growing degree day and precipitation increments).

A limitation of this dataset is that the irrigated attainable yields may not be different from the rainfed attainable yield estimates if little area is actually irrigated within a climate zone. Further, we note that for the comparison with USDA data, the underlying yield dataset upon which these estimates are based (Monfreda et al. 2008) does include county-level

USDA yield data (although these data are a combination of rainfed and irrigated observations).

Global gridded crop models

We used Phase 1 simulation results by global gridded crop model inter-comparison (GGCMI) results (Elliott et al., 2015). The phase 1 of GGCMI includes an unprecedented number of crop models (10) with very different nature of formulas. For example, photosynthesis of crops was simulated with different methods including Farquahar scheme and light use efficiency scheme. The parameters of even the same scheme may differ across models (Folberth et al., EPIC difference paper). A full list of models, their characteristics and their references can be found in Extended Data Table 2. However, all models follow the same simulation protocol (Elliott et al., 2015) with the same forcing of gridded climate and management (planting date and fertilization rate) in order to minimize the impacts of difference in model drivers. All models provided "harmnon" simulations, which simulate historical crop yield forced by historical climate dataset but assuming unlimited nitrogen supply to the croplands (Elliott et al., 2015) are used in the analysis. We use simulations with "harmnon" settings instead of "fullharm" settings forced with more realistic fertilizer rate because 1) it helps to avoid interactive effects of fertilization and irrigation, and 2) it is closer to the assumption used in the climate analogue approach, making the two datasets directly comparable.

Gridded US dataset

The gridded rainfed and irrigated crop yield over US (gridded US) dataset is based on

county rainfed and irrigated yield statistics provided by the US Department of Agriculture (USDA), postprocessed by Elliott et al.. The statistics were gridded to 0.25 degree according to the weighted crop area over each county. The dataset covers 1980–2010, and we use the average across this time period. Further details of the dataset can be found in Schauberger et al. (2017).

The gridded-USDA dataset is suitable for evaluating our reanalysis because 1) it is independent from both products we used in this study, and 2) unlike in many less-developed countries where rainfed farming is often paired with a significantly lower management intensity (e.g. less fertilizer input and pest control measures), the rainfed and irrigated management over the same county in US is more often associated with access to water resources. It may thus more closely approximate spatial variations in the contribution of irrigation alone to crop yield instead of the contribution of co-varying factors.

Runoff and river discharge

The global runoff dataset (UNH-GRDC composite runoff fields) used in this study is a reanalyzed product based on observed river discharge collected by Global Runoff Data Centre (GRDC) and simulations by a climate driven hydrology model (Water Balance Model). This dataset has composite runoff fields, which preserve the accuracy of discharge measurements as well as give the spatial and temporal patterns of the best estimates of runoff. Since the dataset has already accounted contemporary utilization of runoff for all purposes, including irrigation, it serves in this study as an estimate of available water resources that can potentially be used to irrigate the rainfed croplands. UNH-GRDC dataset

has a spatial resolution of 0.5° and temporal resolution of one month over the entire global land surface (Fekete et al., 2000).

River discharge data from Global River Discharge Center (GRDC, 2007) was used as the data source for 405 river basins with mean annual discharge [km³] of the gauging station nearest to the mouth as potentially available water resources to irrigate wheat and maize croplands.

Bayesian model average

We derived Δyield as the ratio of the difference between the irrigated yield and the rainfed yield to the irrigated yield (Eq. 1).

$$\Delta yield = \frac{irrigated\ \ yield - rainfed\ \ yield}{irrigated\ \ yield} \qquad \text{Eq.1}$$

The irrigated yield is chosen as the dividend, instead of the more intuitive rainfed yield, because the rainfed yield can be very small or even zero in extreme cases jeopardizing the stability of the analyses. The reanalysis of Δyield integrating the global gridded crop models and climate analog approaches was performed with algorithm called Bayesian model average (BMA, Raftery et al., 2005), which has been proven to be an effective methods in ensemble weather forecast, but has not yet been applied in agricultural studies. The idea of BMA is to derive posterior probability of each model given a target dataset. The posterior probability of each model is then used to calculate model weights (W_i for the ith model) in the model ensemble and result in reanalyzed estimates that "best" combine information from different datasets. The derivation of W_i follows the Bayesian equation (Eq. 2):

$$W_i = P(M_i|O) \propto P(O|M_i)P(M_i) \qquad \text{Eq.2}$$

where M_i is the *i*th model estimates on Δyield and O is the Δyield estimated from the climate analog approach. In the prior ($P(M_i)$), we assumed each model is equally skillful in projecting Δyield. The conditional probability $P(O|M_i)$ is therefore proportional to the misfits between the *i*th model simulation and climate analog estimates. With Wi, the posterior probability for the best estimate of Δyield in the reanalysis will follows Eq. 3:

$$P(\Delta yield|M_1, M_2, \dots, M_{11}, O) - \sum_{i=1}^{11} W_i P(\Delta yield|M_i, O) \qquad \text{Eq.3}$$

Where $P(\Delta yield|M_i,O)$ is conditional probability density function of Δyield based on M_i and O. A Monte-carlo Markov chain method is used to derive the optimal W_i for each model (Raftery et al., 2005).

Potential Evapotranspiration (PET)

In addition to temperature, we use potential evapotranspiration (PET) as a surrogate to estimate climatic demand of water from croplands. We follow the modified Haude equation (Castellvi et al., 1997) to derive PET, which has been proven effective in building statistical models for regional crop yield (Gornott et al., 2016). The climatic variables used in calculating PET comes from AgMERRA dataset, which was also the climate forcing for GGCM simulations (Elliot et al., 2015).

Balance between irrigation requirements and runoff supply

We first obtain potential irrigation water withdraw calculated by each GGCM (Elliot et al., 2014; Elliot et al., 2015). To ensure consistency between reanalyzed Δyield and

irrigation demand, we use the same model weights (see *Bayesian model average*) to calculate reanalyzed irrigation demands used in the main text. The irrigation demands estimated by GGCMs assuming 100% irrigation efficiency, which is not realistic when comparing with available runoff resources. Therefore, at each grid, we divide the reanalyzed irrigation demand by crop-specific irrigation efficiencies (Jagermeyr et al., 2015) to attain actual irrigation withdrawals from surface water bodies.

On the water supply side, the UNH-GRDC dataset considers today's human water withdrawal for industrial, domestic and agricultural usage from river runoff. River ecosystems provide life- supporting functions that depend on maintaining minimum river discharge, i.e. environmental flow requirements (EFRs) (Pastor et al., 2014, Poff et al. 1997). However, the quantification of EFRs is not trivial as estimation methods vary quite uncertain, which may vary by 4 times with different methods (e.g. EFRs estimated by different methods ranges from 12-48% for Nile and 30-67% for the Amazon). A detailed account of such is beyond the scope of this study and can be found in Jägermeyr et al. (2017). The large uncertainties in EFRs and lack of data for other potential usages make it difficult to estimate the overall sustainable water resources available for irrigating wheat and maize. Therefore, we assumed a fraction of runoff used for irrigating wheat and maize croplands. To make our estimates more conservative, the range of this fraction is set from 20% - 40%. This range of fraction is already 2-4 times larger than global runoff withdraw for all sectors (Jägermeyr et al., 2017). The choice of 20% or 40% will not qualitatively change our findings (Extended Data Figure 3). Confirming our assumptions, Elliott et al.

(2014) assumed that up to 40% of naturalized runoff might be used human needs including irrigation. Given that both current human water withdrawals are already unsustainable across many river basins worldwide (Jägermeyr et al., 2017), and that there are many other irrigation-intensive crops in addition to the here-studied wheat and maize (e.g. rice, cotton and vegetatbles), the estimates of water deficit in our study appear conservative.

References

Asseng S, Ewert F, Martre P *et al.* (2015) Rising temperatures reduce global wheat production. *Nature Clim. Change,* **5**, 143-147.

Berkoff J (2003) China: The South–North Water Transfer Project—is it justified? *Water Policy,* **5**, 1-28.

Cameron KC, Di HJ, Moir JL (2013) Nitrogen losses from the soil/plant system: a review. *Annals Of Applied Biology,* **162**, 145-173.

Cassman KG, Dobermann A, Walters DT, Yang H (2003) Meeting cereal demand while protecting natural resources and improving environmental quality. *Annual Review of Environment and Resources,* **28**, 315-358.

Castellvi, F., Perez, P.J., Stockle, C.O., Ibaiiez, M. (1997) Methods for estimatingvapor pressure deficit at a regional scale depending on data availability. *Agricultural And Forest Meteorology,* **87**, 243–252.

Elliott J, Deryng D, Müller C *et al.* (2014) Constraints and potentials of future irrigation

water availability on agricultural production under climate change. *Proceedings of the National Academy of Sciences,* **111**, 3239-3244.

Elliott J, Müller C, Deryng D *et al.* (2015) The Global Gridded Crop Model Intercomparison: data and modeling protocols for Phase 1 (v1.0). *Geosci. Model Dev.,* **8**, 261-277.

Fekete B, Vörösmarty C, Grabs W (1999) Global, Composite Runoff Fields Based on Observed River Discharge and Simulated Water Balances, WMO-Global Runoff Data Center Report# 22. *WMO GRDC, Koblenz (GERMANY)*.

Folberth C, Skalsky R, Moltchanova E, Balkovic J, Azevedo LB, Obersteiner M, Van Der Velde M (2016) Uncertainty in soil data can outweigh climate impact signals in global crop yield simulations. *Nat Commun,* **7**.

Gornott C, Wechsung F (2016) Statistical regression models for assessing climate impacts on crop yields: A validation study for winter wheat and silage maize in Germany. *Agricultural And Forest Meteorology,* **217**, 89-100.

Gourdji SM, Sibley AM, Lobell DB (2013) Global crop exposure to critical high temperatures in the reproductive period: historical trends and future projections. *Environmental Research Letters,* **8**, 024041.

Houghton RA, House JI, Pongratz J *et al.* (2012) Carbon emissions from land use and land-cover change. *Biogeosciences,* **9**, 5125-5142.

Jägermeyr J, Gerten D, Heinke J, Schaphoff S, Kummu M, Lucht W (2015) Water savings potentials of irrigation systems: global simulation of processes and linkages. *Hydrol.*

Earth Syst. Sci., **19**, 3073-3091.

Jägermeyr J, Gerten D, Schaphoff S, Heinke J, Lucht W, Rockström J (2016) Integrated crop water management might sustainably halve the global food gap. *Environmental Research Letters,* **11**, 025002.

Jägermeyr J, Pastor A, Biemans H, Gerten D (2017) Reconciling irrigated food production with environmental flows for Sustainable Development Goals implementation. *Nature Communications,* **8**, 15900.

Ju X-T, Xing G-X, Chen X-P *et al.* (2009) Reducing environmental risk by improving N management in intensive Chinese agricultural systems. *Proceedings of the National Academy of Sciences,* **106**, 3041-3046.

Laurance WF, Sayer J, Cassman KG (2014) Agricultural expansion and its impacts on tropical nature. *Trends In Ecology & Evolution,* **29**, 107-116.

Lesk C, Rowhani P, Ramankutty N (2016) Influence of extreme weather disasters on global crop production. *Nature,* **529**, 84-87.

Li T, Hasegawa T, Yin X *et al.* (2015) Uncertainties in predicting rice yield by current crop models under a wide range of climatic conditions. *Global Change Biology,* **21**, 1328-1341.

Liu B, Asseng S, Muller C *et al.* (2016) Similar estimates of temperature impacts on global wheat yield by three independent methods. *Nature Clim. Change,*

Lobell DB, Schlenker W, Costa-Roberts J (2011) Climate trends and global crop production since 1980. *Science,* **333**, 616-620.

Lobell DB, Sibley A, Ivan Ortiz-Monasterio J (2012) Extreme heat effects on wheat senescence in India. *Nature Clim. Change,* **2**, 186-189.

Martre P, Wallach D, Asseng S *et al.* (2015) Multimodel ensembles of wheat growth: many models are better than one. *Global Change Biology,* **21**, 911-925.

Monfreda C, Ramankutty N, Foley JA (2008) Farming the planet: 2. Geographic distribution of crop areas, yields, physiological types, and net primary production in the year 2000. *Global Biogeochem. Cycles,* **22**, GB1022.

Mueller ND, Gerber JS, Johnston M, Ray DK, Ramankutty N, Foley JA (2012) Closing yield gaps through nutrient and water management. *Nature,* **490**, 254-257.

Müller C, Elliott J, Chryssanthacopoulos J *et al.* (2017) Global gridded crop model evaluation: benchmarking, skills, deficiencies and implications. *Geosci. Model Dev.,* **10**, 1403-1422.

Neverre N, Dumas P, Nassopoulos H (2016) Large-scale water scarcity assessment under global changes: insights from a hydroeconomic framework. *Hydrol. Earth Syst. Sci. Discuss.,* **2016**, 1-26.

Peng SB, Huang JL, Sheehy JE *et al.* (2004) Rice yields decline with higher night temperature from global warming. *Proceedings of the National Academy of Sciences of the United States of America,* **101**, 9971-9975.

Poff, N. L. et al. The natural flow regime: a paradigm for river conservation and restoration N. BioScience 47, 769–784 (1997).

Portmann FT, Siebert S, Döll P (2010) MIRCA2000—Global monthly irrigated and rainfed

crop areas around the year 2000: A new high-resolution data set for agricultural and hydrological modeling. *Global Biogeochemical Cycles,* **24**, GB1011.

Raftery, A. E., T. Gneiting, F. Balabdaoui, and M. Polakowski (2005), Using Bayesian model averaging to calibrate forecast ensembles, *Mon. Weather Rev.*, *133*(5), 1155-1174, doi: 10.1175/MWR2906.1.

Rosegrant MW, Ringler C, Zhu TJ (2009) Water for Agriculture: Maintaining Food Security under Growing Scarcity. In: *Annual Review of Environment and Resources.* pp Page. Palo Alto, Annual Reviews.

Rosegrant MW, Cai X (2002) Global Water Demand and Supply Projections. *Water International,* **27**, 170-182.

Rosenzweig C, Elliott J, Deryng D *et al.* (2014) Assessing agricultural risks of climate change in the 21st century in a global gridded crop model intercomparison. *Proc Natl Acad Sci U S A,* **111**, 3268-3273.

Schauberger B, Archontoulis S, Arneth A *et al.* (2017) Consistent negative response of US crops to high temperatures in observations and crop models. *Nature Communications,* **8**, 13931.

Schewe J, Heinke J, Gerten D *et al.* (2014) Multimodel assessment of water scarcity under climate change. *Proceedings of the National Academy of Sciences,* **111**, 3245-3250.

Siebert S, Henrich V, Frenken K, Burke J (2013) Update of the Digital Global Map of Irrigation Areas to Version 5. pp Page, Bonn: Institute of Crop Science and Resource Conservation Rheinische Friedrich-Wilhelms-Universität Bonn.

Siebert S, Döll P (2010) Quantifying blue and green virtual water contents in global crop production as well as potential production losses without irrigation. *Journal Of Hydrology,* **384**, 198-217.

Tilman D, Balzer C, Hill J, Befort BL (2011) Global food demand and the sustainable intensification of agriculture. *Proceedings of the National Academy of Sciences,* **108**, 20260-20264.

Figure 1. Comparison of irrigation contribution to yield (Δyield) estimated from US statistics (gridded-US) and from different approaches for wheat (top panel) and for maize (bottom panel) over conterminous US. In the left column (a & d), the y-axis shows Δyield estimated from the climate analogue (CA) approach; In the central column (b & e), the yaxis shows Δyield estimated from gridded crop models; In the right column (c & f), the y-axis shows Δyield estimated from Bayesian model average (BMA). Details of different datasets and approaches can be found in the Methods section. r indicates correlation coefficient between Δyield estimated from gridded-US and other Δyield estimates. **** indicates p<0.01.

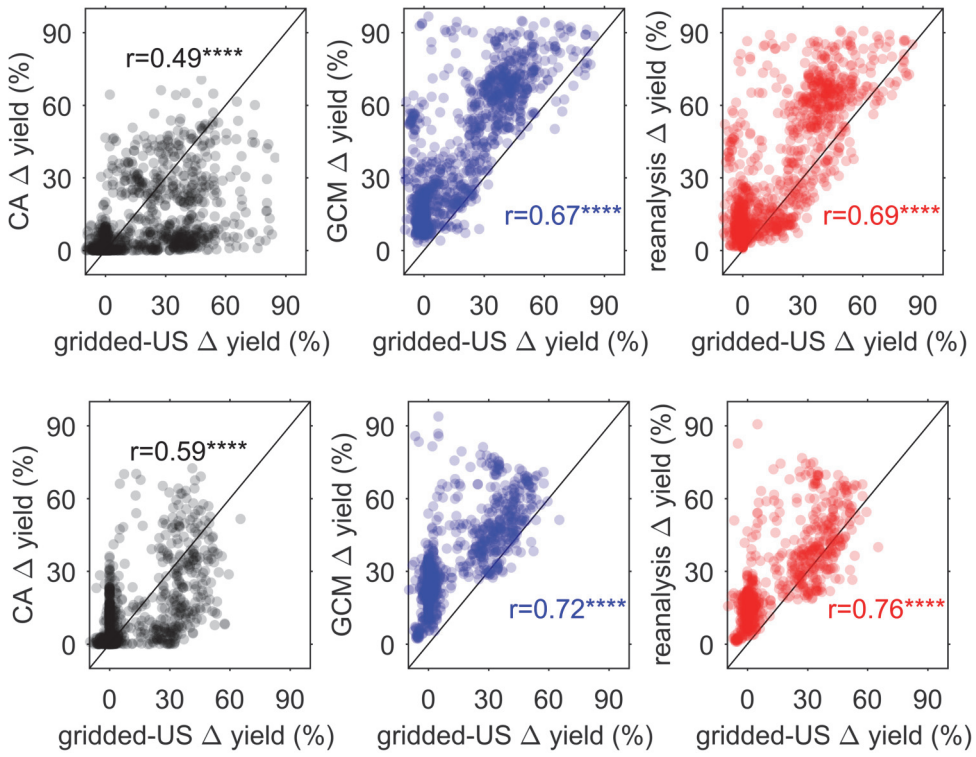

Figure 2. Spatial distribution of Δyield for (a) wheat and (b) maize over contemporary growing area. The right panel shows latitudinal distribution of Δyield for each one degree latitudinal band. The black curve shows Δyield estimated from the climate analogue dataset and the red curve shows Δyield estimated from BMA reanalysis, with shaded area indicates the range of uncertainty.

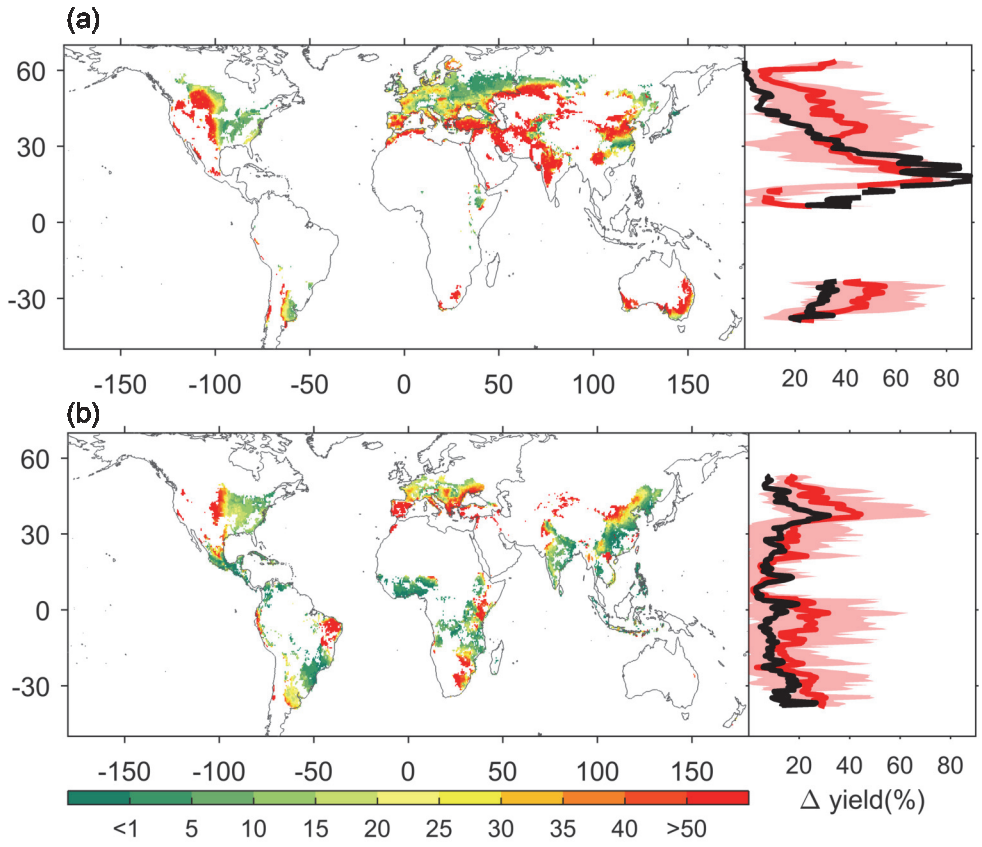

Figure 3. Partial correlation in the spatial domain (3.5°×3.5° moving windows) between Δyield and climatic variables (mean annual temperature (MAT) and mean annual precipitation (MAP)) for wheat (top panel) and for maize (bottom panel). (a,c) bivariate mapping for spatial distribution of the partial correlation coefficient between Δyield and MAT ($R_{\Delta yield,MAT}$) and that between Δyield and MAP ($R_{\Delta yield,MAP}$). (b,d) Percentage of cropland area where Δyield is controlled by temperature or precipitation depending on the chosen threshold (x-axis) for the partial correlation coefficients.

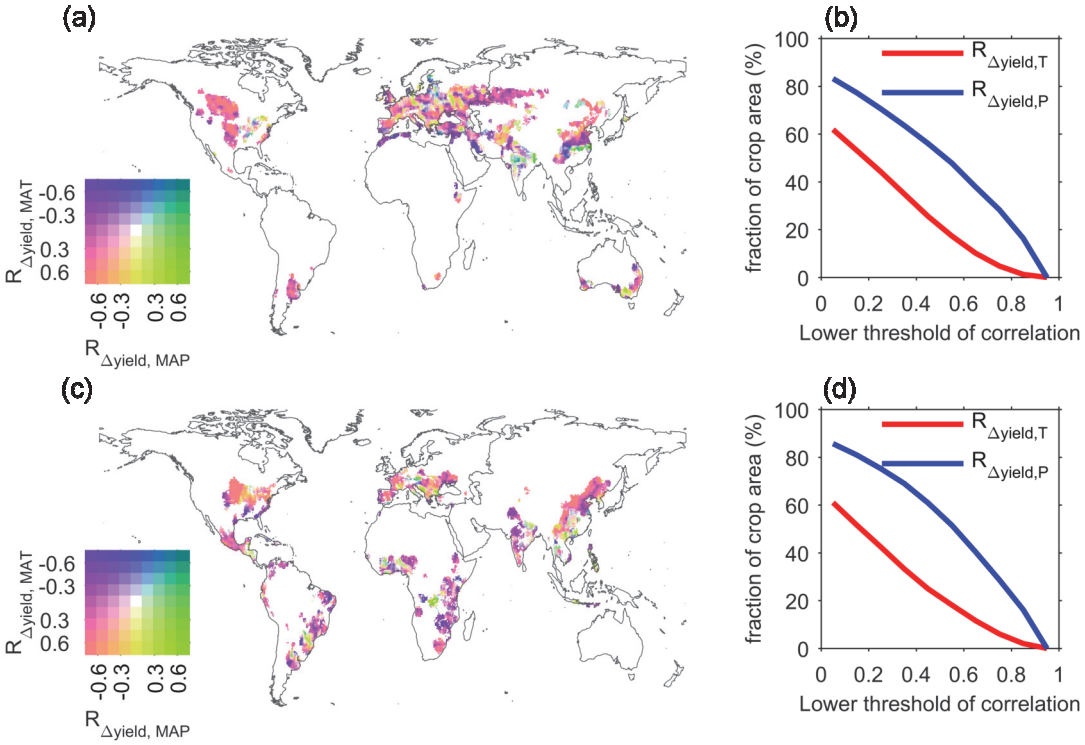

Figure 4. Relationship between irrigation demand estimated from the BMA reanalysis for contemporary rainfed croplands of wheat and maize and available runoff resources. (a) The amount of rainfed crop area when irrigation demand cannot be met with available runoff resources, according to different minimum threshold of Δyield (y-axis) and maximum threshold of runoff consumption (x-axis). (b) the spatial distribution of the difference between irrigation demand and available runoff resources. The spatial pattern is determined with the minimum threshold of Δyield for demanding irrigation is 10% and the maximum usage of runoff is 30% (corresponding to the black circle in (a)). See Extended Data Fig. 3 for spatial pattern of different thresholds of maximum runoff usage.

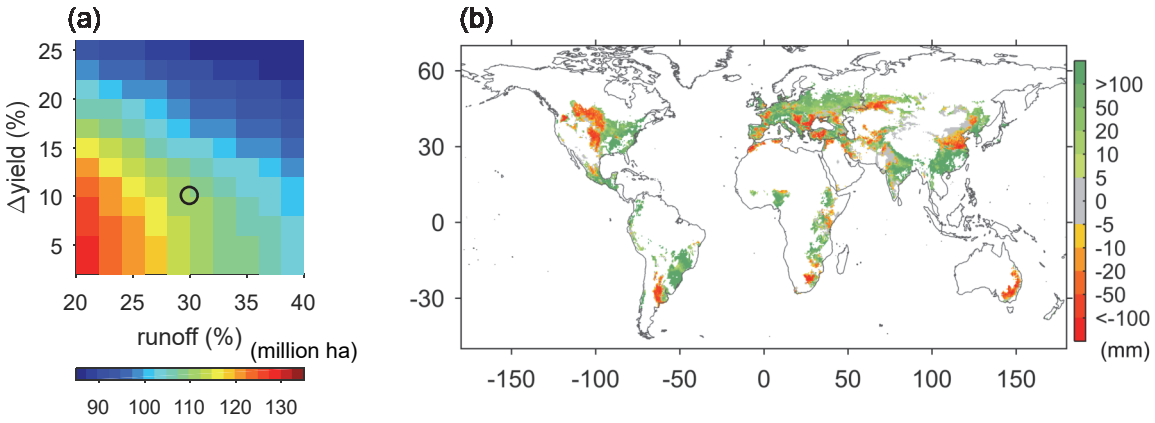

Extended Data Figure 1. Spatial distribution of mean growing season temperature and precipitation for wheat (top panels) and for maize (bottom panels). (a) mean growing season temperature (ºC) for wheat; (b) mean growing season precipitation (mm) for wheat; (c) mean growing seaon temperature (ºC) for maize; (d) mean growing season precipitation for maize (mm).

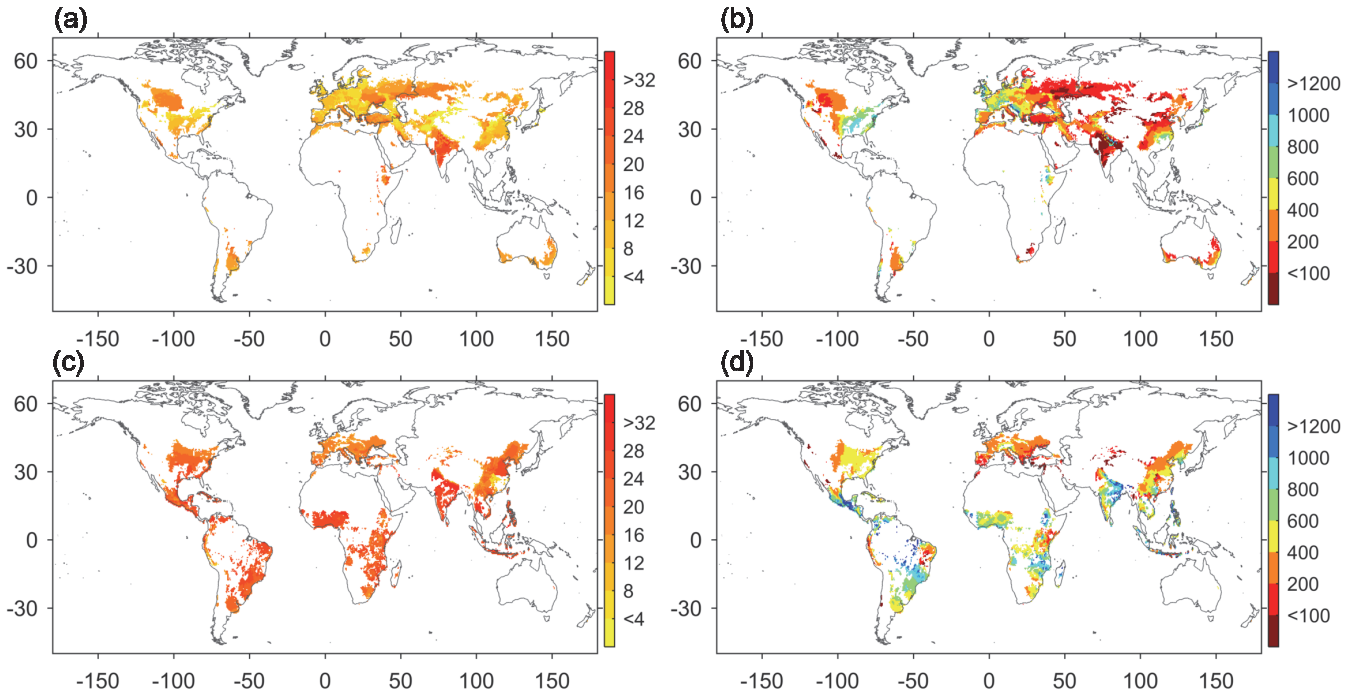

Extended Data Figure 2. Partial correlation in the spatial domain between Δyield and climatic variables (potential evapotranspiration (PET) and mean annual precipitation (MAP)) for wheat (top panel) and for maize (bottom panel). (a,c) bivariate mapping for spatial distribution of the partial correlation coefficient between Δyield and PET ($R_{\Delta yield,PET}$) and that between Δyield and MAP ($R_{\Delta yield,MAP}$). (b,d) Percentage of cropland area where Δyield is controlled by PET or precipitation depending on the chosen threshold (x-axis) for the partial correlation coefficients. Same to Figure 3 but using PET to replace MAT.

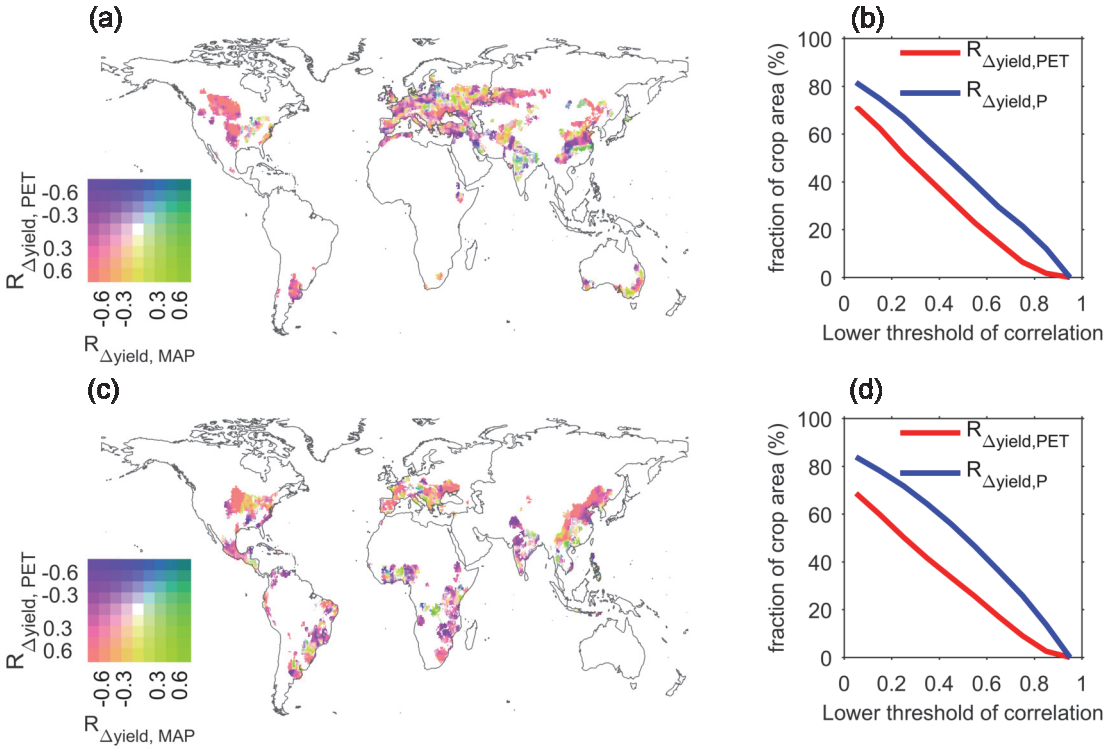

Extended Data Figure 3. The spatial distribution of the difference between irrigation demand and available runoff resources determined with maximum runoff usage threshold of (a) 20% and (b) 40%.

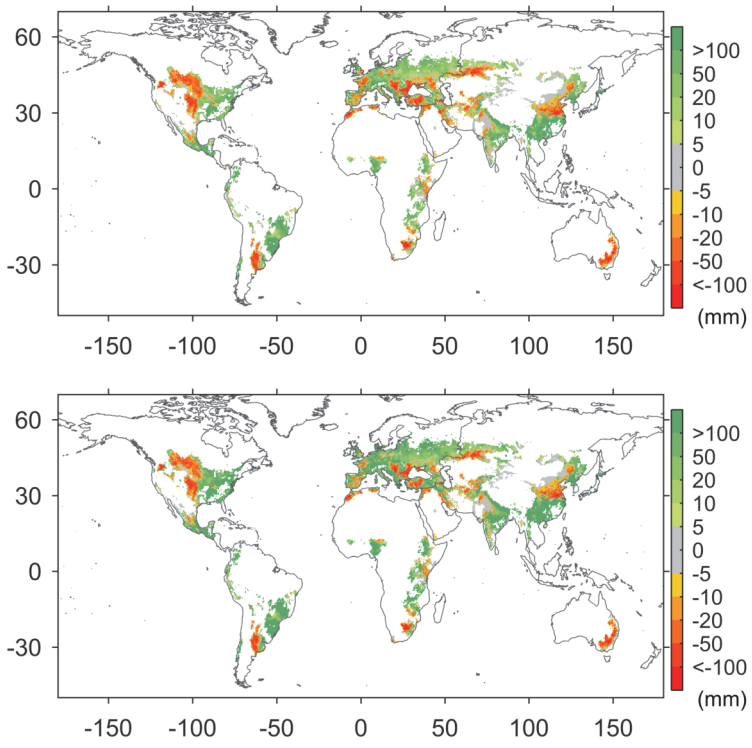

Extended Data Figure 4. Spatial distribution of top 25 river basins having largest rainfed wheat and maize croplands. Colorbar show area of rainfed wheat and maize croplands within the basin according to Monfreda et al. (2008).

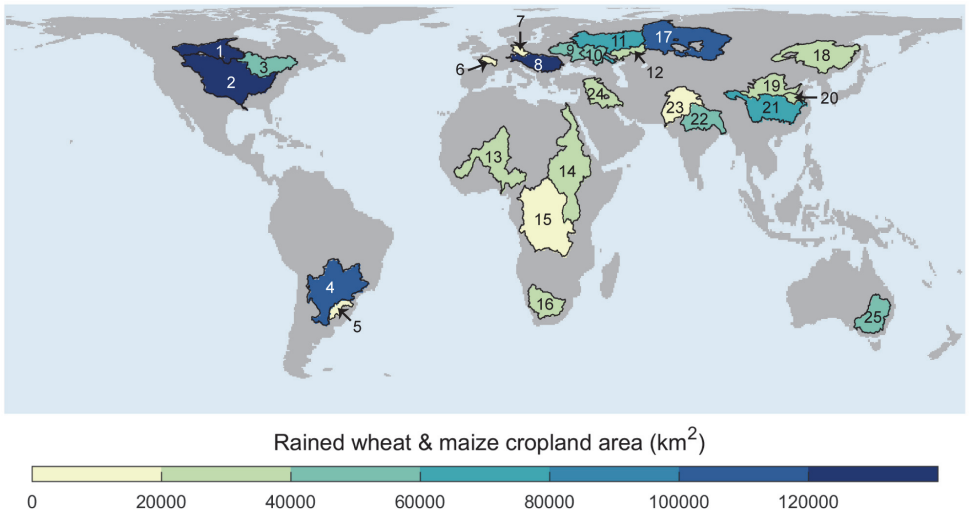

Extended Data Table 1. Balance of river discharge and irrigation demand of contemporary rainfed wheat and maize croplands for 25 river basins with largest rainfed area of wheat and maize. River discharge is the mean annual discharge of the gauging station nearest to the mouth that is represented in GRDC database (GRDC, 2007). Irrigation demand is estimated by reanalyzed irrigation demand by GGCMs (see Methods). Rainfed crop area is derived from Monfreda et al. (2008).

Basin Name	Rainfed area (10^3 km^2)	Discharge (10^3 m^3)	Demand (10^3 m^3)	Demand to supply ratio (%)
Mississippi	367.2	535.0	60.0	11.2
Danube	126.0	202.3	25.0	12.3
Nelson river	120.4	95.5	14.7	15.4
Ob	110.9	400.4	17.2	4.3
Parana	106.5	476.3	10.6	2.2
Volga	64.7	256.7	2.7	1.1
Yangtze river	60.2	899.4	3.7	0.4
Don	56.5	25.5	7.7	30.0
Murray	51.8	6.7	24.9	372.0
Ganges	47.0	379.6	6.4	1.7
Dniepr	46.7	47.1	3.6	7.7
St.lawrence	45.6	268.2	2.0	0.8
Amur	39.4	314.7	4.2	1.3
Huai River	30.4	27.9	7.8	28.0
Tigris &	29.7	37.6	15.6	41.6

euphrates				
Yellow river	27.5	45.0	9.3	20.8
Orange	27.2	9.0	13.7	152.4
Niger	25.7	159.5	0.3	0.2
Ural	25.3	9.4	5.0	53.4
Nile	21.2	39.5	1.8	4.5
Congo	19.5	1269.3	0.1	0.0
Indus	19.2	91.6	3.6	3.9
Uruguay	19.0	170.5	0.3	0.2
Elbe river	17.8	22.4	1.6	7.1
Loire	17.3	26.4	4.3	16.1

Extended Data Table 2. Characteristics of used crop models

Model	Type[1]	CO2 effects[2]	Stresses[3]	Fertilizer application[4]	Calibration[5]	alibrated parameters	Reference
CGMS-WOFOST	Site-based	LF, TE	W, T	NA	Site-specific	sum requirements	De Wit & van Diepen, 2008
EPIC-BOKU	Site-based	RUE, TE	W, T, A, N, P, BD, AL	automatic N input (max 200 kg Ha-1 yr-1) PK (national stat. IFA) dynamic application	Site-specific (EPIC 0810)	A	Izaurralde et al., 2006
EPIC-IIASA	Site-based	RUE, TE	W, T, A, N, P, BD, AL	NP (sub-national stat by Balkovič et al. (2013); Mueller et al. (2012)); P timing: rigid; N timing: automatic (based on N stress)	Site-specific and global	HIpot (ric, mai) F (others)	Izaurralde et al., 2006
EPIC-TAMU	Site-based	RUE, TE	W, T, H, A, N, P, BD, AL	NPK at planting	Site-specific and global	Ipot (maize)	Izaurralde et al., 2012
GEPIC	Site-based	RUE, TE	W, T, A, N, P, BD, AL	NP (national stat: FertiSTAT), dynamic	Site-specific and global	HIpot (for maize and	Liu et al., 2007

				application of N, rigid application of P		rice)	
LPJ-GUESS	Ecosystem	LF, SC	W, T	NA	Uncalibrated	A	Lindeskog et al., 2013
LPJmL	Ecosystem	LF, SC	W, T	NA	National	AImax HI αa	Waha et al., 2012
ORCHIDEE-crop	Ecosystem	LF, SC	W,T,N	Automatic N input (IFA)	Uncalibrated		Wu et al., 2015
pAPSIM	Site-based	RUE	W, T, H, A, N	SPAM by You et al. (2014), (1/2 at planting, 1/2 at day 45)	Site-specific (APSIM)	A	Elliot et al., 2014
pDSSAT	Site-based	RUE (for wheat, rice, maize) and LF (for soybean)	W, T, H, A, N	SPAM by You et al. (2014), (1/2 at planting, 1/2 at day 45)	Site-specific (DSSAT)	A	Elliot et al., 2014
PEGASUS	Ecosystem	RUE, TE	W, T, H, N, P, K	NPK (national stat. IFA), annual application	Global		Deryng et al., 2016

Notes: (NA where not applicable)

[1] Site-based: site-base crop model; Ecosystem: global ecosystem model

[2] Elevated CO_2 effects: LF: Leaf-level photosynthesis (via rubisco or quantum-efficiency and leaf-photosynthesis saturation; RUE: Radiation use efficiency; TE: Transpiration efficiency; SC: stomatal conductance

[3] W: water stress; T: temperature stress; H: specific-heat stress; A: oxygen stress; N: nitrogen stress; P: phosphorus stress; K: potassium stress; BD: bulk density; AL: aluminum stress (based on pH and base saturation)

[4] Fertilizer application, timing of application; NPK annual application of total NPK (nutrient-stress factor); source of fertilizer application data; timing: annual or dynamic

[5] F: fertilizer application rate; HIpot: Potential harvest index; LAImax: maximum LAI under unstressed conditions; HI: harvest index; αa: factor for scaling leaf-level photosynthesis to stand level; β: radiation-use efficiency factor; TH: Total Heat unit required for the maturity; TC: Technological coefficient; TS: Temperature sensitivity of photosynthesis; LR: ratio of leaf to above ground biomass.

Chapter 6 Conclusions and perspectives

Overall, this thesis presented a series of studies detecting and attributing change of crop yield to climate change and management practices. Through these studies, the author not only improved the ORCHIDEE-crop model, but also advanced our ways to integrate crop model outputs and observational data streams. With ensemble of global gridded crop models and observational data-streams, we quantify and reduce uncertainties on how yield of major cereal crops respond to warmer temperature and irrigation practices. The key conclusions for each chapters are as follows.

Firstly, based on the statistical model built upon yield statistics and climate, we found maximum and minimum temperature changes had opposite impacts on maize yield over Northeast China. Maize yield increased by 10.0±7.7% in response to a 1 ºC increase in growing season mean daily minimum temperature (*Tmin*), but decreased by 13.4±7.1% in response to a 1 ºC increase in growing season mean daily maximum temperature (*Tmax*). The responses of maize yield to climate variations were subject to large spatial differences in terms of both the sign and the magnitude. Furthermore, the growing season mean temperature was significantly correlated with the response of maize yield to *Tmax* ($R=-0.67$, $P<0.01$), which changes from positive to negative when the growing season mean temperature exceeds 17.9±0.2 ºC. Precipitation became the dominant climatic factor driving maize yield variations when growing season precipitation was lower than ~400 mm, but had a weaker influence than temperature over most of the study area. These results highlight that spatial variations in the yield response to climate change can be explained by spatial gradients in local climate conditions. The robustness of process models in regional application would have to be carefully calibrated and examined.

Secondly, the particle filter based optimization was developed and applied in optimizing parameters controlling phenological development in ORCHIDEE-crop for three types of rice over China. The calibrated model forced by historical change in climate and transplanting dates was used to attribute the length of growth period (LGP) of rice to

managements and climate change. The results suggest that climate change has an effect on LGP trends dependent on rice types. Climate trends have shortened LGP of early rice (-2.0±5.0 day/decade), lengthened LGP of late rice (1.1±5.4 day/decade) and have little impacts on LGP of single rice (-0.4±5.4 day/decade). ORCHIDEE-crop simulations further show that change in transplanting date caused widespread LGP change only for early rice sites, offsetting 65% of climate change induced LGP shortening. The primary drivers of LGP change are thus different among the three types of rice. Management are predominant driver of LGP change for early and single rice. This study shows that complex regional variations of LGP can be reproduced with an optimized crop model. Better documenting observational error and management practices can help reduce large uncertainties existed in attribution of LGP change through data-model integration.

Thirdly, integrating field warming experiments at 48 sites across the globe and an ensemble of gridded global crop models (Rosenzweig et al., 2014) through emergent constraint approach, we produce field-data-constrained new estimates of the responses of crop yield to changes in temperature (S_T). The new estimates show with >95% probability that warmer temperatures would reduce yields for maize (-7.1±2.8% K^{-1}), rice (-5.6±2.0% K^{-1}) and soybean (-10.6±5.8% K^{-1}). For wheat, S_T was less negative and only 89% likely to be negative (-2.9±2.3% K^{-1}), which is 50% less than previous estimates (Zhao et al., 2017; Liu et al., 2016). The field-observation based constraints from the results of the warming experiments reduced uncertainties associated with modeled S_T by 12-54% for the four crops. The key implication for impact assessments after the Paris Agreement is that with global warming limited within 2 K above pre-industrial levels will still reduce yields of major crops by -3 to -13%, without considering effects of atmospheric CO_2 concentrations. Even if warming was limited to 1.5 K, none of the major producing countries of these crops would likely benefit from the warmer temperatures without effective adaptation. Maize, rice and soybean would be more vulnerable to increasing temperatures than wheat.

Finally, the global reanalysis of irrigation contribution to wheat and maize yield was performed by Bayesian model average to integrate estimates from both data-driven datasets and global crop modelling. The reanalysis was found to have more precision than estimates either by data-driven dataset or by global crop model ensemble when confronted with US

statistics. The reanalysis shows that, at global scale, irrigation contributes to 34%±25% and 22%±23% of irrigated yield for wheat and maize respectively. The further analysis on supply and demand balance of irrigation water shows that the priority of building irrigation facilities is on eastern Europe and India for wheat and Brazil for maize. If shifting global rainfed croplands into irrigated ones, 30% - 47% of contemporary rainfed croplands do not have sufficient local runoff resources to meet irrigation demand, including some hotspots (e.g. northern China and mid-western US), which will have to rely on groundwater or trans-basin water transfer program. The large overestimates (~2 times than the "bottom-up" estimates) and uncertainties (~4 times difference among models) in model simulated irrigation contribution to crop yield suggest that previous model-based analyses of agricultural economy and hydrology will have to be revisited.

During the PhD studies, I have also been developing the ORCHIDEE-crop model by incorporating multiple management practices and a new allocation scheme, which considers phenological growth regulation and the full nutrient cycling of nitrogen and phosphorus. Like many land surface models, the original allocation scheme in ORCHIDEE, and thus earlier version of ORCHIDEE-crop, is photosynthesis centric (Friedlingstein et al., 1998). The carbon assimilation simulated by Farquhar scheme is the "source" of crop growth allocated in a cascading manner to each organ of the crop (Figure 6.1). However, results presented in Chapter 2and 3, and results from FACE experiments (Long et al., 2006) clearly indicates that crop growth dynamics are strongly regulated not only by photosynthesis but also "sink strength" of assimilated carbon, which has been hypothesized to be associated with crop phenology and nutrient availability (e.g. Ainsworth et al., 2004). Therefore, I am going to improve the allocation scheme of ORCHIDEE-crop model, making it from a "cascade" model into a "spiral" model, which consider multiple down-regulations to potential photosynthesis assimilations (Figure 6.1). Such improvement will help the model become a better tool to understand how climate change would have been affecting croplands, though such multiple feedback loops will make the model more unstable and difficult to calibrate (e.g. Goll et al., 2017). The other major shortcoming of ORCHIDEE-crop model is the coverage of crop types is limited to winter wheat, maize and rice at the moment. Though these three crops account substantial portion of global calorie production, they only cover about one-fifth of global croplands. The large cropland area with other crop types can not be

well represented due to lack of parameter sets for other crops. We will expand the model parameter sets for other crops (e.g. soybean, rapseed, millet) in the future studies.

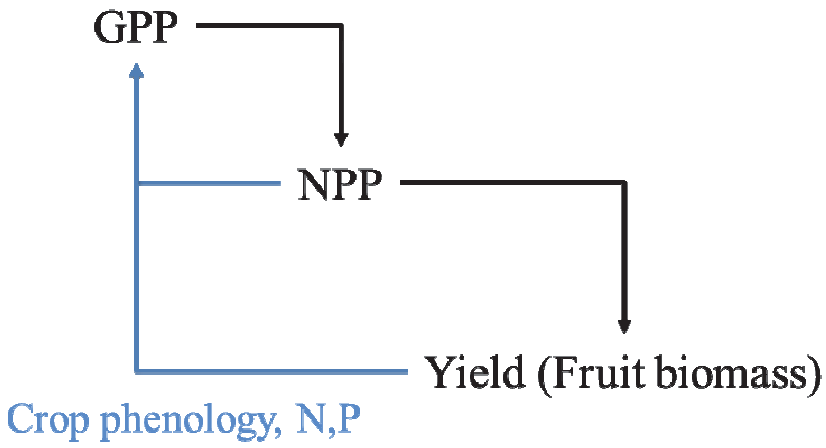

Figure 6.1 Schematic plot showing the change from "cascading" allocation model (black lines, Friedlingstein et al., 1998), where crop growth was controlled by the source to "spiral" allocation model (black + blue lines), which interactively consider source-sink constraint in crop growth.

On the other aspect, as mentioned in Chapter 1 and Chapter 5, climate change not only affect the food production and carbon cycling of croplands, but also the surface water and energy balance of them. Thus, the climate-cropland relationship is not unilateral. The crop-growth related change in surface albedo, evapotranspiration and surface roughness will feed back to the atmosphere and affect the local and regional climate. The significant historical change in cropping intensity, crop productivity and management practices (e.g. irrigation) could have already left a footprint on global climate (e.g. Lobell et al., 2008ab; Jeong et al. 2014). In current version of IPSL earth system model, croplands are represented with very productive C3 and C4 grasslands, which could have dimissed the feedback of crop land surface to the climate. Here, we illustrate the potential influence of surface variables on climate through comparing offline simulations of non-crop version of ORCHIDEE and ORCHIDEE-crop over China during the past three decades.

As shown in Figure 6.2, the land surface properties simulated by non-crop and crop version of ORCHIDEE show drastic differences. Compared with the calibrated

ORCHIDEE-crop model (Wang et al., 2017), the non-crop version of ORCHIDEE under estimate the LAI by 2-6 folds and under estimate the evapotranspiration from rice croplands by a magnitude. The underestimate of LAI reflects the failure of non-crop ORCHIDEE to represent the phenology and growth dynamics of productive Chinese rice, while the underestimate of latent heat flux is related both to the underestimate of LAI and the lack of accounting for irrigation practices. On the other words, the current IPSL earth system model may have underestimated the albedo of the rice croplands and the evaporative cooling effects due to application of irrigation practices.

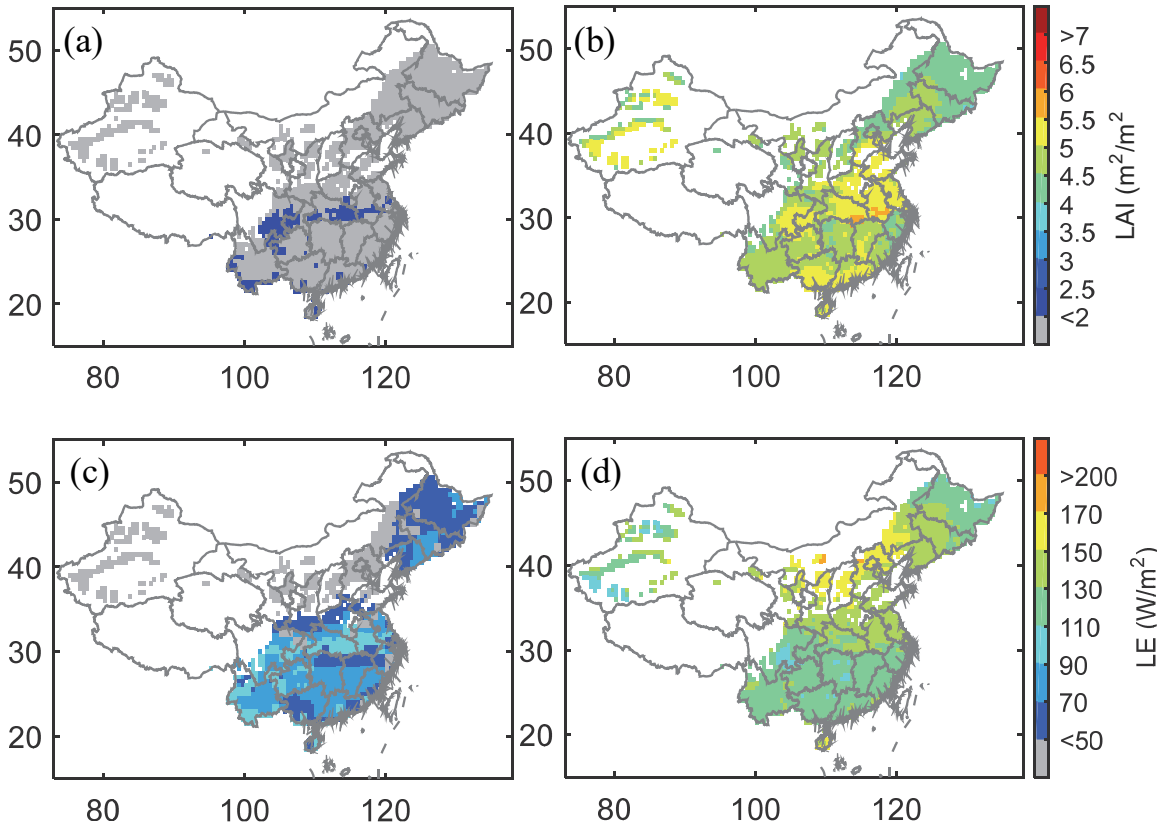

Figure 6.2 Simulated (a-b) leaf area index and (c-d) latent heat flux of rice croplands over China by standard ORCHIDEE model (a, c) and ORCHIDEE-crop model (b,d)

As the land surface component of IPSL model, the crop branch of ORCHIDEE has the potential to be coupled with LMDZ in order to explore the complex interaction between croplands and the atmosphere. Recent studies have demonstrated the capability of such model in estimating, for example, the feedback of LAI increment to historical warming

trend (Zeng et al., 2017; Li et al., in prep). The coupled LMDZ-ORCHIDEE-crop model will contribute to our understanding on how change in crop growth, land use and crop managements may have been influenced the historical change and future evolution of the climate system.

References

Ainsworth EA, Rogers A, Nelson R, Long SP (2004) Testing the "source–sink" hypothesis of down-regulation of photosynthesis in elevated [CO2] in the field with single gene substitutions in Glycine max. *Agricultural And Forest Meteorology,* **122**, 85-94.

Friedlingstein P, Joel G, Field CB, Fung IY (1999) Toward an allocation scheme for global terrestrial carbon models. *Global Change Biology,* **5**, 755-770.

Goll, D. S., Vuichard, N., Maignan, F., Jornet-Puig, A., Sardans, J., Violette, A., et al. (2017). A representation of the phosphorus cycle for ORCHIDEE (revision 3985). *Geoscientific Model Development Discussions*. doi:10.5194/gmd-2017-62.

Jeong S-J, Ho C-H, Piao S *et al.* (2014) Effects of double cropping on summer climate of the North China Plain and neighbouring regions. *Nature Clim. Change,* **4**, 615-619.

Liu B, Asseng S, Muller C *et al.* (2016) Similar estimates of temperature impacts on global wheat yield by three independent methods. *Nature Clim. Change,*

Lobell DB, Bonfils C, Faurès J-M (2008) The Role of Irrigation Expansion in Past and Future Temperature Trends. *Earth Interactions,* **12**, 1-11.

Lobell DB, Bonfils CJ, Kueppers LM, Snyder MA (2008) Irrigation cooling effect on temperature and heat index extremes. *Geophysical Research Letters,* **35**, L09705.

Long SP, Ainsworth EA, Leakey ADB, Nösberger J, Ort DR (2006) Food for Thought: Lower-Than-Expected Crop Yield Stimulation with Rising CO2 Concentrations. *Science,* **312**, 1918-1921.

Rosenzweig C, Elliott J, Deryng D *et al.* (2014) Assessing agricultural risks of climate change in the 21st century in a global gridded crop model intercomparison. *Proc Natl Acad Sci U S A,* **111**, 3268-3273.

Wang X, Ciais P, Li L *et al.* (2017) Management outweighs climate change on affecting length of rice growing period for early rice and single rice in China during 1991–2012. *Agricultural And Forest Meteorology,* **233**, 1-11.

Zeng Z, Piao S, Li LZX *et al.* (2017) Climate mitigation from vegetation biophysical

feedbacks during the past three decades. *Nature Clim. Change,* **7**, 432-436.

Zhao C, Liu B, Piao S *et al.* (2017) Temperature increase reduces global yields of major crops in four independent estimates. *Proceedings of the National Academy of Sciences,* **114**, 9326-9331.